Ecole Doctorale MADIS 631

Université de Lille

Université de Lille

Thèse

pour obtenir le grade de :

Docteur de l'Université de Lille

dans la spécialité

" Automatique, Génie informatique, Traitement du Signal et des Images"

par

Gaël van der Lee

Encadrants

François Cabestaing

Hakim Si–Mohammed

Caractérisation des neuromarqueurs de la vection à l'aide d'ICO passive : vers une atténuation de la cybercinétose

Characterizing Vection Neuromarkers Using Passive BCI: Toward Cybersickness Mitigation

Thèse soutenue le 15 Décembre 2025 devant le jury composé de :

M.	Ronan Boulic	Maître d'Enseignement et de Recherche, EPFL,	(Rapporteur)
M.	Marc Macé	Chargé de recherche, IRISA,	(Rapporteur)
Mme	Raphaëlle N. Roy	Professeure, ISAE-SUPAERO,	(Examinatrice)
M.	Sylvain Chevallier	Professeur, Université Paris Saclay,	(Président)
M.	Hakim Si-Mohammed	Maître de conférences, CRIStAL,	(Co-encadrant)
M.	François Cabestaing	Professeur, CRIStAL,	(Directeur)

CRIStAL Lab, Lille, France

Remerciements

Je tiens tout d'abord à exprimer ma profonde gratitude à mes encadrants de thèse, le professeur François Cabestaing et le maître de conférences Hakim Si-Mohammed, pour leur encadrement, leur disponibilité, leur confiance et leurs conseils tout au long de ces années. Leur rigueur scientifique et leur accompagnement ont été déterminants dans l'aboutissement de ce travail. Je remercie également le projet européen GENESIS, dans le cadre duquel cette thèse a été menée.

J'adresse mes sincères remerciements aux membres du jury qui ont accepté d'évaluer ce travail : Monsieur Ronan Boulic, Maître d'Enseignement et de Recherche à l'EPFL, et Monsieur Marc Macé, Chargé de recherche à l'IRISA, pour m'avoir fait l'honneur de rapporter cette thèse. Madame Raphaëlle N. Roy, Professeure à l'ISAE-SUPAERO, pour avoir accepté d'examiner ce travail. Monsieur Sylvain Chevallier, Professeur à l'Université Paris-Saclay, pour avoir présidé ce jury.

Je remercie les membres permanents de l'équipe BCI, José Rouillard, Marie-Hélène Bekaert et Jean-Marc Vannobel, pour leur présence et leur accompagnement durant la thèse. Je remercie également Anatole Lécuyer et Reinhold Scherer pour leurs relectures, leurs remarques et leur contribution à la solidité de mes articles. Je remercie également les stagiaires qui ont accompagné cette thèse. Je pense à Maxence Naud, dont le travail a posé des bases importantes pour le mien. Je pense à Younes Makhlouf pour son amitié et son aide dans la mise en place de PECS. Je pense à Abdallah Toumji pour avoir été un compagnon de bureau. Je pense enfin à Juliette Meunier pour sa joie de vivre contagieuse, sa gentillesse, son humour et nos conversations aussi loufoques qu'intéressantes.

Je tiens aussi à remercier Pierre Chanais, Pierre Antoine Thouvenin, ainsi que toutes les personnes qui ont rendu mes expériences d'enseignement inoubliables et aussi formatrices pour moi que pour mes étudiants.

Mes déplacements, mes conférences et mes collaborations m'ont aussi offert de très belles rencontres. Je remercie plus particulièrement la communauté BCI française, Valérie Massens, Emile Savalle, Fabien Lotte, Léa Pilette, Camille Jeunet, Laurent Bougrain, Sébastien Rimbert, Loic Bechon, David Trocellier, et bien d'autres, pour son énergie et pour tous les moments partagés.

Au laboratoire CRIStAL, je remercie mes collègues et toutes les personnes qui ont contribué à faire de ces années un cadre de travail stimulant et chaleureux. Je pense en particulier à mes voisins d'en face, et notamment à Clemence Prevauteau, pour son amitié et pour m'avoir accueilli les bras ouverts à Lille. Je remercie Jan Butora pour sa compagnie chaleureuse et ses pizzas délicieuses. Je remercie Markus Grimm pour son amitié, les bons moments passés ensemble et toutes les expériences partagées. Je remercie Pierre Palud pour les séances de grimpe et les moments partagés hors du laboratoire. Je remercie enfin, plus largement, l'équipe SIGMA, ses permanents et ses doctorants.

Je souhaite aussi remercier celles et ceux qui n'ont partagé qu'une partie de ce parcours, mais qui l'ont marqué durablement. Merci à Jimmy Petit pour m'avoir fait découvrir l'université, les équipes, les bons plans et la vie de doctorant, et pour m'avoir accompagné avec gentillesse et bienveillance pendant les premiers mois, qui sont souvent les plus difficiles. Merci à Arne Van Den Kerchove pour les conférences, les moments d'équipe, son écoute attentive et ses remarques toujours pertinentes.

Et enfin, je remercie mes proches, sans qui cette thèse n'aurait jamais vu le jour. À mon pilier, Juliete, merci d'avoir été à mes côtés du début à la fin. Tu as ta part dans chaque idée et de chaque page de cette thèse. Merci à Papa, Maman, Tim et Jo pour votre présence, pour tout ce que vous m'avez transmis, et pour le soutien constant que vous m'avez apporté. Les mots ne suffiront jamais à exprimer ce que je vous dois.

Abstract

Virtual Reality (VR) adoption is constrained by cybersickness: nausea, disorientation, and oculomotor symptoms affecting 60–95% of users. Current assessment relies on retrospective self-report measures that lack temporal resolution and cross-subject comparability, limiting the development of effective mitigation strategies. This dissertation addresses three research objectives: (1) map the research landscape of Brain-Computer Interfaces (BCIs), cybersickness, and vection, including neural markers, algorithms, and methodologies; (2) explore potential neuromarkers for understudied aspects of cybersickness and acceleration perception; (3) contribute to better identification of VR user experience markers suitable for adaptive applications.

Two systematic literature reviews examined BCI-based cybersickness research and Electroencephalography (EEG) correlates of vection. These reviews identified promising neural markers, including increased delta and theta power, decreased alpha power, and parieto-occipital alpha modulation for vection, but revealed substantial methodological heterogeneity limiting cumulative understanding. A controlled VR experiment ($N = 30$) recorded EEG during linear visual acceleration (forward or backward) with concurrent subjective vection ratings and Simulator Sickness Questionnaire (SSQ) assessments. Three spatial filtering techniques (Common Spatial Patterns, Effect-Matched Spatial, xDAWN) were systematically compared for Event-Related Potential (ERP) enhancement.

The findings include the first characterization of neural responses to sudden visual acceleration in VR: a fronto-central positivity emerging 300–700 ms post-stimulus with direction-sensitive activity. We identified the first evoked potential reliably linked to subjective vection perception: a bipolar parietal positivity and frontal negativity at approximately 600 ms (vection P600), representing an objective, inter-subject marker of subjective experience. The spatial filtering evaluation demonstrated that xDAWN outperformed Common Spa-

tial Patterns and Effect-Matched Spatial filtering for enhancing acceleration ERPs, providing a computationally efficient method for ERP enhancement. A complementary protocol named "PECS" extends this work to leverage physical motion with absent or incongruent visual motion to study sensorimotor incongruence in VR.

The temporal sequence from acceleration perception (300–700 ms) to subjective vection experience (600 ms) suggests sequential processing from sensory encoding to conscious perception. The vection P600 topography aligns with cognitive conflict processing, providing support for the sensory conflict theory. Stronger vection is correlated with higher nausea and disorientation, supporting the sensory conflict hypothesis and suggesting that individual differences in conflict resolution modulate cybersickness susceptibility.

The identified neuromarkers enable objective, time-locked cybersickness risk assessment complementing self-report instruments. Real-time ERP detection within the 600 ms window permits neuroadaptive VR interventions, such as field-of-view reduction or velocity modulation, to mitigate cybersickness while preserving immersion. This dissertation demonstrates that EEG holds promise for objective, inter-subject markers of subjective motion perception in VR, establishing a framework integrating sensory conflict theory, predictive coding, and neuroadaptive control for next-generation immersive systems.

Résumé étendu

Introduction et contexte

L'adoption de la Réalité Virtuelle (RV) est freinée par la cybercinétose, un ensemble de symptômes comprenant nausées, désorientation et troubles oculomoteurs affectant 60 à 95% des utilisateurs. Ce phénomène constitue un obstacle majeur à l'utilisation prolongée de la RV dans la recherche, la formation professionnelle et les applications grand public. L'évaluation de la cybercinétose repose principalement sur des mesures subjectives rétrospectives, telles que le Simulator Sickness Questionnaire (SSQ), qui manquent de résolution temporelle et de comparabilité inter-sujets, limitant le développement de stratégies d'atténuation efficaces.

La vection, définie comme l'illusion visuelle de mouvement autonome chez un observateur immobile, semble jouer un rôle central dans l'apparition de la cybercinétose. Selon l'hypothèse du conflit sensoriel, l'intensité de la vection est directement liée à la sévérité des symptômes. Cependant, les mécanismes neurophysiologiques sous-jacents restent mal compris, et leur mesure s'appuie sur des évaluations subjectives sujettes aux biais de rappel et à la désirabilité sociale.

L'Électroencéphalographie (EEG) offre une approche prometteuse pour développer des mesures objectives en temps-réel des états perceptifs en RV. Les interfaces cerveau-ordinateur (ICO) passives permettent de surveiller l'activité cérébrale sans action volontaire, ouvrant la voie à des systèmes adaptatifs ajustant le contenu virtuel selon l'état neurophysiologique détecté. Les potentiels évoqués (PE) présentent un intérêt particulier pour leur analyse temporelle précise des réponses neuronales.

Cette thèse s'inscrit dans le projet européen GENESIS (LeveraGing nEuromarkers for Next-gEn immerSIve Systems), financé par Horizon Europe via le consortium CHIST-ERA. Le projet réunit le Centre de Recherche en Informatique, Signal

et Automatique de Lille (CRIStAL), Inria Rennes, l'ETH Zurich, KOÇ University et l'University of Essex pour développer des systèmes de réalité virtuelle capables de détecter l'état mental en temps-réel et d'adapter le contenu pour améliorer l'immersion et réduire la cybercinétose.

Objectifs de recherche

Cette thèse poursuit trois objectifs principaux :

1. Cartographier le paysage de la recherche sur les ICO, la cybercinétose et la vection, incluant les marqueurs neuronaux, les algorithmes et les méthodologies.
2. Explorer les neuromarqueurs potentiels pour des aspects peu étudiés de la cybercinétose et de la perception de l'accélération.
3. Contribuer à une meilleure identification des marqueurs de l'expérience utilisateur en RV adaptés aux applications adaptatives.

Ces objectifs répondent à des lacunes identifiées concernant l'hétérogénéité méthodologique, l'absence de marqueurs objectifs en temps-réel et la compréhension limitée des mécanismes neurophysiologiques sous-jacents à la cybercinétose et à la vection.

Méthodologie générale

Revues systématiques

Deux revues systématiques ont été conduites selon les directives PRISMA. La première a examiné l'utilisation des ICO pour la caractérisation et la prédiction de la cybercinétose (marqueurs neurophysiologiques, méthodes de classification, protocoles). La seconde a synthétisé les connaissances sur les corrélats EEG de la vection (signatures oscillatoires et potentiels évoqués).

Protocole expérimental

Une cohorte de 30 adultes jeunes en bonne santé (extension d'une cohorte initiale de 20) a été exposée à des stimuli visuels de vection rectiligne (avant ou arrière) via un casque de réalité virtuelle. L'EEG (14 électrodes) a été enregistré en continu pendant l'exposition. Après chaque essai, les participants évaluaient l'intensité de vection perçue sur une échelle de Likert à 4 points (aucune, faible, modérée, forte). Le SSQ était administré avant l'expérience et après chaque bloc pour quantifier les symptômes de cybercinétose.

Les stimuli consistaient en sphères blanches sur fond noir se déplaçant radialement, créant une illusion de mouvement rectiligne. Chaque essai comprenait une phase de repos (vitesse constante basse), une accélération soudaine et une vitesse élevée constante, permettant d'isoler les réponses neuronales à l'accélération et à la vection. En complément, le protocole PECS (Potentiels Évoqués par des Conflits Sensoriels), présenté en annexe, étudie les réponses neuronales à un mouvement physique lorsque le mouvement visuel est absent, congruent ou conflictuel en RV.

Traitement du signal

Les données EEG ont été prétraitées de façon standard : filtrage passe-bande (0,3–10 Hz pour les analyses PE), suppression d'artefacts par analyse en composantes indépendantes (ICA), re-référencement au moyen commun (CAR) et segmentation. Les analyses ont porté sur les potentiels évoqués moyens, les analyses spectrales temps-fréquence, les statistiques par permutations, et la comparaison de techniques de filtrage spatial (Common Spatial Patterns, Effect-Matched Spatial, xDAWN) pour améliorer la séparabilité des PE.

Résultats principaux

État de l'art sur les ICO et la cybercinétose

La revue systématique a analysé 83 études (2001–2025). L'EEG domine comme modalité d'imagerie grâce à sa résolution temporelle élevée et sa compatibilité avec la RV. Les marqueurs neurophysiologiques les plus rapportés incluent une augmentation de la puissance spectrale dans les bandes delta (1–4 Hz) et thêta (4–8 Hz), et une diminution de la puissance alpha (8–13 Hz), particulièrement dans les régions fronto-centrales et pariéto-occipitales.

Les méthodes de classification se répartissent entre approches classiques (Support Vector Machines, k-Nearest Neighbors, Linear Discriminant Analysis) et apprentissage profond (réseaux convolutifs, récurrents, architectures hybrides). Les performances rapportées montrent des précisions moyennes de 92,5% pour la validation intra-sujet (plage : 73–100%) et 86,8% pour la validation inter-sujets (plage : 68–100%), reflétant une hétérogénéité méthodologique importante.

La revue identifie plusieurs limitations récurrentes : absence de standardisation des protocoles, échantillons petits et trop homogènes, manque de validation croisée inter-sujets, rapports méthodologiques incomplets, et confusion entre caractérisation, prédiction et détection. Ces résultats motivent le besoin d'investigations fondamentales sur les mécanismes neurophysiologiques et de protocoles standardisés.

Corrélats EEG de la vection

La seconde revue a synthétisé 16 études sur les signatures neuronales de la vection. Les modulations dans la bande alpha (8–13 Hz), particulièrement pariéto-occipitales, constituent un marqueur oscillatoire robuste. Une diminution de la puissance alpha est observée pendant la vection, reflétant possiblement une inhibition de l'activité visuelle de base et une augmentation du traitement cortical du mouvement.

Concernant les potentiels évoqués, les modulations précoces (N2, 200 ms) sont associées aux caractéristiques du stimulus plutôt qu'à la vection elle-même. Les composantes tardives (P3, 300–600 ms) montrent des associations avec la susceptibilité individuelle, mais aucun potentiel évoqué spécifique de la vection subjective n'avait été identifié de manière fiable.

L'hétérogénéité méthodologique (types de stimuli, paradigmes, évaluations) limite les comparaisons inter-études. Les lacunes incluent l'absence de PE spécifique de la vection subjective et la compréhension limitée de la hiérarchie temporelle du traitement neuronal.

PE de l'accélération en réalité virtuelle

L'étude expérimentale sur 20 participants a révélé la première caractérisation systématique des réponses neuronales à l'accélération visuelle soudaine en RV. Un potentiel évoqué distinct émerge 300 à 700 ms après le début de l'accélération, caractérisé par une positivité fronto-centrale représentant

l'encodage neuronal des changements soudains de flux optique, indépendamment de la direction.

Une activité neuronale sensible à la direction a été identifiée au niveau de l'électrode Cz, suggérant des flux de traitement parallèles pour l'accélération avant et arrière. Cette différenciation directionnelle indique que le cerveau distingue la direction du mouvement à des stades précoces du traitement perceptif.

Ces résultats établissent un lien causal temporellement précis entre l'onset du stimulus et la réponse neuronale, fournissant un marqueur objectif de la perception de l'accélération. La robustesse de ce marqueur a été confirmée par sa réplication, l'étude ayant été étendue de 20 à 30 participants pour l'analyse de vection.

Potentiel évoqué de la vection (P600)

L'étude sur 30 participants a identifié le premier potentiel évoqué relié de manière fiable à la perception subjective de vection. Le P600 de vection est caractérisé par un pic positif pariétal et un pic négatif frontal simultané, apparaissant environ 600 ms après le début du stimulus.

Malgré une variabilité inter-individuelle substantielle dans la susceptibilité à la vection, le P600 distingue significativement les essais avec vection forte des essais avec vection faible ou absente, établissant un marqueur objectif d'une expérience perceptive subjective.

La topographie bipolaire pariéto-frontale ressemble aux composantes cognitives de résolution de conflit documentées dans la littérature des PE (paradigmes d'oddball vestibulaire, traitement de l'humour). Le profil temporel s'aligne avec les complexes positifs tardifs de mise à jour contextuelle et de surveillance de conflit, suggérant que le P600 de vection reflète la résolution active de conflit sensoriel.

L'intensité de vection rapportée est significativement corrélée avec les scores SSQ : score total ($r = 0,55$, $P < 0,01$), nausée ($r = 0,62$, $P < 0,003$), désorientation ($r = 0,51$, $P < 0,02$) et oculomoteur ($r = 0,45$, $P < 0,04$). La corrélation la plus forte avec la nausée et la désorientation est cohérente avec les symptômes caractéristiques de la cybercinétose. Cette convergence de preuves neuronales et comportementales renforce l'hypothèse du conflit de vection, selon laquelle les processus neuronaux sous-jacents à la vection contribuent directement à la cybercinétose.

La contribution centrale réside dans l'identification d'un marqueur PE inter-sujets d'un état perceptif subjectif, permettant des comparaisons objectives entre participants et démontrant des processus neuronaux communs sous-jacents à la variabilité individuelle.

Techniques de filtrage spatial

L'évaluation a comparé CSP, EMS et xDAWN pour améliorer la détectabilité des PE d'accélération. xDAWN surpasse significativement CSP et EMS en séparabilité entre conditions avant/arrière, produisant les différences les plus nettes avec des pics bien définis.

Les analyses temporelles confirment que xDAWN améliore la détection de différences spectrales dans les fenêtres temporelles d'intérêt (300–700 ms). Les courbes d'apprentissage montrent que xDAWN atteint les meilleures performances de séparabilité avec moins de données d'entraînement.

Ces résultats s'expliquent par la conception de xDAWN pour optimiser le rapport signal-sur-bruit des réponses temporellement verrouillées, contrairement à CSP (maximisant la variance sans considération temporelle) et EMS (sensible au bruit). L'efficacité computationnelle de xDAWN permet son application en temps-réel dans des systèmes ICO passifs.

Contributions théoriques

Hiérarchie temporelle du traitement du mouvement

Les résultats révèlent une hiérarchie temporelle se déployant séquentiellement de l'encodage sensoriel à la perception subjective. Le PE d'accélération (300–700 ms, positivité fronto-centrale) représente la réponse neuronale initiale aux changements soudains de mouvement visuel. Le P600 de vection (600 ms, positivité pariétale/négativité frontale) reflète un traitement d'ordre supérieur associé à la perception consciente de mouvement autonome.

Cette séquence suggère que l'encodage sensoriel de l'accélération précède les processus neuronaux sous-jacents à la vection, s'intégrant aux modèles de traitement prédictif où les signaux précoces d'erreur de prédiction précèdent la mise à jour de modèle d'ordre supérieur.

Éléments de preuve en faveur de la théorie du conflit sensoriel

Le P600 de vection fournit des éléments de preuve mesurables cohérentes avec la théorie du conflit sensoriel, historiquement fondamentale pour comprendre le mal des transports induit visuellement. La topographie bipolaire pariéto-frontale s'aligne avec les mécanismes de contrôle inhibiteur et le traitement de conflit cognitif.

Les corrélations entre intensité de vection et symptômes (nausée, désorientation) renforcent l'hypothèse du conflit de vection. Les différences individuelles dans l'efficacité de résolution de conflit pourraient moduler la susceptibilité à la cybercinétose.

Cadre du codage prédictif

Le PE d'accélération peut représenter la détection d'erreurs de prédiction lorsque le mouvement visuel viole le modèle interne de l'observateur, tandis que le P600 de vection correspondrait à la mise à jour du modèle. Les participants avec un début rapide de vection pourraient posséder des modèles prédictifs plus flexibles, cohérent avec les différences individuelles dans l'efficacité du traitement neuronal.

Implications pratiques

Les neuromarqueurs identifiés permettent une évaluation objective et temporellement précise du risque de cybercinétose, complétant les instruments d'auto-évaluation comme le SSQ. La détection d'un PE en temps-réel dans la fenêtre de 600 ms permet des interventions neuroadaptatives : réduction du champ de vision, modulation de la vitesse ou ajout de repères visuels stabilisateurs lors de la détection d'accélérations soudaines.

Cependant, détecter la variabilité à essai unique reste un défi. Les algorithmes doivent tenir compte des différences inter-sujets tout en maintenant la précision temporelle. Les stratégies adaptatives doivent équilibrer l'atténuation de la cybercinétose avec la préservation de l'immersion.

L'approche PE avec un montage EEG 14 électrodes facilite les comparaisons reproductibles entre laboratoires, s'alignant avec les mouvements vers des algorithmes de traitement standardisés. L'évaluation du filtrage spatial xDAWN

montre l'intérêt d'utiliser cette technique de filtrage dans les neurotechnologies en temps-réel, où l'efficacité computationnelle et les contraintes de latence sont critiques pour l'adaptation en boucle fermée.

Limitations

Le montage EEG 14 électrodes limite la localisation de source et l'interprétation au niveau des réseaux neuronaux, reflétant un compromis entre validité en situation réelle et fidélité de mesure. Les stimuli contrôlés (sphères blanches sur fond noir), nécessaires pour isoler les PE, peuvent ne pas se généraliser aux environnements VR complexes.

L'échantillon (jeunes adultes en bonne santé) limite la généralisabilité aux populations plus âgées ou avec des déficiences vestibulaires ou visuelles. La variabilité inter-sujets dans la morphologie, l'amplitude et la latence des PE complique la classification à essai unique. Des facteurs (fatigue, engagement, conditions environnementales) peuvent influencer les réponses neuronales.

La robustesse des résultats de vection serait renforcée par une étude sur un échantillon plus large et plus diversifié, permettant une meilleure caractérisation de la variabilité individuelle.

Perspectives de recherche

Objectifs à court terme

Les priorités immédiates incluent l'application de xDAWN aux données de vection pour améliorer le rapport signal-sur-bruit du P600, et le développement d'algorithmes de classification pour la détection en ligne en temps-réel, équilibrant précision temporelle et variabilité inter-sujets.

L'analyse des données pilotes du protocole PECS (Potentiels Évoqués par des Conflits Sensoriels), avec la possiblité d'avoir un mouvement physique sans mouvement visuel, fournira des éclairages sur l'intégration sensorielle lorsque les mouvements physique et visuel sont découplés. Ce paradigme examine si les PE d'accélération et de vection persistent ou présentent de nouveaux motifs lorsque la perception vestibulaire contredit ou complète la perception visuelle.

Objectifs à moyen terme

L'augmentation de l'ensemble de données PECS permettra une analyse statistique robuste des corrélats neuronaux lorsque les mouvements physique et visuel sont systématiquement découplés, clarifiant les mécanismes neuronaux sous-jacents à la vection et à la cybercinétose.

L'investigation de neuromarqueurs spécifiquement liés à la vection induisant la cybercinétose est essentielle pour distinguer la perception bénigne des réponses pathogènes. Identifier les signatures neuronales différenciant la vection sans symptômes de la vection induisant une nausée permettra des interventions ciblées.

L'augmentation de la diversité et de la taille d'échantillon renforcera la généralisabilité. La localisation de source et l'analyse de connectivité cartographieront les réseaux corticaux, fournissant des éclairages mécanistes sur la séquence de traitement hiérarchique.

Vision à long terme

Le développement de systèmes ICO en boucle fermée adaptant le contenu VR en temps-réel basé sur les PE détectés représente l'objectif translationnel ultime. De tels systèmes pourraient dynamiquement ajuster le champ de vision, les profils de vitesse ou les ancres visuelles dans la fenêtre de 600 ms pour prévenir le début de vection ou atténuer la cybercinétose.

Les applications s'étendent à la formation (réduction du mal des simulateurs), l'accessibilité (personnalisation pour individus avec sensibilités sensorielles) et les contextes thérapeutiques (thérapie d'exposition pour phobies, rééducation vestibulaire).

La validation dans des environnements VR en situation réelle (navigation, jeux vidéos, simulations) établira la robustesse des marqueurs pour le déploiement réel. L'incorporation de stimulation vestibulaire physique examinera comment l'entrée vestibulaire congruente module les PE visuels, informant la conception de simulateurs de mouvement.

Conclusion

Cette thèse démontre que l'EEG peut fournir des marqueurs objectifs et inter-sujets de la perception subjective de mouvement en réalité virtuelle. L'identification des PE d'accélération et de vection établit des voies neuronales temporelles et hiérarchiques sous-jacentes à la perception de mouvement, reliant l'encodage sensoriel précoce à l'expérience perceptive consciente.

Le P600 de vection constitue la première composante d'un PE reliée de manière fiable à la perception subjective de vection, fournissant des preuves mesurables cohérentes avec la théorie du conflit sensoriel. Les corrélations entre intensité de vection et symptômes de cybercinétose renforcent l'hypothèse du conflit de vection et suggèrent que les différences individuelles dans la résolution de conflit modulent la susceptibilité.

Les contributions méthodologiques, notamment la supériorité de xDAWN pour l'amélioration des PE, fournissent une base computationnellement efficace pour les implémentations ICO passives en temps-réel. Ces résultats s'inscrivent dans les agendas en neuroergonomie, interaction homme-machine et technologies immersives, soutenant des pratiques standardisées et reproductibles permettant des benchmarks inter-laboratoires et des études translationnelles.

En définitive, cette recherche montre l'intérêt de développer des systèmes de réalité virtuelle conscients de l'état cérébral capables de détecter objectivement l'état de l'utilisateur et d'adapter le contenu pour améliorer le confort, la sécurité et l'expérience immersive.

Contents

Chapter 1

Introduction

> *Je n'ai fait celle-ci plus longue que parce que je n'ai pas eu le loisir de la faire plus courte.*
> *If I had more time I would have written a shorter letter*
>
> Blaise Pascal

This chapter introduces the core concepts and tools used throughout the dissertation. It defines Virtual Reality through the lenses of immersion and presence, motivates the problem of cybersickness, and reviews leading explanatory theories alongside the central role of vection. We outline limitations of current (primarily subjective) measures and motivate objective monitoring with Brain–Computer Interfaces. We then survey neuroimaging modalities with a focus on Electroencephalography (EEG), describe Brain Computer Interfaces (BCI) paradigms and the standard processing pipeline, and justify the use of event-related potentials for Virtual Reality (VR). The chapter closes by stating the research aims and the overall structure of the dissertation.

I.1 What is Virtual Reality?

In science, a simple question often earns a familiar answer: "it depends". At the outset of this dissertation, we meet the same difficulty with a seemingly simple question: *what is Virtual Reality?* Kardong-Edgren et al. (2019) show that definitions of Virtual Reality (VR) are numerous and sometimes contradictory. Studies range from Head-Mounted Displays (HMDs) to desktop screens and smartphones. This plurality can stall cumulative progress by fragmenting methods, expectations, and evaluation. They propose a tiered taxonomy of VR based on its level of immersion: low, medium, and high. Illustrative setups are shown in Figure 1.1. This work helps compare studies and advances the field by providing a common language for discussing VR. However, for the purposes of this dissertation, we need to identify what VR fundamentally is. Given the lack of consensus, this dissertation provisionally adopts the seminal, experience-centered definition of Steuer (1992). Rather than defining VR by hardware (e.g., "goggles and gloves"), Steuer grounds it in telepresence, after defining presence as "the sense of being in an environment," and telepresence being "the experience of presence in an environment by means of a communication medium". He defines VR as follows:

Virtual Reality

A "virtual reality" is defined as a real or simulated environment in which a perceiver experiences telepresence (Steuer 1992).

This definition was chosen because it captures what makes VR special: it stimulates your senses, and especially your visual system, to elicit the feeling of being transported, of disconnecting from the physical world and feel fully present somewhere else. This sense of presence is not only central to the VR experience, but also provides a lens for studying how the brain responds in real-world scenarios. VR technologies have permeated numerous sectors beyond entertainment, becoming integral tools in fields such as healthcare, professional training, and education (Chatain et al. 2022). The technology's applications span diverse domains, offering immersive experiences that can support learning, clinical interventions, and training environments that would

[1] Image source: `https://www.istockphoto.com/fr`
[2] Image source: `https://gametyrant.com`
[3] Image source: `https://www.atomicgear.com`

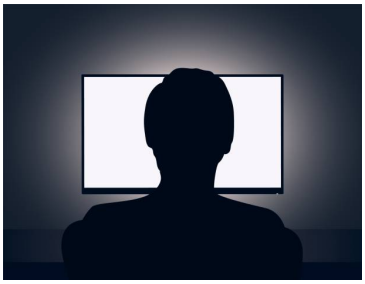

Image source:

https://www.istockphoto.com/fr

(a) *Low immersion: VR limited to one sense (monitor display with mouse), with low fidelity visuals and no alignment between visual and proprioceptive feedback.*[1]

Image source: https://gametyrant.com

(b) *Medium immersion: VR engaging one or two senses (projection and sound), with moderate fidelity visuals tracking.*[2]

Image source: https://www.atomicgear.com

(c) *High immersion: VR engaging multiple senses (visual, auditory, motor), with high-fidelity displays (HMD) and full-body motion capture matching proprioceptive feedback.*[3]

Figure 1.1: *Although all three of these setups are referred to as "VR" in the literature, Kardong-Edgren et al. (2019) proposes a tiered taxonomy of immersion: low, medium, and high, to separate them into different levels of immersion.*

be logistically infeasible or impossible in the physical world. To use this definition productively, we next distinguish immersion (a property of systems) from presence (a user response), terms we use throughout the dissertation.

Immersion

Immersion refers to the objective level of sensory fidelity a VR system provides (Bowman et al. 2007).

Presence

Presence refers to a user's subjective psychological response to a VR system (Bowman et al. 2007).

Steuer's telepresence can be viewed as the experience of presence mediated by the system (i.e., presence in an environment by means of a communication medium), consistent with this separation (Steuer 1992).

A high immersion VR system typically comprises: (1) a head-mounted display (HMD) with stereoscopic lenses whose resolution and refresh rate shape visual detail and motion smoothness; (2) tracked controllers or hand tracking to capture user actions; (3) head and controller tracking (inside-out or outside-in) to compute head pose and motion; (4) a compute unit (PC or integrated) that runs the simulation and renders images; and (5) optionally,

haptic feedback devices (e.g., vibration, force) to reinforce immersion. A game engine or equivalent software integrates inputs and produces the rendered environment.

Key determinants of immersion include field of view (instantaneous visual angle), field of regard (total viewable sphere), display size and resolution, stereoscopy, head-based rendering (head-tracked viewpoint updates), realism of lighting/shading, and temporal dynamics (frame and refresh rates). These are system properties that, collectively, drive immersion; presence is the user's psychological response to this level of immersion (Bowman et al. 2007; Cummings et al. 2016; Slater 2003).

In sum, we adopt an experience-centered definition of VR (Steuer 1992) and distinguish system-level immersion from the user's presence response. With this foundation, we turn to a major challenge at the heart of VR user experience, cybersickness.

I.2 The Problem of Cybersickness

If you've worn a head-mounted display for extended periods, you've likely felt it: a queasiness, disorientation that builds. That unsettling sensation is cybersickness (CS). Virtual Reality adoption is constrained by user experience problems, with cybersickness representing a barrier to widespread implementation across research and home applications. The phenomenon affects 60% to 95% of participants (Caserman et al. 2021), with 6% to 12.9% of participants prematurely ending their exposure and up to 42% unable to complete experimental sessions (Nesbitt et al. 2017), severely degrading user experience and impairing task performance (Mimnaugh et al. 2023).

To anchor terminology, we adopt the following concise definition:

Cybersickness

Cybersickness (CS) is a term used to refer to symptoms, such as nausea, headache, and dizziness, that users experience during or after virtual reality immersion (Caserman et al. 2021).

Cybersickness is closely related to motion sickness (MS), which is an unpleasant physiological response to real motion characterized by autonomic, oculomotor, and disorientation symptoms (L.-L. Zhang et al. 2016). The two share symptom clusters and explanatory frameworks (notably sensory conflict),

and questionnaire tools such as the Simulator Sickness Questionnaire are often used across both[1]. At the same time, important distinctions apply. Cybersickness typically arises during compelling visually simulated self-motion while the body remains stationary, whereas classical motion sickness can be provoked by vestibular stimulation alone. Cybersickness tends to present stronger disorientation symptoms compared to the oculomotor profile of simulator sickness (Stanney et al. 1997), and severity in HMD VR is frequently higher than in non-immersive setups (Davis et al. 2014; Weech et al. 2019). Vomiting, prominent in some motion-sickness contexts, is comparatively rare in HMD VR.

Related terms include simulator sickness (SS), motion sickness (MS), visually induced motion sickness (VIMS), and virtual reality sickness (VRS). Some authors consider CS a form of VIMS (Weech et al. 2019); others argue CS is distinct due to its characteristic disorientation profile (Rebenitsch et al. 2016). Here we retain the term CS for HMD VR contexts and note overlaps with VIMS/MS when discussing measures.

There is significant inter-subject variability in symptom onset and severity (L. M. Berger et al. 2025; L. M. Berger et al. 2024), with individual susceptibility influenced by demographic factors including age and gender, prior VR experience, and motion sickness susceptibility (Davis et al. 2014). Age-related susceptibility patterns reveal that children under 2 years do not experience motion sickness, with susceptibility emerging at 6 years and peaking at 9 years (Nürnberger et al. 2021). This variability creates challenges for systematic study and intervention development.

A meta review by Weech et al. (2019) shows that the relationship between presence, immersion, and cybersickness is complex and often contradictory. While most studies suggest an inverse relationship, where higher presence suppresses cybersickness by diverting attention from sensory conflict, others report positive or null correlations, often attributed to methodological differences. Immersion itself complicates the picture: increasing system fidelity (e.g., higher field-of-view, stereoscopy, or intuitive controls) can simultaneously heighten presence and increase susceptibility to cybersickness. The leading explanatory framework emphasizes sensory mismatch (particularly visual–vestibular conflict), but empirical findings remain inconsistent, partly due to low-powered studies and heterogeneous methodologies. This persistent

[1]The Simulator Sickness Questionnaire (SSQ) (Kennedy et al. 1993) remains the most widely used instrument; in practice, total scores (TS) of ≥ 18 are often taken to indicate the presence of sickness symptoms (e.g., (Cortes et al. 2023a)).

lack of clarity underscores the need for more systematic and theoretically grounded investigations into the mechanisms underlying cybersickness.

I.3 Theories of Cybersickness

Although we have outlined what cybersickness is, important questions remain about its neural origins and mechanisms. In the following section, we present the principal explanatory models of cybersickness to clarify the problem's complexity and motivate a neurophysiological approach. Situating this thesis within these frameworks prepares the interpretation of EEG-based findings and delineates the gaps that motivate our research.

The precise etiology of cybersickness remains a subject of investigation, with several theories to explain its multifaceted nature. These theories are not always mutually exclusive and often provide complementary perspectives on the phenomenon. The most dominant framework is the **Sensory Conflict Theory**, which posits that cybersickness arises from discrepancy between visual, vestibular, and proprioceptive systems (Davis et al. 2014; L.-L. Zhang et al. 2016). Several specific hypotheses branch from this core theory. The **Vection conflict hypothesis** states that cybersickness occurs when the visual system perceives compelling self-motion while the vestibular and proprioceptive systems report a stationary or incongruent physical state (Hettinger et al. 1990). The **Subjective Vertical Mismatch Theory** stems from a discrepancy between the sensed vertical, integrated from sensory information (eyes, vestibular system, proprioceptors), and the subjective vertical, which is the expected vertical based on previous experience (Bles et al. 1998). The **Rest Frame Conflict Hypothesis** attributes sickness to ambiguity in identifying a stable, stationary frame of reference within the environment (Prothero et al. 2003). The **Poison Theory** offers an evolutionary explanation, proposing that the brain misinterprets the sensory mismatch as a sign of neurotoxin ingestion, triggering a defensive response that includes nausea and vomiting (Treisman 1977). Consistent with an evolutionary perspective, cybersickness-like responses occur across mammalian species such as rats and also in fish (Nürnberger et al. 2021).

A second prominent framework is the **Postural Instability Theory**, which proposes that cybersickness results from a prolonged inability to maintain stable postural control rather than direct sensory mismatch (Cortes et al. 2023a). Other theories focus on specific physiological mechanisms. The **Vergence-**

Accommodation Conflict, unique to stereoscopic displays, describes the mismatch between the distance at which the eyes converge to fuse a stereoscopic image and the fixed focal distance of the device's screen (Kramida 2016). The **Eye Movement Theory** suggests that sickness is caused by specific patterns of eye movements generated by the vestibular system in an attempt to compensate for perceived motion (Ebenholtz 1992). More recently, these concepts have been integrated within a **Predictive Coding** framework (Nürnberger et al. 2021). This re-contextualizes sensory conflict as a failure of predictive processing where the brain fails to update its internal model when faced with persistent and unresolvable prediction errors between expected and actual sensory signals. An engineering-focused theory, often termed the **Display Lag Theory**, posits that cybersickness can be triggered by time-varying discrepancies between the user's physical head pose and the rendered virtual pose. These discrepancies arise from motion-to-photon latency and related tracking/optical factors. In summary, these theories can be viewed as complementary lenses on overlapping mechanisms. A concise comparison is provided in Table 1.1. Taken together, they underscore that core processes are still debated and that substantial research is needed to precisely characterize the mechanisms that underlie cybersickness. These perspectives converge on the central role of visually driven self-motion signals in creating and resolving sensory conflicts.

I.4 Understanding Vection

You have probably experienced it in everyday life: when a train next to you begins to move and, for a moment, it feels as though you yourself are moving. This sensation has been studied and is formally known as Vection (Dichgans et al. 1978; Hettinger et al. 1992). To situate the present research, it is essential to first define the concept of vection and its central role in cybersickness.

Vection

A visual illusion of self motion in a stationary observer (Palmisano et al. 2015).

Vection occurs when visual input creates a sensation of movement despite the observer remaining physically stationary. The term was first coined by von Helmholtz (1896) through observations of river flow beneath a bridge.

Table 1.1: *Concise summary of major cybersickness theories. Rows marked with † denote sub-theories within the Sensory Conflict framework.*

Theory	Trigger	Limitations
Sensory Conflict Theory	Mismatch between visual, vestibular, proprioceptive signals or prior expectations.	Weak predictive power; often unfalsifiable post-hoc.
Vection Conflict†	Illusion of self-motion while physically stationary.	No definitive link between vection and sickness.
Subjective Vertical Conflict†	Disagreement between sensed and expected gravity-based vertical.	Sickness occurs when vertical is unchallenged.
Rest Frame Conflict†	No single stable stationary reference in scene.	Mixed evidence; sickness occurs with clear rest frames.
Postural Instability Theory	Prolonged difficulty maintaining stable posture/control.	Instability ill-defined; mixed sway–sickness evidence.
Poison Theory	Sensory disturbance interpreted as neurotoxin ingestion.	Poor stimulus prediction; vomiting rare in HMD VR.
Eye-Movement Theory	Excessive, unsuccessful oculomotor error correction.	Hard to explain minimal eye-movement cases; vestibular role unclear.
Vergence Accommodation Conflict	Mismatch between vergence (disparity-driven depth) and fixed accommodation in HMDs.	Primarily visual fatigue/eye strain; solutions add complexity and design trade-offs.
Predictive Coding	Persistent prediction-error from unresolved sensory mismatch.	Explanatory more than predictive; causal direction and specifics need validation.
Display lag theory	Time-varying head pose discrepancy due to motion-to-photon latency and related factors.	HMD-specific; limited account of adaptation/individual differences; triggers need specification.

Initially conceptualized as a sensory failure or "illusion," it was later recognized as serving important functional roles in spatial orientation and motion perception.

Mechanistically, vection emerges from the integration of visual and vestibular sensory information. The visual system compensates for limitations of the vestibular system, which can only detect acceleration but cannot distinguish between absence of motion and constant velocity (Dichgans et al. 1978). This integration occurs within shared neural loci that construct unified models of spatial orientation, making vection a window into multisensory perception and sensory conflict resolution.

Vection is central to cybersickness research for several reasons. It operationalizes the core sensory conflict implicated in visually induced motion sickness: compelling visual cues signal self-motion while vestibular organs indicate stationarity, producing the mismatch at the heart of leading theories

(Hettinger et al. 1990). The vection–conflict theory proposes that stronger vection increases the likelihood or severity of sickness, potentially helping differentiate susceptible from resilient observers (Palmisano et al. 2020). Vection also contributes to presence and immersion in VR, further underscoring its dual role in user experience (Nürnberger et al. 2021). Vection frequently co-occurs with cybersickness (Keshavarz et al. 2015b; Kooijman et al. 2022; Nooij et al. 2017; Pöhlmann et al. 2021) and can exacerbate symptoms (Pöhlmann et al. 2022; Teixeira et al. 2022).

However, the empirical picture is nuanced. Some studies report stronger vection accompanying greater sickness, whereas others find weak or negative associations (Palmisano et al. 2020). Individuals with bilateral vestibulopathy (a loss of function in both vestibular organs) can still experience vection while remaining immune to vection-induced nausea (Cheung et al. 1991). This observation suggests that while visual mechanisms can elicit the percept of self-motion, an intact vestibular system may be necessary for the development of nausea in response to sensory conflict. These observations have motivated refinements to conflict-based theories (e.g., emphasis on mismatches in the subjective vertical (Bles et al. 1998)) and engineering-focused hypotheses about HMD-specific triggers (e.g., display lag; see Table 1.1).

I.5 Limitations of Current Approaches

Despite these theoretical insights, the field's measurement practice, dominated by retrospective self-reports, heterogeneous protocols, and modalities with limited temporal precision for event-locked phenomena, faces substantive limitations that impede cumulative, reproducible progress toward solutions. Assessment has relied heavily on subjective, post-hoc measures like the Simulator Sickness Questionnaire for cybersickness (Kennedy et al. 1993) and non-standardized rating scales for vection (Keshavarz et al. 2015a; Palmisano et al. 2015). These measures are retrospective, prone to recall bias, and may not capture the dynamic nature of the experience (Chang et al. 2023; Dennison et al. 2019). Questionnaire-based approaches are further compromised by social desirability bias, with meta-analytic evidence indicating that approximately 50% of questionnaire studies document effects of social desirability on their results (Weech et al. 2019).

For vection specifically, researchers have highlighted additional challenges. These include misreported onset latencies, difficulty obtaining real-time mea-

surements, susceptibility to experimenter influence, potential confusion with other sensations, and variability in confidence about capturing true self-motion perception (Palmisano et al. 2015). The lack of well-validated, objective measures capable of consistently identifying or characterizing vection experiences leads to substantial variability across subjects and studies (Berti et al. 2019; Palmisano et al. 2015). While alternative subjective measures including the Fast Motion Sickness Scale, Virtual Reality Sickness Questionnaire, and continuous rating methods have been developed (Keshavarz et al. 2011), they remain fundamentally limited by their subjective nature.

The field is hampered by significant methodological heterogeneity, a lack of standardized protocols and ground-truth labels, and frequent reliance on small, demographically-limited samples. This reliance on subjective reports creates a critical need for objective, real-time metrics to accurately track users' states and complement self-report measures (Kooijman et al. 2023; Palmisano et al. 2016). Electroencephalography (EEG) offers a promising avenue for such objective assessment. The following section introduces Brain–Computer Interfaces (BCIs) and EEG as the methodological basis for such objective monitoring.

I.6 Introduction to Brain–Computer Interfaces

I.6.1 What is a BCI? Definitions and scope

A brain–computer interface (BCI) measures brain activity and translates it, in real time, into functionally useful outputs. The term was first introduced by Jacques Vidal in the 1970s to describe the use of EEG signals for controlling external devices (Vidal 1973). For alignment with contemporary community consensus, we adopt the BCI Society's working definition:

Brain Computer Interface

A brain-computer interface is a system that measures brain activity and converts it in (nearly) real-time into functionally useful outputs to replace, restore, enhance, supplement, and/or improve the natural outputs of the brain, thereby changing the ongoing interactions between the brain and its external or internal environments. It may additionally modify brain activity using targeted delivery of stimuli to create functionally useful inputs to the brain.[a]

[a] https://bcisociety.org/bci-definition/

BCIs can enable hands-free interaction and provide access to users' cognitive state. This is particularly useful for individuals with motor impairments who lack alternative means of interacting with devices. In VR contexts, BCIs can detect cerebral states that are otherwise invisible to the system, such as motor intentions or mental fatigue. This dissertation leverages BCIs for passive monitoring to study the neurophysiological mechanisms underlying cybersickness and to develop objective detection methods that could enable adaptive VR systems.

I.6.2 How do we measure brain activity?

Different neuroimaging modalities offer distinct trade-offs in temporal precision, spatial resolution, portability, and suitability for VR applications:

Noninvasive, direct electrophysiology. Here, "noninvasive" means sensors remain outside the body, and "direct electrophysiology" means we measure neural electrical activity itself rather than a downstream proxy. It measures electrical brain activity using external sensors. Electroencephalog-

raphy (EEG) uses an array of electrodes (typically 4–128) placed on the scalp to detect electrical signals from cortical neurons, and was first demonstrated in humans by H. Berger (1929). It offers millisecond temporal resolution but limited spatial resolution due to volume conduction and signal blurring through the skull and scalp (Wolpaw et al. 2012). Rhythms are EEG components characterized by their frequency bands, they are conventionally categorized as delta (1–4Hz), theta (4–7Hz), alpha/mu (8–13Hz), beta (13–30Hz) and gamma (>30Hz). EEG systems are lightweight, portable, and relatively affordable, which facilitates use in VR applications. Magnetoencephalography (MEG) uses superconducting quantum interference devices (SQUIDs) housed in a helmet-like apparatus to measure the magnetic fields generated by neural electrical activity. MEG provides millisecond-scale temporal resolution with improved spatial localization relative to EEG, but requires participants to remain motionless within a magnetically shielded room and involves high system and operating costs, which constrain use in VR applications.

Noninvasive, indirect hemodynamics. Here, "noninvasive" again denotes sensors outside the body, while "indirect hemodynamics" indicates that neural activity is inferred from blood-flow and oxygenation changes rather than measured electrically. Functional near-infrared spectroscopy (fNIRS) uses lightweight scalp-mounted optical sensors to emit near-infrared light and quantify absorption differences between oxygenated and deoxygenated hemoglobin in underlying tissue, offering portability but seconds-level temporal resolution that limits detection of brief events. Functional magnetic resonance imaging (fMRI) employs strong magnetic fields (typically 1.5–7 T) in large cylindrical scanners to map blood-oxygenation changes throughout the brain, providing millimeter-scale spatial sampling but requiring participants to remain motionless within the scanner bore. The blood-oxygen-level–dependent (BOLD) response lags underlying neural activity by approximately 4–6 s, and sampling is constrained by the repetition time (TR), typically 0.5–2 s. This seconds-scale latency, together with substantial capital and operating costs, limits suitability for interactive VR.

Invasive electrophysiology. "Invasive" indicates surgically implanted sensors that contact neural tissue, and "electrophysiology" denotes direct measurement of neural electrical activity. It requires surgical implantation of recording devices directly on or within brain tissue. Electrocorticography (ECoG) uses electrode grids or strips placed directly on the brain surface during neurosurgical procedures, providing high signal-to-noise with high

Image source:
https://www.gtec.at/

EEG (scalp electrodes)[1]

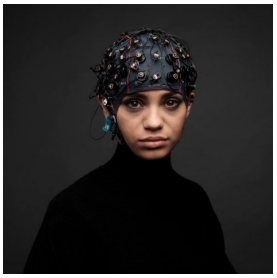

Image source:
https://www.gtec.at/

fNIRS (optical sensors)[1]

Image source:
https://www.ndcn.ox.ac.uk

fMRI (MRI scanner)[2]

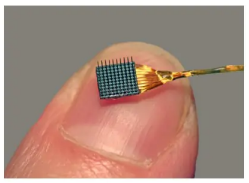

Image source:
https://brainlatam.com

ECoG (cortical grid)[3]

Figure 1.2: *Illustrative hardware for common brain measurement modalities: EEG uses scalp electrodes; fNIRS uses near-infrared optical sensors; fMRI uses a high-field magnetic resonance scanner; ECoG uses electrode grids on the cortical surface (invasive).*

spatial and temporal resolution. Intracortical recordings use microelectrode arrays inserted into brain tissue to record from individual neurons or small neural populations. Both approaches provide the highest signal quality but are limited to clinical populations undergoing neurosurgery, making them unsuitable for healthy-user VR studies.

Given our need to time-lock brain responses to brief VR events such as acceleration onsets, noninvasive EEG aligns with the requirements of this research.

I.6.3 BCI paradigms and signals

Within BCI research, systems are commonly grouped into active, reactive, and passive paradigms, which differ in whether brain activity is self-generated, stimulus-evoked, or opportunistically monitored (Si-Mohammed 2019):

Active BCIs require users to intentionally perform specific mental tasks, generating endogenous brain signals that are detected and translated into control commands. Such tasks include motor imagery, the mental rehearsal of movement (e.g., imagining hand or foot movement) without overt muscle activity; it modulates sensorimotor rhythms over corresponding cortical areas. Other commonly used tasks include mental arithmetic and word generation. These systems typically rely on spontaneous, self-generated neural activity

[1] Image source: `https://www.gtec.at/`
[2] Image source: `https://www.ndcn.ox.ac.uk`
[3] Image source: `https://brainlatam.com`

including sensorimotor rhythms and slow cortical potentials.

Reactive BCIs detect exogenous brain signals elicited in response to external stimuli. A neuromarker is a measurable feature of brain activity (e.g., a component, pattern, or spectral change) that is reliably associated with a specific sensory, cognitive, or motor process. Often, this signal is an evoked potential, a neuromarker that occurs in response to an external stimulus (Chiappa 1997). An event-related potential (ERP) is a type of evoked potential that occurs in response to a sensory, cognitive, or motor event. ERPs form a central class of neuromarkers for reactive BCIs (Cabestaing et al. 2016). Common reactive paradigms include the P300, a positive-going ERP component that typically occurs about 300 ms after an infrequent, task-relevant stimulus in an "oddball" sequence. Another reactive paradigm is the steady-state visually evoked potentials (SSVEPs), a periodic neural response elicited by flickering visual stimuli; the EEG response is phase-locked to the stimulus frequency and its harmonics.

Passive BCIs continuously monitor ongoing brain activity without requiring intentional control or specific tasks from the user (Zander et al. 2011). Instead, they infer the user's cognitive or affective state to adapt system behavior or improve human-computer interaction (Wolpaw et al. 2012). Passive BCIs have been applied to monitor cognitive workload, typically showing decreased alpha power and increased theta and delta activity under high load (Gevins et al. 2000). An error-related potential (ErrP) is a brief ERP that occurs when users perceive a mismatch or error in system behavior (e.g., after incorrect feedback); these responses can be leveraged to trigger corrective adaptation.

I.6.4 The BCI processing pipeline

BCI systems can be thought of as following a six-step pipeline (Mason et al. 2003): acquisition → preprocessing → feature extraction → classification → translation → feedback illustrated in Figure 1.3. Signal preprocessing typically includes filtering and artifact removal to improve signal quality (Wolpaw et al. 2012). Appropriate filter design is crucial for ERP studies, as improper filtering can introduce temporal smearing that distorts event-locked responses. Then spatial filtering techniques can find electrodes combinations of interest to improve signal-to-noise ratio (Wolpaw et al. 2012). Chapter 6 benchmarks these spatial filtering methods for enhancing acceleration-related ERPs in our VR paradigm.

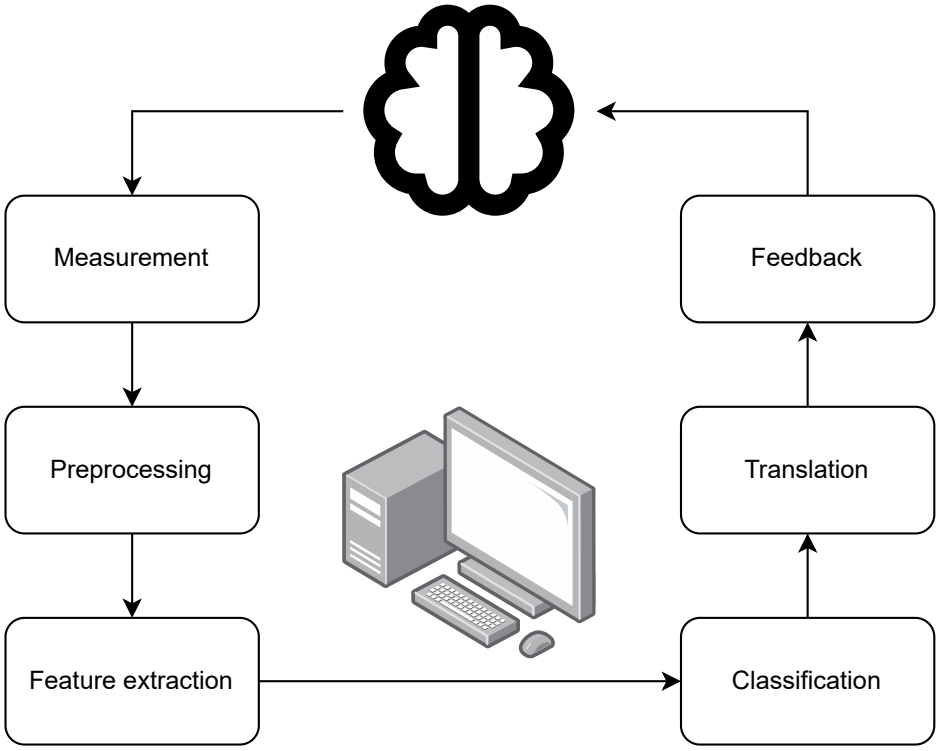

Figure 1.3: *Illustrative BCI processing pipeline (diagram by the author, conceptually based on Mason et al. (2003)): acquisition, preprocessing, feature extraction, classification, translation, and feedback.*

I.6.5 Choosing a modality

The general goal of this thesis is to study neuromarkers of user experience in VR. We advance the central hypothesis that specific VR events elicit distinct, event-locked neural responses that track the user's perceptual and physiological experience. This hypothesis motivates the line of work developed in this thesis and explains our methodological choices. Chapter 1 and Chapter 3 indicate a growing body of literature at the intersection of EEG, VR, cybersickness, and vection, but very limited work on evoked potentials specifically. Consequently, we adopt an event-locked perspective to test whether salient VR events produce reliable neural signatures. In particular, acceleration onsets and vection transitions are brief, well-defined events whose detection benefits from millisecond-precise measurements. Event-related potentials (ERPs) are well suited for uncovering such time-locked responses.

Within this context, EEG emerges as an appropriate modality for conduct-

ing ERP based experiments in VR settings. It is noninvasive, portable, and compatible with head-mounted displays, while offering millisecond temporal resolution necessary to resolve event onset and component latency. By contrast, fNIRS provides seconds-level temporal resolution that limits detection of sub-second responses, and MEG/fMRI impose practical and ecological-validity constraints in immersive VR settings. Invasive approaches like ECoG are not appropriate for healthy-user VR studies.

Accordingly, we adopt EEG and ERPs to test this hypothesis throughout the thesis. The subsequent chapters pursue and evaluate this claim, leveraging the synthesis in Chapter 2 and Chapter 3 to motivate and contextualize event-locked analyses in VR.

I.6.6 From BCIs to cybersickness

Designing VR-ready BCIs for monitoring and adaptation requires specifying what the system should detect, how that state is currently measured, and under what conditions it emerges. For cybersickness, this entails clarifying proposed mechanisms, operational measures and labels, and the neurophysiological markers reported to date. Reports of spectral changes (e.g., low-frequency increases and alpha decreases) and emerging ERP-based approaches suggest multiple promising directions (Krokos et al. 2022). Yet the literature remains heterogeneous in stimuli, hardware, and methods, complicating synthesis and translation to practice.

Accordingly, we begin with a systematic review of EEG and cybersickness to establish the current state of knowledge, identify robust markers, and surface methodological gaps. This sets the stage for subsequent chapters that build toward event-locked investigations (including vection) and signal-processing methods suited for VR.

I.7 Research Aims

Having established the conceptual and methodological foundations, we now outline the aims and key contributions of this dissertation. This dissertation pursues three concrete aims to advance the understanding and detection of cybersickness.

1. Map the research landscape of BCIs, cybersickness, and vection, including neural markers, algorithms, and methodologies.

2. Explore potential neuromarkers for understudied aspects of cybersickness and acceleration perception.
3. Contribute to better identification of VR user experience markers suitable for adaptive applications.

The research is conducted within the framework of GENESIS, a European research project that includes the Centre de Recherche en Informatique, Signal et Automatique de Lille in France, the Centre de Recherche Inria Rennes - Bretagne Atlantique, ETH Zurich, KOÇ UNIVERSITY's Intelligent User Interfaces Laboratory, and University of Essex. GENESIS (LeveraGing nEuromarkers for Next-gEn immerSIve Systems) is focused on improving virtual reality experiences using brain-computer interface methods. It is funded by Horizon Europe within the European Innovation Council's Pathfinder programme through the CHIST-ERA consortium. This dissertation uses EEG-based passive BCIs to study and detect vection- and acceleration-related processes that underlie cybersickness, and proposes signal-processing and protocol advances to enable objective, real-time detection. By leveraging neurophysiological markers, the GENESIS project aims to enable the next generation of virtual reality systems.

This dissertation contributes novel findings and methodological advances across multiple domains of passive BCI research for virtual reality applications. The contributions include two systematic literature reviews synthesizing current knowledge on BCI correlates of cybersickness and EEG correlates of vection. We discovered novel neuromarkers associated with acceleration and its direction, including a significant difference between perceived forward and backward acceleration. We identified a novel event-related potential of vection. Methodological contributions identify a filter for enhancing acceleration-related ERPs.

Ethical approval was obtained with special attention given to informing participants that they could withdraw should they experience cybersickness, and written informed consent was obtained from all participants. Given the heterogeneity in stimuli, hardware, and protocols that poses a threat to replicability and impedes cumulative progress in this evolving field, the following chapters present systematic reviews to establish the current state of knowledge and identify gaps that justify the empirical investigations that follow.

I.8 Dissertation Structure

This dissertation follows a structured progression from foundational reviews to empirical investigations and methodological advances:

- Chapter 2: synthesizes BCI–cybersickness literature to map neuromarkers and methodological gaps. Pending publication as *The Neurophysiology of Cybersickness: A Review of BCI-based Characterization and Prediction*.
- Chapter 3: reviews EEG correlates of vection to identify consistent spectral/ERP patterns. Published as *EEG Correlates of Vection: A Systematic Literature Review*.
- Chapter 4: experimental EEG–VR paradigm and methodology for studying acceleration and vection perception.
- Chapter 5: demonstrates ERP markers of acceleration perception in VR as a mechanistic step toward objective monitoring. Published as *EEG Markers of Acceleration Perception in Virtual Reality*.
- Chapter 6: introduces a vection-locked ERP (P600) linking subjective vection to time-locked neural responses. Pending publication as *Towards the Automatic Detection of Vection in Virtual Reality Using EEG*.
- Chapter 7: benchmarks spatial filters (CSP, EMS, xDAWN) to enhance acceleration-related ERPs. Published as *Enhancing Detection of Acceleration-Related ERPs using Spatial Filtering Techniques*.
- Chapter 8: integrates findings across chapters, relating mechanisms and methods to cybersickness mitigation.
- Chapter 9: concludes with overarching contributions and outlines future research opened by this work.
- Appendix A: In the annex, we explore potential future research directions with the PECS protocol, investigating sensorimotor conflicts with physical motion in VR (pilot stage; not yet published).

The PECS protocol appears after the conclusion as an annex as data collection and analysis are ongoing. This dissertation follows a compilation format where published papers are inserted as standalone chapters (except for Chapter 4, which describes the experimental methodology), each preceded by a contextualization section that situates the chapter within broader research

objectives and explicitly states changes from the published version to maintain transparency regarding peer-reviewed content.

Chapter 2

State of the Art on BCIs and Cybersickness research

> *Verum et factum convertuntur*
> *The truth and the made are reversible*
>
> — Giambattista Vico

Prelude — *This chapter, except for the abstract, the Introduction, the entire subsection on The Etiology of Cybersickness within the Theoretical and Methodological Background section, the condensed objectives statement, the transition sentence introducing the Theoretical and Methodological Background section (all covered in the Introduction), and the final two paragraphs of section 2.5, was submitted as "The Neurophysiology of Cybersickness: A Review of BCI-based Characterization and Prediction" and is currently under review at the IEEE Transactions on Visualization and Computer Graphics journal.*
Paragraphs in italics were added to improve readability.

Before conducting empirical research, we begin with a summary of the current state of knowledge in the field. This chapter provides a systematic literature review of research at the intersection of Brain-Computer Interfaces and cybersickness, examining how neuroimaging approaches, particularly EEG, have been employed to characterize, predict, and mitigate cybersickness. Extending the contextual background established in the Introduction, this

chapter focuses on methodological approaches and empirical findings from BCI applications.

2.1 Introduction

Having established cybersickness as a barrier to VR adoption, this chapter synthesizes current knowledge on using Brain-Computer Interfaces to characterize and predict cybersickness. Since related terms are often used interchangeably, we consider findings across studies referring to cybersickness, visually induced motion sickness, simulator sickness, and motion sickness, where relevant.

2.1.1 Neuroimaging Modalities for Cybersickness Research

While cybersickness assessment has traditionally relied on subjective measures such as questionnaires, the need for objective, real-time metrics has driven researchers toward neuroimaging approaches to measure corresponding brain activity. Electroencephalography (EEG) is the most widely adopted modality in the reviewed literature. Its principal advantages are its excellent temporal resolution, allowing for the tracking of rapid changes in neural dynamics, its portability, which facilitates studies in mobile and interactive VR paradigms (Cortes et al. 2023a; Krokos et al. 2022), as well as its relative affordability. Functional Near-Infrared Spectroscopy (fNIRS) is an emerging optical imaging technique that measures hemodynamic changes in superficial cortical blood flow. It offers greater portability and robustness to motion artifacts than Functional Magnetic Resonance Imaging (fMRI), making it suitable for cybersickness research involving movement (Yamamura et al. 2021; C. Zhang et al. 2020). However, its depth sensitivity remains limited and its temporal resolution is orders of magnitude lower than that of EEG because it reflects slower vascular responses rather than rapid neural dynamics. Finally, fMRI provides unparalleled spatial resolution, enabling the precise localization of activity in both cortical and subcortical structures. However, it also has a lower temporal resolution and requires the subject to be immobile, which can be problematic for the study of cybersickness. Despite these limitations, fMRI has been instrumental in identifying the core brain networks underlying nausea and sensory integration, such as the insular and cingulate cortices (Napadow et al. 2013; Toschi et al. 2017).

2.2 Review Methodology

2.2.1 Search Strategy

A systematic literature search was conducted on March 27, 2025, to identify all relevant peer-reviewed articles. The search was performed across three major academic databases: PubMed, Web of Science, and Scopus. No date restrictions were applied to ensure a comprehensive historical overview of the field. The following search query, designed to capture studies at the intersection of BCI and cybersickness, was utilized:

```
(Brain Computer Interface OR EEG OR electroencephalogram OR
   neuromarkers OR MEG OR fMRI OR ECoG OR fNIRS)
AND
(Cybersickness OR ((virtual reality OR VR) AND motion sickness
   ) OR simulator sickness OR visually induced motion sickness
    OR Virtual Reality Motion Sickness)
```

2.2.2 Study Selection and Eligibility Criteria

The initial search yielded a total of 360 articles. Following the removal of 119 duplicate entries, 241 unique records remained for screening. This systematic review was conducted in accordance with the Preferred Reporting Items for Systematic Reviews and Meta-Analyses (PRISMA) 2020 statement, an evidence-based guideline for transparent and complete reporting. This framework enables readers to appraise the review's methodological quality and to ensure the reproducibility of the search and selection strategy. The full selection process is detailed in the PRISMA flow diagram (Figure 2.1).

Each of the 241 records underwent a manual screening process based on titles and abstracts to assess relevance according to predefined eligibility criteria. The inclusion criteria for this chapter were as follows:

- The study employed a neuroimaging or BCI methodology (e.g., EEG, fMRI, fNIRS) to measure brain activity.
- The study focused on cybersickness or a closely related term (e.g., VIMS, simulator sickness) within a VR or simulated environment.
- The study presented original empirical data from a human-subject study.

Conversely, articles were excluded if they met any of the following criteria:

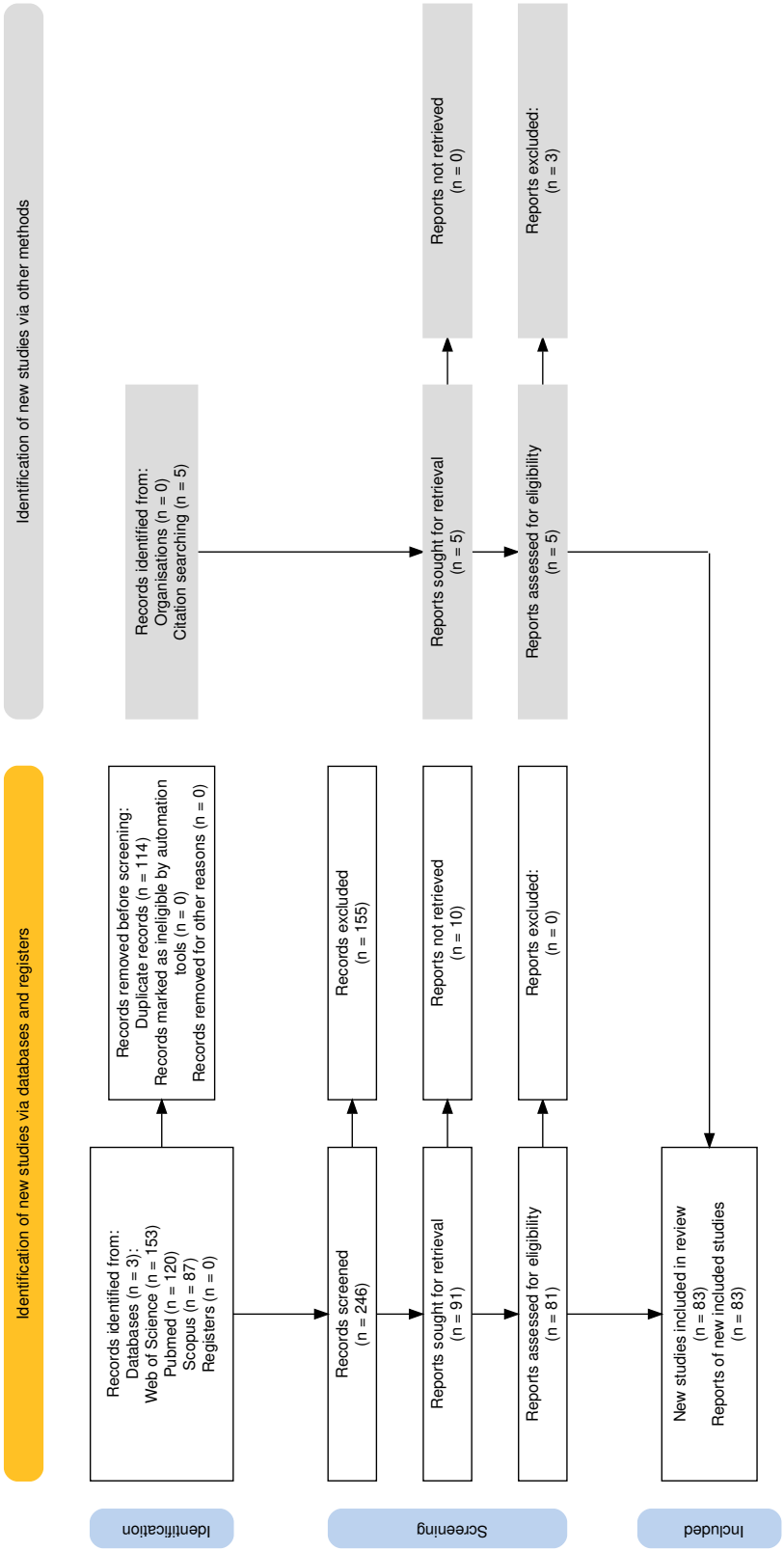

Figure 2.1: *PRISMA flow diagram illustrating the study identification, screening, eligibility, and inclusion process.*

- The work was non-empirical, such as literature reviews, meta-analyses, editorials, letters, or conference abstracts without a corresponding full paper.
- The full text of the article was unobtainable.

This screening process resulted in the exclusion of 155 articles, leaving 91 for full-text assessment. An additional two relevant articles were identified through manual citation searching and included. Of these 93 articles, 10 were subsequently removed due to the unavailability of their full text. This resulted in a final corpus of 83 peer-reviewed articles for detailed analysis.

The exclusion of these ten records was due to their appeareance in journals or conference proceedings owned by publishers such as Springer, World Scientific, and IEEE, for which the University of Lille does not currently hold specific subscription licenses. Secondary attempts to locate author-archived versions on repositories such as ResearchGate proved unsuccessful, as only metadata entries were available without the accompanying full text. Consequently, we restricted our final analysis to the corpus where full content could be found.

2.2.3 Data Extraction and Thematic Synthesis

For each of the 83 included articles, a structured data extraction process was performed to systematically capture and catalogue key information. This process was guided by a predefined protocol designed to ensure consistency and facilitate subsequent comparison and synthesis. The following data points were extracted from each paper:

1. **Summary of Contribution:** A concise summary of the study's primary objective and its main contribution to the field of BCI-based cybersickness research.
2. **Cybersickness Measurement:** The methods used to measure or label cybersickness, distinguishing between subjective questionnaires (e.g., SSQ, FMS) and objective physiological or behavioral metrics (e.g., galvanic skin response, postural sway).
3. **BCI Methodology:** A detailed breakdown of the neuroimaging pipeline, including: (a) the measurement modality (e.g., EEG, fMRI), (b) the key feature extraction techniques (e.g., power spectral density, event-related potentials, functional connectivity), and (c) the primary analysis or classification methods (e.g., statistical tests, machine learning models).

4. **Theoretical Framework:** The explicitly stated or implicitly assumed theory of cybersickness (e.g., Sensory Conflict, Postural Instability) that guided the study's design or interpretation of results.
5. **Quantitative Performance:** Reported performance measures, such as classification accuracy, correlation coefficients (e.g., PLCC, SROCC), root mean square error (RMSE), or statistical significance values.
6. **Empirical Study Details:** For empirical studies, specific details of the experimental protocol, including the VR environment, display hardware, cybersickness-inducing stimulus, and the number of human subjects.
7. **Reported Shortcomings:** Any limitations, caveats, or weaknesses explicitly identified by the authors or apparent from the study's design.

Following data extraction, a quantitative analysis was conducted to structure the review and identify overarching trends, methods, and results. To facilitate this synthesis, each paper was assigned to a primary research objective category. An initial set of objective categories was defined *a priori* based on established research paradigms in the field. This set was iteratively refined during the data extraction process to accurately capture the full spectrum of research goals present in the literature. The final categories, which form the organizational structure of the subsequent results section, include: Classification (Binary, Likert, Continuous), Correlates (e.g., Brain Regions, Rhythms, Physiological), Mitigation (A/B Testing, Real-time), User Differences, Dataset Provision, Recovery, and studies on the Effects of Cybersickness on other cognitive or performance metrics.

2.3 Results

The selected studies address several distinct objectives, which we categorize as follows. These include: (1) Observed study characteristics, (2) the identification of neurophysiological and physiological correlates of the cybersickness state; (3) the development of computational models for the classification and prediction of sickness; (4) the characterization of neurophysiological factors underlying individual susceptibility; (5) the testing of BCI-driven mitigation and intervention strategies; and (6) ancillary investigations encompassing recovery dynamics, dataset contributions, cognitive performance effects, and hardware-specific neural response patterns. The research demonstrates temporal evolution in research focus, with early investigations concentrating pri-

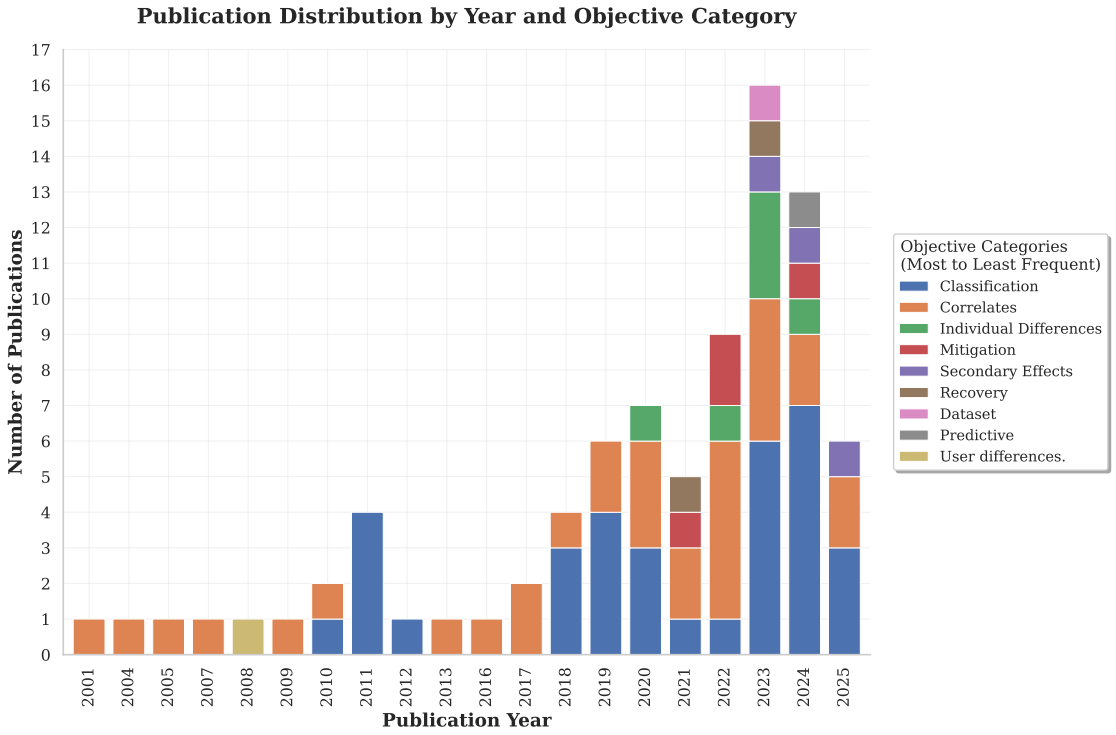

Figure 2.2: *Distribution of reviewed papers by year and research objective category*

marily on correlates and classification of cybersickness, while recent research has diversified into additional fields of study, as illustrated in Figure 2.2.

The following section synthesizes the findings from this literature, structured thematically according to these primary research objectives.

2.3.1 Study Characteristics

The synthesis encompasses 83 empirical studies spanning from 2001 to 2025, with a notable acceleration in research activity observed in recent years: 59.0% of studies were conducted from 2021 onwards. The total participant population across all investigations comprises 2213 individuals, with studies employing a mean of 26.7 ± 25.7 participants per investigation (median: 20, range: 6-202). Age demographics show a mean of 24.0 ± 2.3 years (median: 23.7, range: 20.4-29.9) across the 49 studies that reported participant age, reflecting a predominant focus on young adult populations. An overview of age distributions across all studies is presented in Figure 2.5.

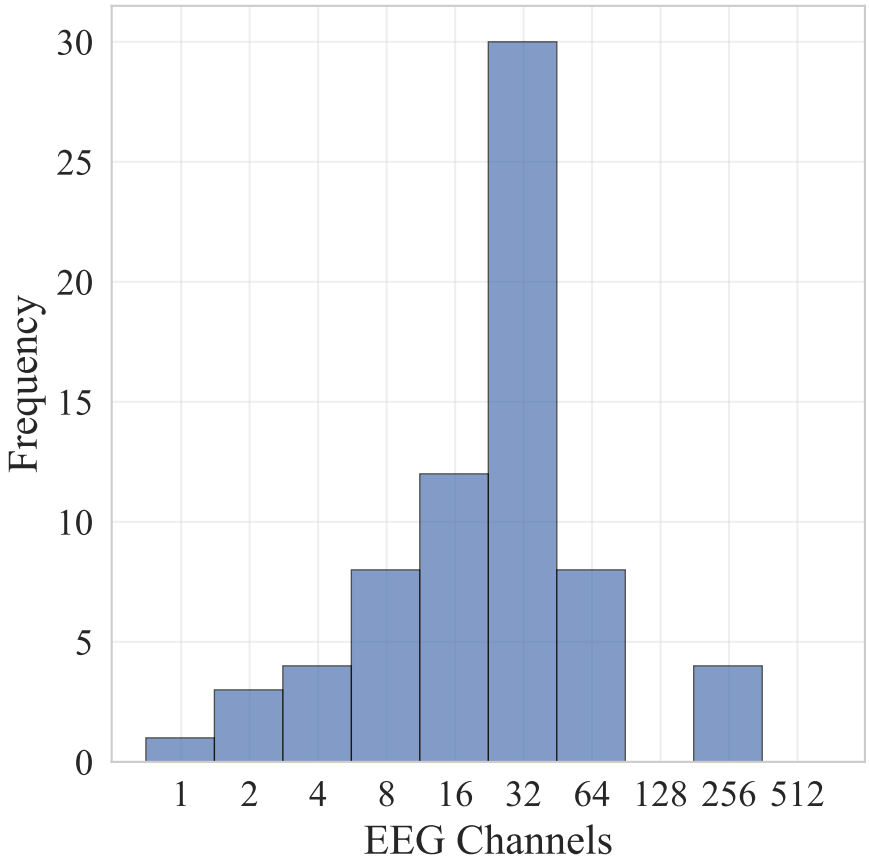

Figure 2.3: *Distribution of EEG channel configurations across cybersickness studies*

Neuroimaging and Physiological Recording Modalities

EEG represents the predominant neuroimaging modality, employed in 89.2% of studies (74 of 83), followed by fNIRS at 6.0% (5 studies) and fMRI at 4.8% (4 studies). EEG configurations demonstrate substantial variability, with a mean of 38.9 ± 56.4 channels (median: 30, range: 1-256). The distribution reveals a predominance of standard montages, with the most frequently employed configurations including 32-channel (21 studies), 14-channel (7 studies), 64-channel (7 studies), 256-channel (4 studies), and 30-channel (4 studies) setups. A visual representation of the distribution of EEG channel configurations across studies is presented in Figure 2.3.

Beyond primary neuroimaging modalities, studies frequently incorporate additional physiological measurements. Multi-modal approaches are employed in 55.4% of investigations, with electrocardiography (ECG) being the most common supplementary modality (15.1% of studies), followed by joystick input (12.8%) and head tracking (11.6%). Other recorded signals include galvanic

skin response (GSR) (8.1%), electrooculography (EOG) (8.1%), eye tracking (5.8%), photoplethysmography (PPG) (4.7%), skin temperature (4.7%), electrogastrography (EGG) (3.5%), button box (3.5%), heart rate monitor (3.5%), and respiration monitor (3.5%). Additional modalities encompass motion capture systems (2.3%), blood pressure monitor (2.3%), balance board (2.3%), and various other devices including Kinect, pulse oximeter, electromyography (EMG), keyboard, force plate, mouse, and accelerometer (each 1.2%).

Experimental Design and Data Collection Protocols

Study designs predominantly employ within-subject comparisons (75.9%), with 7.2% employing between-subject designs exclusively, and 16.9% utilizing both within-subject and between-subject approaches. Session protocols demonstrate considerable variation, with the majority implementing single-session designs and the remainder conducting multiple sessions (mean: 1.4 ± 0.8 sessions, range: 1-4). Experimental sessions last a mean of 49.8 ± 34.9 minutes (median: 48.5, range: 2-180), while cybersickness-inducing stimulus exposure durations average 17.2 ± 17.8 minutes (median: 10.0, range: 0-90).

Virtual reality exposure is delivered through head-mounted displays in 56.0% of studies, screen-based displays in 15.5%, projection systems in 19.0%, other configurations in 6.0%, and television displays in 3.6%. Virtual environments encompass navigation tasks (24.4%), driving simulations (20.0%), video content (15.6%), roller coaster experiences (13.3%), games (7.8%), and other scenarios (16.7%). The relationship between VR device types and virtual environments is illustrated in Figure 2.6.

Cybersickness Assessment Methods

Cybersickness measurement employs questionnaire-based approaches in 67.0% of studies, continuous rating methods in 17.6%, Likert scale assessments in 8.8%, and other methodologies in 6.6%. The Simulator Sickness Questionnaire (SSQ) represents the predominant assessment instrument, utilized in 63.4% of studies, followed by the Fast Motion Sickness Scale (FMS) (9.8%) and Motion Sickness Susceptibility Questionnaire (MSSQ) (4.9%). Continuous input mechanisms include joystick-based ratings (48.0% of continuous studies), other methods (44.0%), and keyboard input (8.0%).

Data Processing and Signal Analysis

EEG signal preprocessing demonstrates considerable heterogeneity across studies in terms of filtering approaches and frequency ranges. Band-pass filtering is employed across a wide spectrum of frequency ranges, from very low frequencies (0.01 Hz) to high gamma ranges (100 Hz), with the majority of studies applying filters in the 1-50 Hz range. The distribution of band-pass filter configurations across studies is presented in Figure 2.4, illustrating the substantial variability in preprocessing approaches employed in the literature.

2.3.2 Neural and Physiological Correlates of Cybersickness

A primary objective across a substantial portion of the literature has been to identify objective, physiological markers that co-vary with the subjective experience of cybersickness. This research addresses the question of what physiological changes occur when a user becomes sick. The studies have identified a set of neural and physiological correlates, which form the basis for the development of predictive models.

EEG Spectral Power and Connectivity

The most frequently reported neural signature of cybersickness is a modulation of EEG spectral power. Across numerous studies employing diverse VR stimuli and hardware, a pattern emerges characterized by an increase in low-frequency power and a corresponding decrease in alpha-band activity. Quantitative analysis across studies examining specific brain rhythms reveals patterns accross the literature. Delta rhythm changes show increases in 79.3% of studies, decreases in 10.3%, mixed findings in 6.9%, and no change in 3.4%. Theta rhythm investigations report increases in 73.3% of studies, with decreases in 13.3%, mixed results in 10.0%, and no change in 3.3%. Specifically, an increase in power within the delta (1-4 Hz) and theta (4-8 Hz) frequency bands has been associated with the onset and increasing severity of CS (Andrievskaia et al. 2023; Jang et al. 2022; Y. Y. Kim et al. 2005; Krokos et al. 2022; Nürnberger et al. 2021). Concurrently, a commonly observed phenomenon is a suppression of power in the alpha band (8-13 Hz), particularly over central, parietal, and occipital cortices (Chen et al. 2010; Cortes et al. 2023a; Y. Kim et al. 2001). Alpha rhythm findings demonstrate greater variability, with 45.7%

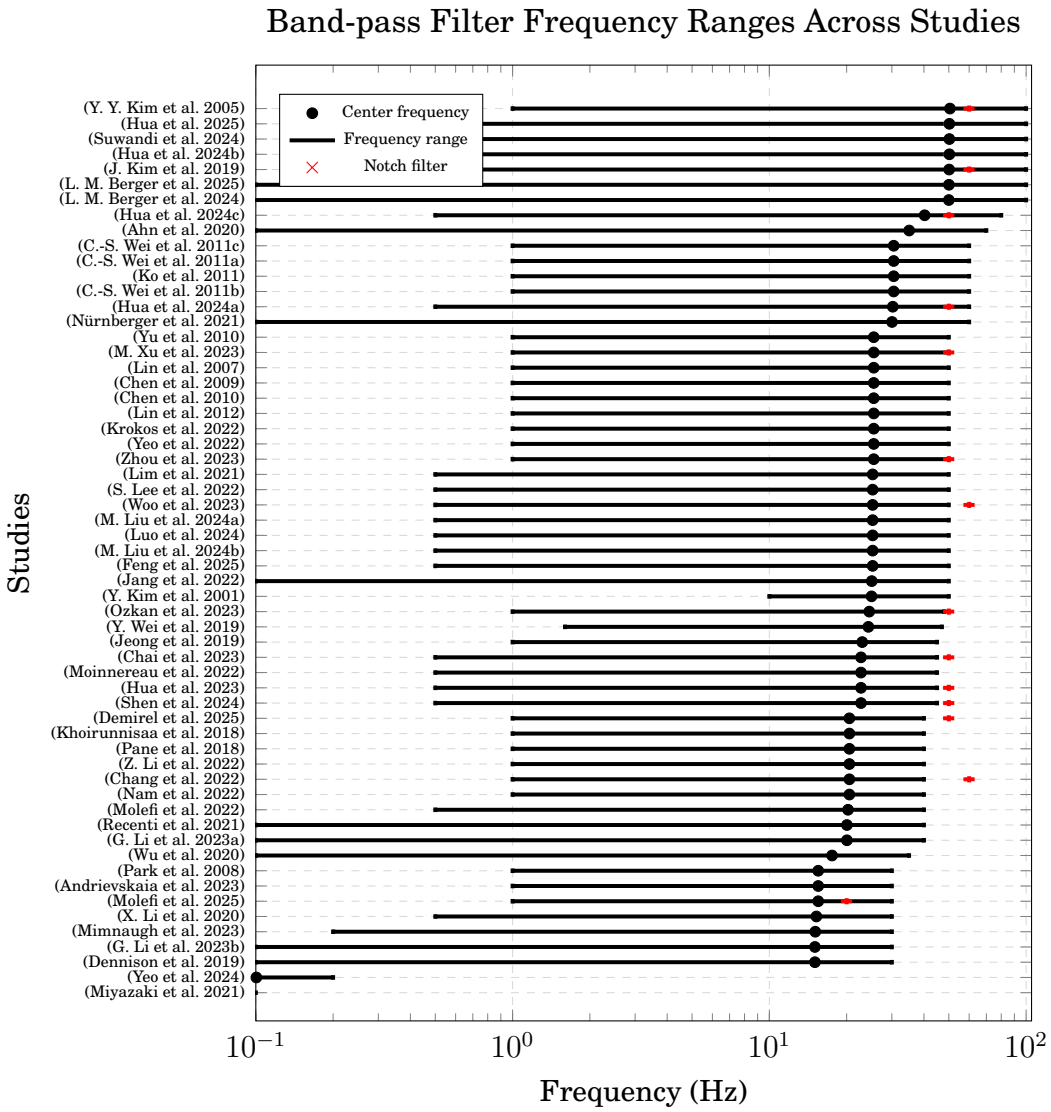

Figure 2.4: *Band-pass filter frequency ranges across studies showing center frequency (black dots) with frequency ranges (black error bars) and notch filter frequencies (red crosses). The frequency range shows the low and high cutoff frequencies of the band-pass filters, while red crosses indicate notch filter frequencies used to remove specific interference (e.g., 50 / 60 Hz power line noise).*

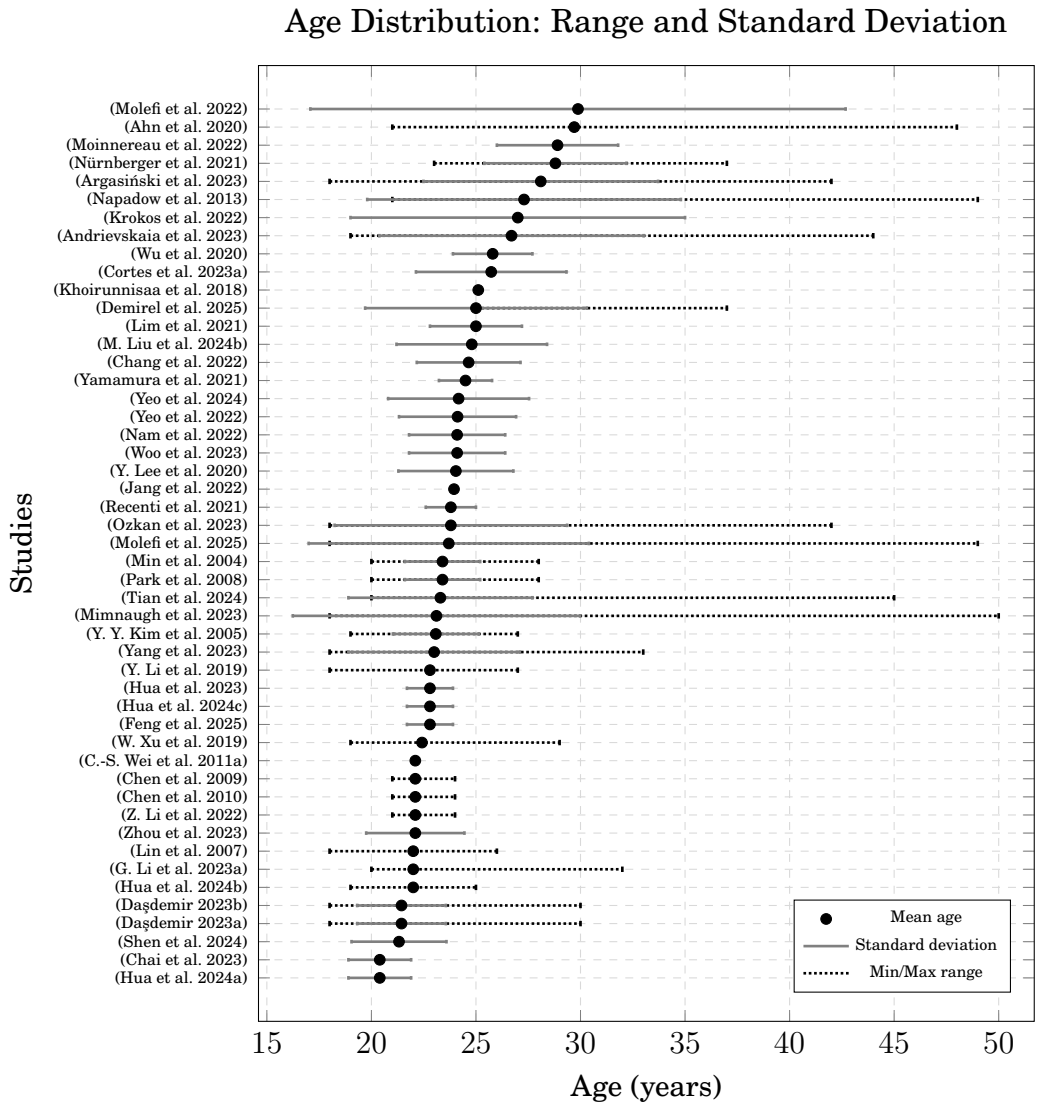

Figure 2.5: *Age distribution across studies showing mean age (black dots) with age ranges (dotted black error bars) and standard deviations when available (solid gray error bars). The age range shows the minimum and maximum participant ages, while the standard deviation shows the typical spread around the mean age.*

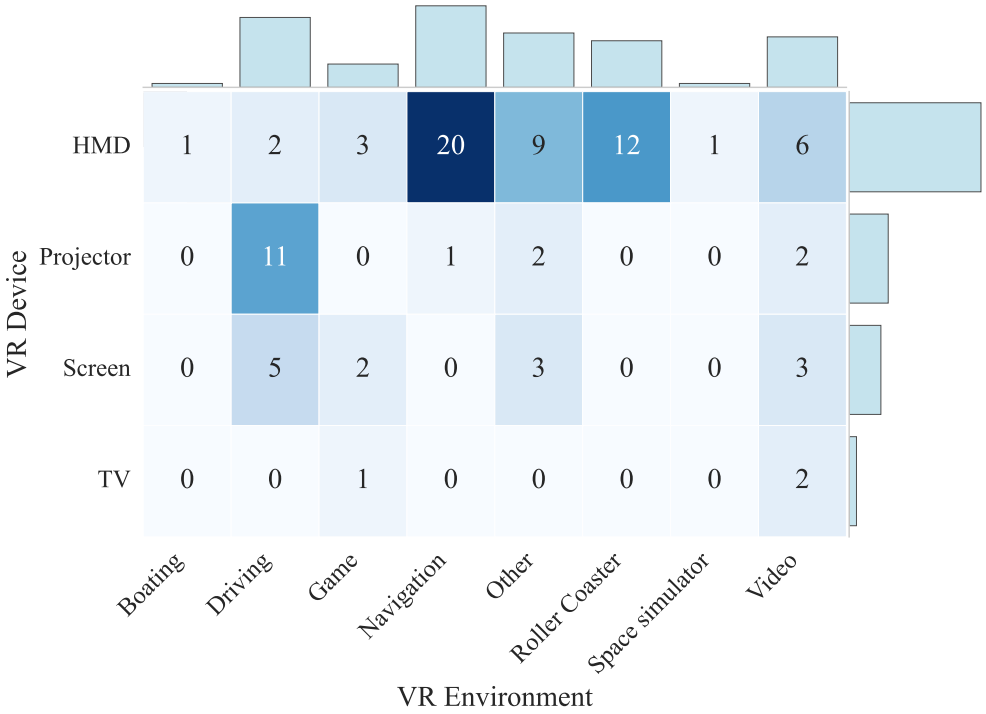

Figure 2.6: *Heatmap of the distribution of VR device types and virtual environments across studies. Studies employing multiple devices or environments contribute towards each.*

reporting increases, 31.4% showing decreases, 14.3% presenting mixed results, and 8.6% finding no change. This alpha suppression is often interpreted as a marker of increased cognitive load, potentially reflecting the brain's attempt to manage sensory conflict or maintain postural control (Cortes et al. 2023a). While less consistent, changes have also been reported in higher frequency bands, with some studies noting decreases in beta power (Y. Y. Kim et al. 2005) and others reporting increases (Suwandi et al. 2024) or its utility for channel selection (Khoirunnisaa et al. 2018). Beta rhythm studies show increases in 41.4% of investigations, no change in 24.1%, decreases in 24.1%, and mixed findings in 10.3%. Gamma rhythm research reports increases in 40.0% of studies, no change in 33.3%, decreases in 20.0%, and mixed results in 6.7%. A comprehensive analysis of rhythm changes across different brain regions is presented in Figure 2.7. The test-retest reliability of these spectral markers has been formally assessed, with one study demonstrating good reliability for delta, theta, and alpha power changes in frontal and central areas across multiple sessions (Lim et al. 2021).

Furthermore, the normalization of delta wave power has been shown to serve as an objective marker for the dissipation of symptoms during the

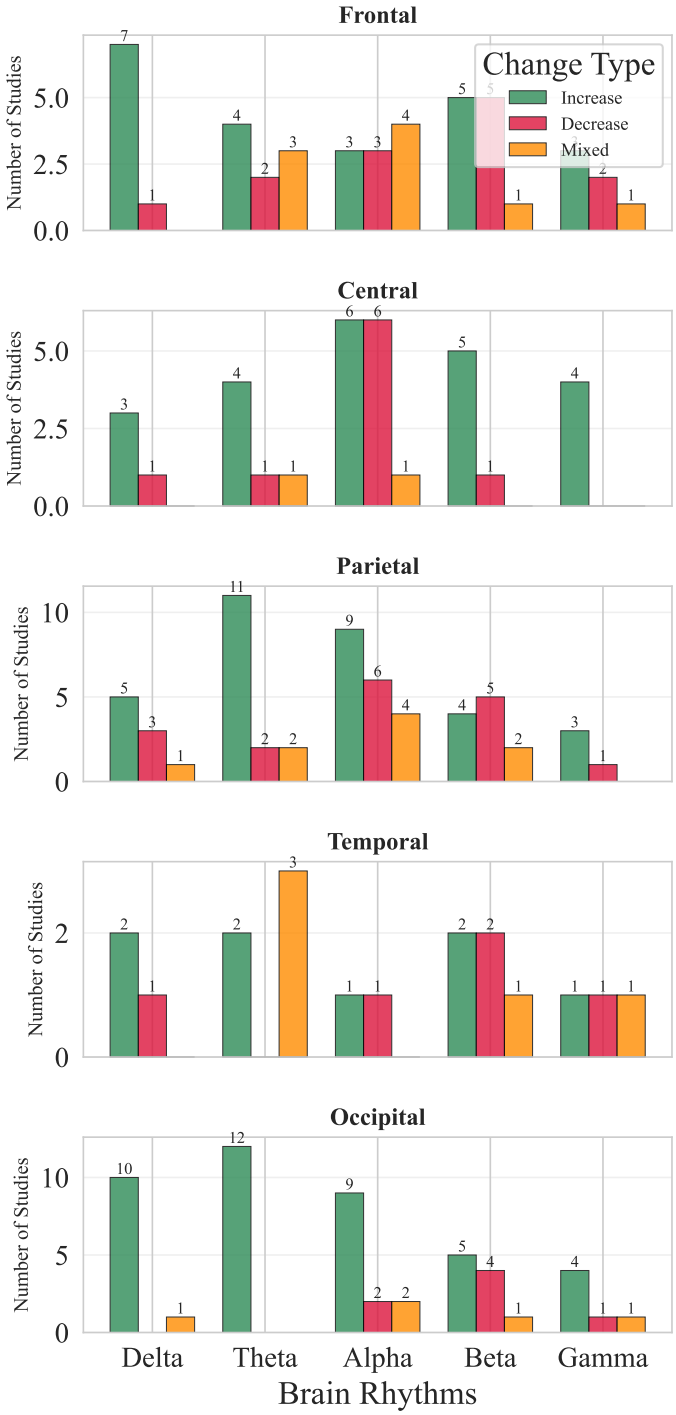

Figure 2.7: *Brain rhythm changes across anatomical regions during cybersickness*

recovery phase (Woo et al. 2023).

In addition to band power, researchers have explored more complex features derived from the EEG signal. These include metrics such as spectral entropy and skew (Feng et al. 2025), Gravity Frequency, and Kolmogorov Com-

plexity (R. Liu et al. 2017, 2020), as well as amplitude modulation features, which one study identified as significant for CS characterization (Rosanne et al. 2025). Others have used the mean frequency of the theta band as a direct indicator of motion sickness level (Z. Li et al. 2022). Investigations into functional connectivity provide information on more systemic CS-related brain dynamics. Functional connectivity investigations reveal mixed findings in 56.2% of studies, increases in 18.8%, decreases in 18.8%, and no change in 6.2%. One finding is a general decrease in information transfer, measured via transfer entropy, with the onset of VIMS (Nürnberger et al. 2021). More specifically, studies using EEG microstate analysis have shown that CS alters the temporal dynamics of canonical brain networks and is associated with decreased functional connectivity between the visual cortex (V5) and vestibular processing regions (Nam et al. 2022). Connectivity-based features are also used as direct inputs for deep learning models, often based on metrics like the Phase-Locked Value (PLV) (Hua et al. 2025; Shen et al. 2024). The causal relevance of these spectral patterns is suggested by intervention studies where symptom mitigation correlates with a normalization of these same EEG bands (Molefi et al. 2022; Yeo et al. 2022).

Hemodynamic and Regional Brain Activity (fNIRS & fMRI)

EEG offers high temporal resolution, whereas fMRI and fNIRS provide high spatial localization, identifying the specific brain regions involved in the cybersickness experience. fNIRS and fMRI each represent 4.8% of studies, reflecting their complementary but less prevalent role compared to EEG-based investigations. fMRI studies have delineated a “nausea network”. One study dissociated the temporal evolution of nausea, identifying a network including the amygdala and putamen that was active preceding a transition to stronger nausea, and a broader network including the insular, anterior cingulate, and orbitofrontal cortices that was active following the transition (Napadow et al. 2013). Furthermore, motion sickness has been shown to increase the functional connectivity between the visual motion processing area (MT+/V5) and nausea-associated regions like the insula and mid-cingulate cortex (Toschi et al. 2017). The involvement of this network is highlighted by findings that its functional connectivity is also modulated during the post-exposure recovery phase (Miyazaki et al. 2021). This central processing has been linked to peripheral physiology, with activity in distinct brain networks correlating with sympathetic and parasympathetic autonomic outflow during nausea (Sclocco

et al. 2014).

fNIRS studies, which offer greater portability, have corroborated and extended these findings. Research using fNIRS has identified deactivation in the bilateral angular gyrus (Yeo et al. 2024) and activation changes in the occipital lobe (C. Zhang et al. 2020) and parieto-temporal regions (Gavgani et al. 2018) that correlate with subjective sickness scores. Others have linked an increase in total hemoglobin concentration directly to cybersickness (Ren et al. 2023; Yamamura et al. 2021). This body of work indicates a complex hemodynamic response, with evidence for both increased regional perfusion in some cortical areas and a decrease in global cerebral perfusion during cybersickness episodes (Gavgani et al. 2018).

Event-Related Potential (ERP) and Evoked Potential

Beyond ongoing oscillations, a subset of studies has used ERPs to probe how cybersickness impacts discrete cognitive processes. These studies indicate that cybersickness is accompanied by measurable changes in cognitive function. One finding is that VR sickness is associated with a reduction in the amplitude of the P3b component in a dual-task paradigm, a classic marker of diminished attentional resources (Mimnaugh et al. 2023). Relatedly, VIMS has been shown to impair response inhibition, as reflected by a larger N2 amplitude and a smaller, delayed P3 component in an oddball task (Wu et al. 2020). Other work has shown that trait-like susceptibility to cybersickness is associated with distinct baseline ERP characteristics, such as excessive N2 amplitudes (Y. Wei et al. 2019) and higher P3 amplitudes during sensory mismatch conditions (Ahn et al. 2020). An approach using heartbeat-evoked potentials (HEPs) has linked the subjective experience of disorientation to a significant suppression of fronto-central HEP amplitudes, providing a potential link between interoceptive processing and a key symptom of cybersickness (Chang et al. 2022).

Other Physiological Correlates

Many studies have adopted a multimodal approach, recording other physiological signals alongside neuroimaging data. This work indicates that cybersickness is a whole-body phenomenon. Electrogastrography (EGG) has been identified as a measure for detecting nausea-specific symptoms (Tian et al. 2024). Measures of autonomic nervous system arousal, such as heart

rate variability (HRV) and galvanic skin response (GSR), are also consistently modulated by cybersickness and have been integrated into predictive models (S. Lee et al. 2022; Sameri et al. 2024; Sclocco et al. 2014). In a study that integrated VR with a motion platform, electromyography (EMG) signals were reported to be more informative for classifying motion sickness than the concurrently recorded EEG signals (Recenti et al. 2021). Finally, electrooculography (EOG) has been used to show that an increased eye blink rate correlates with subjective cybersickness reports (Moinnereau et al. 2022).

2.3.3 Classification and Prediction of Cybersickness

A substantial body of research has focused on using the previously identified neural correlates to automatically classify or predict a user's cybersickness state. This line of inquiry seeks to determine if these physiological changes can be reliably detected and quantified by computational models. The research objective is to develop objective, real-time assessment systems that can operate continuously and implicitly during VR use. Analysis of computational approaches across the literature reveals that deep learning architectures are employed in 15 studies (34.1%), traditional machine learning classifiers in 14 (31.8%), regression models in 13 (29.5%), thresholding in 1 (2.3%), and unsupervised approaches in 1 (2.3%). We defined statistical and correlational analysis as studies that identify and validate statistically significant relationships between physiological signals and cybersickness without building predictive models, including methods such as t-tests, ANOVA, and correlation analyses. Traditional machine learning was defined as studies employing established algorithms with engineered features for discrete state classification, including Support Vector Machines, Linear Discriminant Analysis, and k-Nearest Neighbors. Deep learning encompasses studies utilizing multi-layered neural networks for automatic feature learning from raw data, including Convolutional Neural Networks, Recurrent Neural Networks, and hybrid architectures. Regression models were defined as studies predicting continuous cybersickness severity values using methods such as Support Vector Regression and linear regression approaches. The distribution of these classification approaches is illustrated in Figure 2.8, with detailed breakdowns of specific methods within each category shown in Figure 2.9. Additionally, 55.4% of studies adopt multi-modal approaches, combining EEG with other physiological measurements. The most common additional modalities are

Electrocardiography (ECG) and Head tracking, which are used in 15.1% and 11.6% of studies, respectively. Model validation strategies predominantly employ k-fold cross-validation (65.7%), with additional approaches including train-test splits (14.3%), other methods (11.4%), and leave-one-subject-out cross-validation (8.6%). Performance evaluation reveals mean classification accuracies of 92.5% ± 8.6% for within-subject validation (range: 73.3%-99.9%) and 86.8% ± 9.8% for cross-subject validation (range: 68.0%-100.0%).

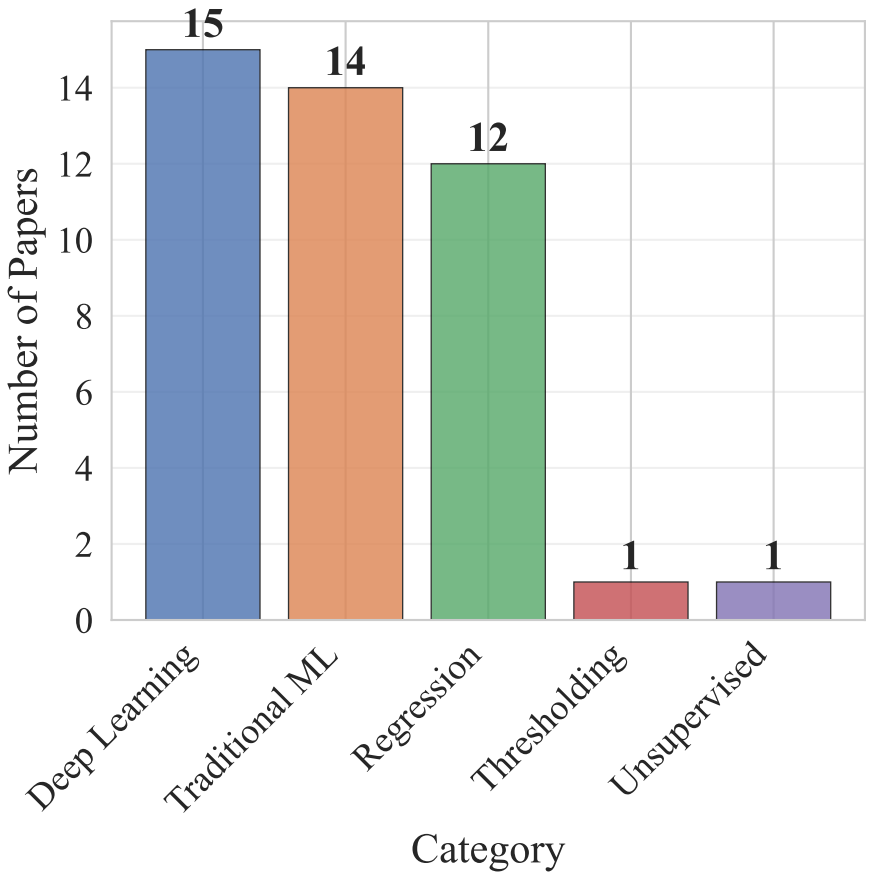

Figure 2.8: *Distribution of classification method categories across cybersickness studies*

Methodological Approaches and Feature Engineering

The methodologies for automated cybersickness detection have evolved in parallel with advances in machine learning. One set of approaches relies on traditional machine learning classifiers fed with pre-selected, or "handcrafted," features. These models include Support Vector Machines (SVM), k-Nearest Neighbors (k-NN), and Linear Discriminant Analysis (LDA) (Chai et al. 2023; Yu et al. 2010). Features extracted from EEG for these models are frequently

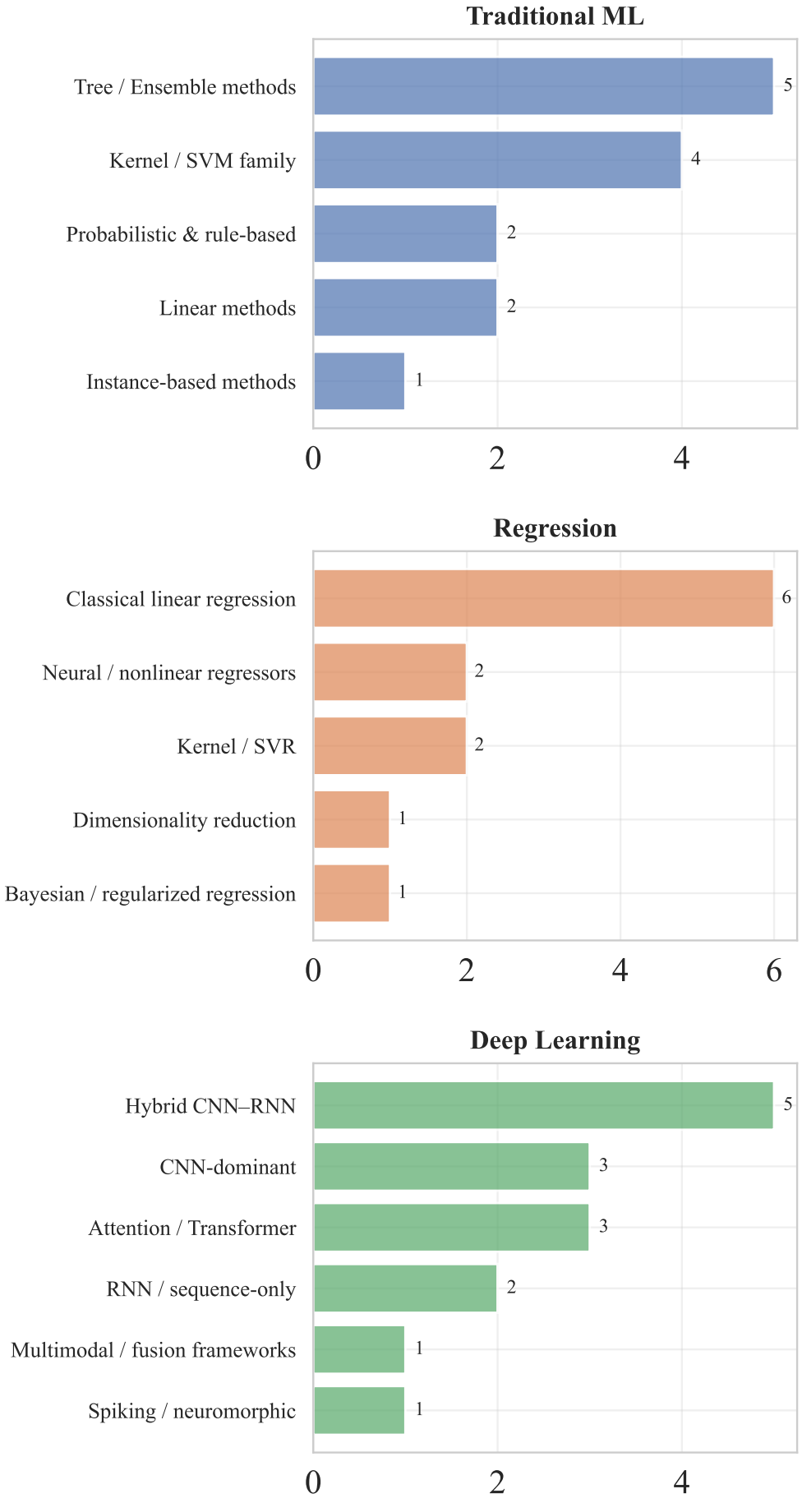

Figure 2.9: *Detailed breakdown of specific methods within each classification category*

based on Power Spectral Density (PSD), wavelet-derived energy ratios (X. Li et al. 2020), or spectral entropy and skew (Feng et al. 2025). Other work has employed time-domain statistical features such as signal variance (Mawalid et al. 2018). To reduce dimensionality and improve model performance, some studies focus on feature selection algorithms, using methods like Correlation Feature Selection (CFS) (Khoirunnisaa et al. 2018) and genetic algorithms (C.-S. Wei et al. 2011c).

A second set of approaches utilizes deep learning architectures, which can learn relevant features directly from the data. Convolutional Neural Networks (CNNs) are widely used to extract spatial and spectral features from EEG time series, spectrograms, or topological scalp maps (Jeong et al. 2019). To capture the temporal evolution of cybersickness, these are often combined with Recurrent Neural Networks (RNNs) like Long Short-Term Memory (LSTM) (Liao et al. 2020) or Gated Recurrent Units (GRU) (Luo et al. 2024). Other explored architectures include spiking neural networks (Yang et al. 2023) and specialized shallow CNNs designed for real-time detection in mitigation systems (Uyan et al. 2024). More recent models frequently employ hybrid architectures, such as combining CNNs and LSTMs (Shen et al. 2024) or implementing dual-pathway CNNs that process raw EEG and functional connectivity data in parallel (Hua et al. 2025). These models may be enhanced with attention mechanisms to weigh the importance of different channels or time points (Hua et al. 2024b). The inputs to these models have also diversified, incorporating functional connectivity matrices (Shen et al. 2024) or features such as entropy and cross-frequency coupling asymmetry (Hua et al. 2024a).

Beyond EEG-only models, a number of studies have demonstrated the utility of multimodal data fusion. This involves combining neural signals with peripheral physiological data, such as galvanic skin response (GSR) and blood volume pulse (BVP) (Sameri et al. 2024), or with non-neural signals like electromyography (EMG) from postural muscles, which was found to be highly informative (Recenti et al. 2021). Other modalities, including fNIRS, have also been used as input for regression models (Ren et al. 2023). A different approach involves knowledge transfer, where a model trained on EEG data is used to enable prediction based solely on features extracted from the VR video content (J. Kim et al. 2019). To improve model interpretability, some studies have incorporated explainable AI (XAI) techniques (Sameri et al. 2024).

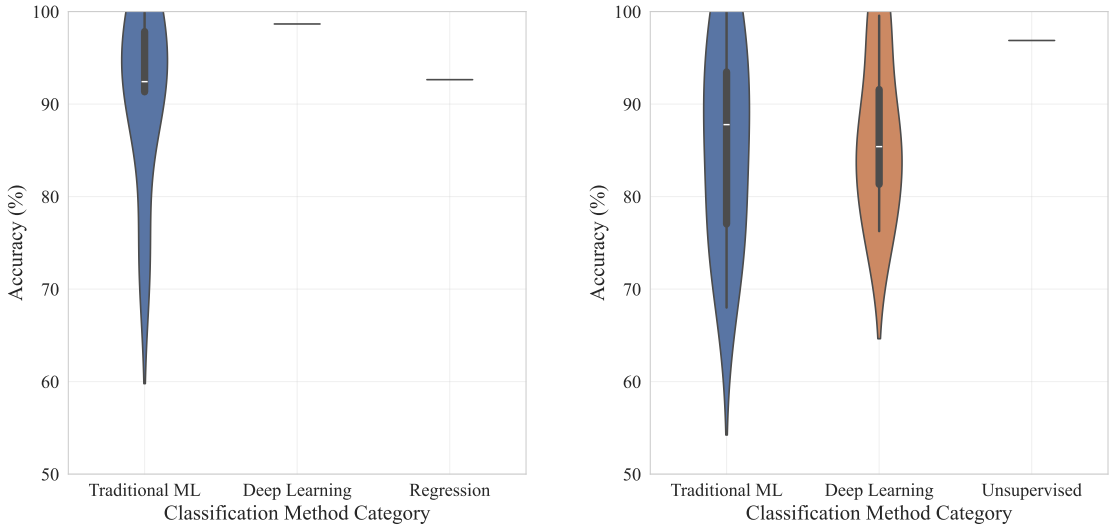

(a) *Within-subject accuracy* **(b)** *Cross-subject accuracy*

Figure 2.10: *Classification accuracy distributions by method category for within-subject and cross-subject validation approaches*

Classification Tasks and Performance

Model performance is typically evaluated across three main tasks. The most common task is binary classification, which distinguishes between a "sick" and "not sick" state. In within-subject validation paradigms, many studies report accuracies exceeding 95% (Daşdemir 2023b; Hua et al. 2024a,b; Jeong et al. 2019; Shen et al. 2024; Yu et al. 2010). Quantitative analysis of reported performance metrics reveals that within-subject models achieve a mean accuracy of 92.5% ± 8.6% (median: 92.7%, range: 73.3%-99.9%). Cross-subject models, which are trained on a group of users and tested on a new user, yield accuracies typically in the range of 68.0%-100.0% (X. Li et al. 2020; Luo et al. 2024), with a mean accuracy of 86.8% ± 9.8% (median: 86.7%). The accuracy distributions for both validation approaches are compared in Figure 2.10.

A second task is multi-level classification, which categorizes cybersickness into several discrete levels of severity. Studies have demonstrated three-level classification using multimodal data fusion (Dennison et al. 2019; Y. Li et al. 2019) and EEG alone, for instance with a rule-based induction algorithm (Pane et al. 2018) or a genetic algorithm with an SVM (Lin et al. 2012).

A third task is continuous prediction or regression, where the objective is to predict a continuous value, such as a total SSQ score. Performance is measured by correlation coefficients and error metrics. Deep learning models have demonstrated high correlations between predicted and actual SSQ scores

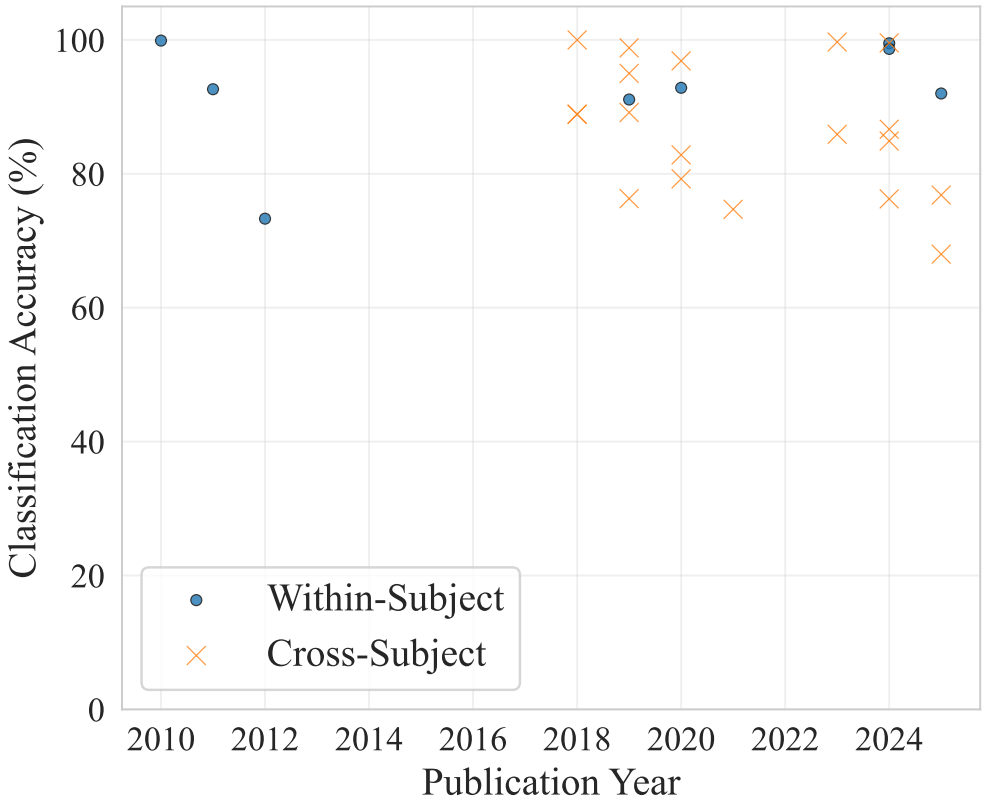

Figure 2.11: *Classification accuracy over time comparing within-subject and cross-subject validation approaches*

(Hua et al. 2023; M. Liu et al. 2024a,b; M. Xu et al. 2023). Earlier work in this area used methods such as Support Vector Regression (SVR) (Ko et al. 2011; C.-S. Wei et al. 2011b) and linear regression (C.-S. Wei et al. 2011a). Current architectures include Siamese LSTMs (Hua et al. 2024c) and frameworks that fuse physiological signals with VR video features (S. Lee et al. 2022). Addressing the challenge of relying on discrete, post-hoc subjective labels, some research has focused on developing methods for continuous, calibration-free detection directly from physiological data (Demirel et al. 2025). The temporal evolution of classification performance across both validation approaches is depicted in Figure 2.11.

2.3.4 Individual Differences and Susceptibility

A well-established observation in cybersickness research is the significant inter-subject variability in symptom onset and severity. This has motivated a specific line of inquiry focused on identifying the neurophysiological basis of individual susceptibility. The goal of this research is to understand why some individuals are highly vulnerable to cybersickness while others remain resistant, and to determine if these differences can be predicted from brain activity.

A key finding in this area is that an individual's susceptibility to cybersickness can be predicted from their resting-state brain activity, even before any VR exposure. One study, using a spiking neural network, demonstrated the ability to predict whether a user would later become sick with 85.9% accuracy, based solely on pre-exposure resting-state EEG (Yang et al. 2023). Other work has identified specific features of the resting-state signal as being predictive. For instance, one study found that EEG beta power in the left parietal region was a significant predictor of subsequent motion sickness ratings in an in-car VR platform (G. Li et al. 2023b). Another EEG study found that aperiodic components of the signal predicted an individual's susceptibility to rotational motion (Tian et al. 2024). These findings suggest the existence of pre-existing neural traits that predispose individuals to cybersickness.

Beyond prediction, studies have also identified distinct neural signatures that differentiate susceptible and resistant individuals during a nauseogenic experience. In a comparison between groups, resistant individuals were found to exhibit enhanced theta activity in the left parietal cortex, a potential biomarker of resilience (G. Li et al. 2023a). Conversely, susceptible individuals show unique patterns of brain activity. One study found that VIMS-susceptible participants exhibited excessive parietal N2 ERP amplitudes and impaired theta-band phase synchronization compared to their resistant counterparts, suggesting a systematic impairment in dynamic cortical coordination (Y. Wei et al. 2019). Similarly, another ERP study found that individuals with high sickness levels presented with higher P3 amplitudes during sensory mismatch conditions, indicating a greater demand on cognitive resources (Ahn et al. 2020). Analyses of spectral power and source-space activity have further revealed differential patterns of activation between susceptible and non-susceptible groups during vection (Zhou et al. 2023). For instance, one study noted that while the cybersickness condition increased

delta and decreased alpha power in both sensitive and non-sensitive groups, the sensitive group showed significantly lower absolute power in the beta and gamma bands at baseline (Jang et al. 2022). An early study also found that the ratio of theta to total EEG power in the frontal and parietal lobes differed significantly between sick and non-sick groups during a long-duration driving task, suggesting it as a potential physiological index of sensitivity (Park et al. 2008).

In addition to neurophysiological traits, demographic factors have been shown to contribute to susceptibility. Specifically, several studies have consistently reported a higher incidence and severity of cybersickness in female participants compared to male participants (L. M. Berger et al. 2025; L. M. Berger et al. 2024). Together, this research demonstrates that individual susceptibility to cybersickness is not random but is rooted in measurable differences in baseline brain function, neural responses to sensory conflict, and demographic variables.

2.3.5 Mitigation and Intervention Strategies

A primary applied objective of cybersickness research is the development of mitigation and prevention strategies. A number of studies are focused on this area, developing and testing systems that use neurophysiological signals to trigger interventions. This research can be divided into two categories: real-time adaptive systems that modify the VR environment, and interventions that aim to directly modulate the user's brain state.

Real-Time Adaptive Systems

One approach involves creating closed-loop systems that can detect the onset of cybersickness and dynamically adapt the virtual environment to reduce its nauseogenic properties. These systems differ from static VR experiences by creating environments that are responsive to the user's internal state. Only two studies in the corpus implemented this approach, indicating that this area of study remains in early-stage development. One study developed a system that uses a two-stage shallow convolutional network to first detect cybersickness from EEG and then to infer a likely causal factor (Uyan et al. 2024). The system then selectively modifies the identified parameter (e.g., navigation speed or scene complexity) in real-time, resulting in a significant reduction in user-reported sickness compared to control conditions. Another

approach utilized fNIRS to monitor total hemoglobin concentration in the brain (Yamamura et al. 2021). Upon detecting an increase in hemoglobin correlated with sickness, the system dynamically reduced the user's field of view (FOV), demonstrating the feasibility of an fNIRS-based closed-loop system for symptom alleviation.

Neurostimulation, Neurofeedback, and Other Interventions

A second category of mitigation research investigates the efficacy of external interventions while measuring their effect on brain activity. Five studies in our corpus have taken this approach. One study demonstrated that transcutaneous auricular vagus nerve stimulation (taVNS) significantly reduced motion sickness symptoms (Molefi et al. 2025). The reduction in symptoms was correlated with taVNS-induced neural activation in specific brain regions, as measured by EEG source localization, providing a neurophysiological correlate for the treatment's effect. Another study explored Vibro-motor Reprocessing Therapy (VRT) and found its application was associated with significant reductions in alpha, delta, and theta spectral power (Molefi et al. 2022). Beyond stimulation, modifying other sensory inputs has also been shown to be effective. One study found that providing synchronized auditory and physical motion cues during a simulated bicycle ride reduced VIMS scores compared to conditions with mismatched or absent cues, an effect that was reflected in concurrent EEG recordings (Yeo et al. 2022).

Some protocols leveraged neurofeedback (NF), where users are trained to volitionally modulate their own brain activity. However, research in this area has identified a significant confounding variable: the presence of cybersickness symptoms can directly impair a user's ability to successfully perform the neurofeedback training task (L. M. Berger et al. 2025). Further complicating the study of such interventions, another experiment found that a placebo transcranial direct current stimulation (tDCS) procedure, while having no significant effect on reported sickness symptoms, paradoxically degraded performance on a concurrent NF task (L. M. Berger et al. 2024). These findings illustrate a critical challenge for BCI-based interventions, where the physiological state being targeted can interfere with the user's ability to engage with the intervention itself.

2.3.6 Additional Findings: Recovery, Datasets, Cognition, and Confounding Factors

Beyond the primary research thrusts of correlation, prediction, and mitigation, several studies address additional aspects relevant to cybersickness. These include: (1) the neurodynamics of recovery after exposure, (2) publicly released datasets that support benchmarking and reproducibility, (3) the effects of cybersickness on cognition and task performance, and (4) identification of confounding factors such as hardware platform and virtual environment type that systematically influence neural response patterns.

The Neurodynamics of Recovery

While the majority of research focuses on the onset and progression of cybersickness, a subset of studies has investigated the neural processes that underlie recovery after the nauseogenic stimulus is removed. One study sought to objectively quantify the duration of recovery using both subjective SSQ reports and objective EEG measures (Woo et al. 2023). The authors found that both measures indicated a recovery period of at least 11.5 minutes, with EEG delta wave power serving as a reliable objective marker of the recovery time course. Investigating the underlying network dynamics with fMRI, another study found that the recovery period from VIMS was characterized by enhanced resting-state functional connectivity patterns involving the insular, cingulate, and visual cortical regions, which are the same networks implicated in the emergence of sickness (Miyazaki et al. 2021). This body of literature suggests that recovery is not a passive return to a baseline state but an active neurophysiological process.

Public Datasets

The advancement of robust and generalizable machine learning models is dependent on the availability of large, high-quality, and publicly accessible datasets. Several research groups have contributed to the field by providing such resources. One dataset was released by (J. Kim et al. 2019), containing EEG data from over 200 subjects experiencing 44 different VR contents, which was used to develop a model for predicting sickness from video features. Another contribution is a dataset containing EEG and subjective measures collected while participants used ten different VR locomotion techniques, pro-

viding a resource for studying the impact of interaction design on cybersickness (Daşdemir 2023a). More recently, a dataset was released alongside a method for continuous, calibration-free cybersickness detection, addressing the need for data with dynamic, real-time ground-truth labels rather than post-hoc questionnaires (Demirel et al. 2025). These open datasets are necessary for benchmarking new algorithms and fostering reproducible science.

Effects of Cybersickness on Cognition and Performance

A final ancillary theme explores the consequences of cybersickness on a user's ability to perform tasks within the virtual environment. This research demonstrates that cybersickness is an issue of both comfort and functional impairment. Studies using event-related potentials (ERPs) have provided direct neurophysiological evidence of this impairment. For instance, one study found that VR sickness severity was associated with a reduction in the P3b component amplitude, a classic ERP marker of diminished attentional resources available for a secondary task (Mimnaugh et al. 2023). Relatedly, VIMS has been shown to impair executive functions such as response inhibition, an effect indexed by a larger N2 amplitude and a smaller, delayed P3 component during an oddball task (Wu et al. 2020).

This functional impairment also presents a specific challenge for BCI applications. In a pair of studies investigating VR-based neurofeedback (NF), it was found that the presence of cybersickness symptoms significantly hampered the user's ability to successfully perform the NF training task (L. M. Berger et al. 2025). These studies also found that a placebo tDCS treatment, while having little effect on sickness symptoms, paradoxically impaired NF success, and consistently observed that female participants experienced more cybersickness and had worse NF performance than their male counterparts (L. M. Berger et al. 2024). These findings highlight a challenge for BCI applications in VR: the physiological state being targeted can interfere with the user's ability to engage with the intervention itself.

Confounding Factors: Hardware Platform and Virtual Environment Effects

Meta-analysis of neural response patterns reveals differences based on hardware platform and experimental conditions. Head-mounted display studies demonstrate distinct alpha band response patterns compared to non-HMD

configurations, with HMD studies showing alpha increases in 20.9% of cases while non-HMD studies show alpha decreases in 29.2% of cases, suggesting different underlying neural mechanisms. Mann-Whitney U analysis with Cliff's delta effect size revealed a statistically significant difference in alpha rhythm changes between HMD-based and screen-based cybersickness studies (p=0.044, Cliff's δ=0.455, large effect). *This comparison should nevertheless be interpreted cautiously. The percentages reported in the published text summarize selected alpha outcomes, but do not by themselves establish opposite subgroup profiles. The evidence for a platform-related difference rests primarily on the Mann-Whitney analysis ($p = 0.044$, Cliff's $\delta = 0.455$), and may also be influenced by associated differences in exposure duration.*

This large effect size indicates that VR display technology substantially modulates alpha frequency responses during cybersickness, providing empirical support for device-specific neural response patterns that justify separate analytical treatment of HMD versus screen-based VR paradigms. Stimulus duration analysis reveals that HMD studies employ significantly shorter exposure periods (mean: 11.6 ± 16.6 minutes) compared to non-HMD studies (mean: 23.7 ± 15.0 minutes; U=242.0, $p < 0.001$, Cohen's $d = 0.76$), potentially reflecting comfort limitations with immersive displays or accelerated symptom onset in HMD environments. Virtual environment type demonstrates additional specificity in neural responses, with driving simulations exhibiting increased alpha responses 46.7% of the time while navigation tasks exhibit increased alpha only 15.8% of the time, potentially reflecting the distinct sensorimotor demands of driving scenarios.

2.4 Discussion

This work follows a recent scoping review by (Chang et al. 2023), which provides an overview of the use of EEG in cybersickness research. Their work, based on a literature search conducted in September 2021, systematically analyzed 33 EEG-based studies. The review reported that frequency or time-frequency analysis was the predominant method for feature extraction. Key neurophysiological findings identified in their analysis included an increase in delta power and a decrease in beta power associated with cybersickness, while results for the alpha band were noted as being inconsistent across studies. The authors also reported that classification models achieved accuracies between 79% and 100%, and that studies frequently used head-mounted displays with

portable EEG systems and recruited participants primarily in their 20s. The volume of research in this domain has increased substantially since the conclusion of their search. Our analysis includes 49 additional studies published after their search date.

2.4.1 Methodological Challenges and Critical Perspective

While the reviewed literature demonstrates significant progress in applying BCI methods to cybersickness research, a critical appraisal reveals substantial methodological challenges. These issues temper the interpretation of many findings and present considerable barriers to the generalization, replication, and practical application of the reported results. This section highlights four main challenges identified in the literature (1) optimistic accuracy estimates, (2) the lack of standardized cybersickness thresholds, (3) protocol disparities and (4) conceptual variability.

A prominent trend in the classification literature is an "accuracy arms race," with a proliferation of studies reporting exceptionally high performance. Numerous papers claim binary classification accuracies exceeding 95%, and in some cases, approaching 99% (Daşdemir 2023b; Hua et al. 2024a, 2025, 2024b; Shen et al. 2024). However, these impressive figures are often a product of experimental designs that limit their generalizability. Many are achieved using within-subject validation on small, homogeneous participant pools, which may not translate to new, unseen users. Furthermore, the choice of data used for classification also plays a role. For example, some high-performing models compare resting-state EEG data collected before and after VR exposure (Chai et al. 2023; Hua et al. 2024b), a paradigm that, while useful for identifying state changes, is ill-suited for the real-time detection required by adaptive systems.

The foundation of any supervised learning model is the quality of its "ground truth" labels, and in cybersickness research, this foundation is ill-defined. The vast majority of predictive models are trained on subjective data, most commonly post-exposure SSQ scores or in-task ratings from scales like the FMS (Rosanne et al. 2025). The SSQ is retrospective and coarse, while continuous ratings can lead the model to classify signals related to the motor action of reporting. A more fundamental issue is the lack of standardized thresholds for defining sickness states. Individual studies frequently devise their own arbitrary cut-offs to convert continuous SSQ scores into binary

(“sick” vs. “not sick”) or multi-level (“mild,” “moderate,” “severe”) labels. This means that the very definition of the target variable is inconsistent across the literature, severely undermining the comparability of different models and their reported accuracies.

This lack of standardization extends to many aspects of experimental design, creating a profound heterogeneity that hinders scientific synthesis. First, there is significant variability in display technology and the nature of the stimulus. Experiences in fully immersive HMDs are not equivalent to those on large-screen monitors or in CAVE-like projection systems (Lim et al. 2021; C. Zhang et al. 2020), or smartphone based VR systems (Molefi et al. 2022), yet findings are often discussed interchangeably. Similarly, passive viewing of a 360-degree video (Suwandi et al. 2024) is fundamentally different from active navigation in an interactive game (Cortes et al. 2023a). Our meta-analysis supports these concerns, revealing statistically significant differences in neural response patterns between different hardware platforms and virtual environment types (see subsection 2.3.6). Second, experimental protocols are inconsistent, with wide variance in exposure duration, the inclusion and length of rest periods, and the definition of a valid baseline. A particularly problematic practice is the use of an "eyes-closed" baseline, which artificially inflates alpha power and directly confounds the interpretation of alpha suppression, one of the most commonly reported neural markers of cybersickness. Third, the recording itself varies, ranging from research-grade, high-density EEG systems to low-cost, consumer-grade devices with fewer channels and potentially lower signal quality, which may impact the reliability of the derived results (R. Liu et al. 2020). Additionally, reporting quality across studies demonstrates substantial deficiencies in critical methodological parameters. For example, EEG reference electrode configuration is reported in only 49.4% of studies, and notch filter frequency in 22.9%, hampering reproducibility and meta-analytic synthesis. A quantitative analysis of the included literature reveals a reliance on low-density EEG systems, with 82.9% of studies employing 32 or fewer electrodes, and 21.4% employing 10 or fewer electrodes. While such systems are appropriate for applied BCI paradigms that target well-characterized and localized neural signals, their use in the context of cybersickness research presents a significant methodological limitation. The neural underpinnings of cybersickness are not yet fully elucidated, and the research objective for many studies remains fundamentally exploratory. Low-density electrode montages have insufficient spatial resolution for reliable

source localization and are blind to activity originating from large, un-sampled cortical areas. This practice, therefore, risks generating an incomplete understanding of cybersickness neurophysiology, potentially overlooking critical contributions from distributed neural networks and biasing the literature towards the few cortical sites that are consistently measured.

The appropriateness of low-density electrode systems depends on the research objective. For exploratory studies attempting to comprehensively map cybersickness neurophysiology or perform source localization, sparse spatial sampling presents significant limitations. However, for hypothesis-driven investigations targeting well-characterized neural signals at known locations (e.g., event-related potentials at specific scalp sites guided by prior literature), strategic electrode placement may be methodologically sound and more appropriate than comprehensive cortical coverage. The key distinction lies in whether the research question requires broad spatial coverage or can be adequately addressed through focused sampling of expected signal locations.

Finally, the field suffers from a degree of conceptual imprecision. A significant conceptual issue is the frequent absence of an explicit theoretical framework guiding experimental design and interpretation. Many of the reviewed studies adopt a data-driven, correlational approach, identifying statistical relationships between physiological signals and subjective sickness reports without explicitly stating which theory of cybersickness, such as Sensory Conflict Theory or Postural Instability Theory, they are operating under. This lack of theoretical grounding is problematic for scientific synthesis. Without a stated theoretical context, the interpretation of findings becomes ambiguous, hindering meaningful cross-study comparisons. Furthermore, it weakens the basis for generalizing results, as a "neuromarker" identified in a purely correlational manner lacks a principled foundation for predicting its validity in a new VR application that may stress a different underlying causal mechanism. Moreover, the terms "cybersickness," "motion sickness", "VIMS", "simulator sickness" and more are often used interchangeably, despite evidence that they may represent distinct phenomena. There are fundamental differences, such as the fact that motion sickness occurs in the presence of vestibular motion, while cybersickness occurs with visual motion and is related to visually induced motion also known as vection. Those semantic discrepancies can result in measurable differences. For instance, Rebenitsch et al. (Rebenitsch et al. 2016) found that motion sickness and cybersickness present distinct symptom profiles, while Stanney et al. (Stanney et al. 1997)

highlight differences between cybersickness and simulator sickness. Furthermore, there is a tendency to label any statistically significant feature as a "neuromarker" without sufficient validation of its specificity, sensitivity, and reliability across different contexts. Compounding these issues is the prevalent use of small sample sizes and demographically biased populations (e.g., young, male university students), which severely limits the statistical power and external validity of the findings (Jang et al. 2022; Molefi et al. 2022).

Taken together, this landscape of methodological and conceptual variability poses a significant threat to replicability and impedes the cumulative progress of the field.

2.4.2 Future Directions

The successful identification of cybersickness correlates and the development of high-performing classifiers mark a significant first phase of research. However, to transition from a collection of isolated, proof-of-concept studies to a mature scientific field capable of producing robust, real-world applications, a concerted effort toward methodological rigor and conceptual clarity is required. Based on the challenges identified in this chapter, we propose the following roadmap for future research.

First, the field must embrace standardization and open science. The profound heterogeneity in stimuli, hardware, and protocols is the single greatest impediment to comparing results and building cumulative knowledge. We advocate for a community-led effort to develop standardized experimental protocols and benchmark datasets. These datasets should encompass a variety of common VR experiences (e.g., passive roller coasters, active navigation) and include high-quality, multimodal data (e.g., EEG, EOG, ECG, head-motion) alongside well-defined subjective labels. The public release of such resources, as pioneered by a few research groups (Daşdemir 2023a; Demirel et al. 2025; J. Kim et al. 2019), is essential for validating new methods and ensuring fair, direct comparisons between different classification and prediction models. Accompanying this should be a commitment to open-sourcing analysis code and pre-trained models to enhance transparency and facilitate replication.

Second, research must move beyond correlation to causal mechanisms. While the literature has established strong correlations between specific neural patterns and cybersickness, the causal nature of these relationships remains largely unexplored. Future work should employ interventional techniques

to probe these connections. For instance, non-invasive brain stimulation methods like transcranial alternating current stimulation (tACS) could be used to exogenously modulate specific neural oscillations (e.g., alpha or theta power) to determine if this directly influences sickness susceptibility or severity. Such studies, when combined with sophisticated computational neuroscience models based on frameworks like predictive coding, can help disentangle epiphenomenal correlates from the core causal drivers of the cybersickness experience.

Third, for BCI systems to be practical, they must be generalizable and validated in ecologically valid contexts. The performance of many current classifiers drops significantly in cross-subject paradigms. Future research should prioritize the development of advanced machine learning techniques, such as transfer learning and domain adaptation, to create models that are robust to inter-subject and inter-session variability without requiring burdensome user-specific calibration. Furthermore, validation must move beyond the laboratory. Studies conducted in more naturalistic, uncontrolled settings, such as the at-home gaming paradigm explored by Moinnereau et al. (Moinnereau et al. 2022), are crucial for assessing the real-world viability of these systems.

Fourth, there is a critical need to innovate on the measurement of ground truth. The field's heavy reliance on subjective questionnaires is a persistent limitation. Future work should focus on developing and validating objective, implicit behavioral markers of cybersickness that can supplement or, in some cases, replace subjective reports. These could include metrics derived from user behavior within the VR environment, such as changes in task performance, head motion dynamics (e.g., freezing or reduced exploration), or eye-tracking metrics (e.g., blink rate, saccadic velocity). Integrating these behavioral measures with neurophysiological signals could provide a more holistic and objective picture of the user's state.

Finally, the field should adopt longitudinal study designs to investigate adaptation and recovery. The vast majority of studies are single-session experiments, leaving the neurodynamics of how users adapt to VR over time, or "get their VR legs", largely unknown. Multi-session, longitudinal studies are needed to track the neural changes that accompany this adaptation process. Similarly, while a handful of studies have examined the recovery period immediately following exposure (Miyazaki et al. 2021; Woo et al. 2023), a deeper understanding of the neural mechanisms governing the dissipation of symptoms is required to develop effective post-exposure recovery strategies.

2.5 Conclusion

This synthesis reveals both significant progress and critical gaps in BCI-based cybersickness research. The evidence points toward an emerging neurophysiological signature of cybersickness, primarily characterized by increased low-frequency (delta, theta) power and suppression of alpha-band oscillations in EEG recordings. Spatially precise modalities like fMRI and fNIRS have localized these dynamics to brain networks including the insula, cingulate cortex, and visual-vestibular processing areas, enabling the development of computational models that show promise for real-time classification and adaptive system control.

Despite these advances, methodological challenges remain, including heterogeneous protocols, limited standardization, and small sample sizes that constrain generalizability. The path toward robust BCI applications requires addressing these limitations through standardized protocols, larger datasets, and validation in ecologically relevant contexts.

A notable gap emerges from this synthesis: while cybersickness theories consistently implicate vection as a mechanism underlying sensory conflict, the neurophysiological correlates of vection itself remain incompletely characterized. The Sensory Conflict Theory and its variants, particularly the Vection Conflict Hypothesis, position vection as the perceptual phenomenon that triggers cybersickness when visual self-motion perception conflicts with vestibular and proprioceptive signals. However, the BCI literature has primarily focused on cybersickness as an endpoint rather than examining the neural mechanisms of its underlying components. Understanding vection's neurophysiological signatures represents a more tractable approach to cybersickness research, potentially revealing biomarkers that address the phenomenon at its perceptual source rather than merely detecting symptomatic manifestations.

Chapter 3

State of the art on EEG and Vection research

> *A man with one watch knows what time it is. A man with two watches is never sure*
>
> Segal's law

Prelude — *This chapter, except for the abstract, the opening paragraph of the Introduction, the EEG methodology description, the condensed objectives statement, and the final two paragraphs of the Conclusion (all covered in the Introduction), was published as "EEG Correlates of Vection: A Systematic Literature Review" at the MetroXRAINE conference. Paragraphs in italics were added to improve readability.*

Leading cybersickness theories, particularly the Vection Conflict Hypothesis, position vection as the perceptual mechanism underlying sensory conflict between visual self-motion perception and vestibular stationarity signals (Hettinger et al. 1990). Vection frequently co-occurs with cybersickness (Keshavarz et al. 2015b; Nooij et al. 2017; Pöhlmann et al. 2021) and can exacerbate symptoms (Pöhlmann et al. 2022; Teixeira et al. 2022), yet the neurophysiological correlates of vection itself remain incompletely characterized. Understanding vection's neural signatures offers a more tractable approach to the complex cybersickness phenomenon by targeting its underlying perceptual components.

This synthesis of sixteen peer-reviewed studies represents the first systematic examination of EEG-based vection research, identifying neural patterns and methodological approaches that inform both fundamental understanding and virtual reality applications.

3.1 Introduction

Cybersickness theories often implicate vection as the perceptual phenomenon that operationalizes sensory conflict between visual self-motion perception and vestibular stationarity signals (Hettinger et al. 1990). However, the previous chapter revealed that while BCI research has characterized cybersickness endpoints, the neurophysiological correlates of vection itself remain incompletely characterized. EEG provides the temporal resolution necessary to investigate the rapid neural dynamics accompanying vection onset and maintenance. A growing number of studies have employed EEG to identify potential neural signatures of vection, warranting systematic examination of this emerging literature.

The review characterizes consistent EEG patterns associated with vection, examines modulation by stimulus and individual factors, and evaluates the potential for robust biomarkers to inform both fundamental research and virtual reality applications.

3.2 Methods

This systematic review adheres to Preferred Reporting Items for Systematic Reviews and Meta-Analyses (PRISMA) reporting guidelines (Page et al. 2021), aiming to provide a transparent account of the study identification, selection, and synthesis process.

3.2.1 Search Strategy

A systematic literature search was conducted on May 1, 2025, across three scientific databases: PubMed, Scopus, and Web of Science. These databases were selected for their comprehensive and overlapping coverage of the biomedical, engineering, and psychological literature relevant to this interdisciplinary topic. No publication start date was applied in order to ensure a comprehensive historical retrieval of all relevant studies. The search included

all articles published up to the search date. The following search query was employed uniformly across each database: `"Vection" AND ("EEG" OR "Electroencephalogram")`. No other databases were systematically searched, as the selected sources were deemed sufficient to capture the relevant literature. This initial search yielded 18 results from PubMed, 27 from Web of Science, and 23 from Scopus, for a total of 68 records before duplicate removal.

3.2.2 Study Selection and Eligibility Criteria

Retrieved records were aggregated, and duplicate entries were identified and removed using custom Python scripts, primarily based on Digital Object Identifiers (DOIs) and PubMed IDs (PMIDs) where available. This process identified and removed 36 duplicate records, leaving 32 unique records for screening.

The articles were independently screened using the titles and abstracts of these 32 unique records against predefined eligibility criteria. Full texts were retrieved and assessed when abstract information was insufficient for a decision. The eligibility criteria were defined as follows:

Inclusion Criteria:

- Original research articles (i.e., reporting primary data).
- Studies explicitly investigating visually induced vection (the illusory perception of self-motion).
- Studies utilizing electroencephalography (EEG) as a measurement technique for assessing neural correlates related to vection.

Exclusion Criteria:

- Review articles, meta-analyses, editorials, letters, or conference abstracts without corresponding full papers.
- Studies where the full text was unavailable.
- Studies not utilizing EEG.
- Studies focused solely on motion sickness, simulator sickness, or other phenomena without specifically analyzing EEG correlates of the vection experience itself.

Following the screening process, 15 records were excluded as they did not meet the inclusion criteria. Of the remaining papers, one could not be accessed in its entirety. This resulted in a final selection of 16 studies deemed

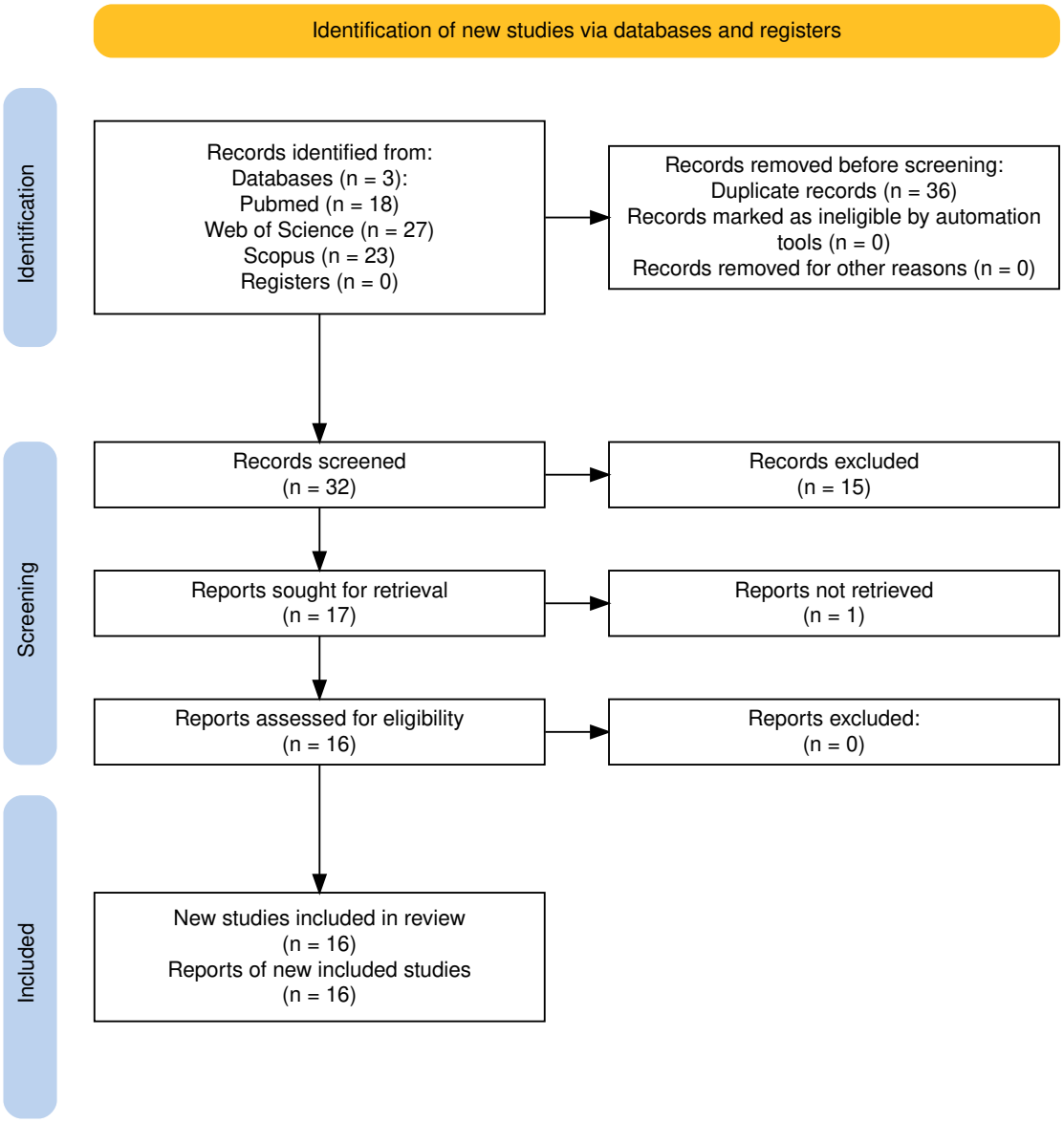

Figure 3.1: *PRISMA Diagram of the retrieval and selection process*

relevant for inclusion in this systematic review. The study selection process is summarized in a PRISMA flow diagram Figure 3.1.

3.2.3 Data Extraction

A standardized data extraction form was developed. For each included study, we systematically extracted publication details (authors, year, title) and core study design information (objectives, number of subjects). We recorded methods related to vection, including induction stimuli (parameters, display system) and assessment techniques. Comprehensive EEG methodology details were extracted, covering the setup, signal processing steps (e.g., filtering, artifact

correction), and primary analysis approaches (e.g., spectral analysis, ERPs, connectivity, source localization, statistical tests). Key findings regarding EEG markers of vection were noted, along with influencing factors investigated, such as stimulus characteristics, individual differences (e.g., handedness, motion sickness susceptibility), and task interactions. Finally, reported quantitative results were documented where available. The extracted data were consolidated into a structured table to facilitate synthesis and comparison across studies.

3.2.4 Data Synthesis

Given the heterogeneity anticipated in methodologies and reported metrics across studies, a qualitative narrative synthesis approach was employed. The extracted findings were organized and synthesized thematically based on the objectives of the EEG analysis and the research question addressed. The main themes identified *a priori* were refined during data extraction, resulting in the following five primary categories used to structure the results of this chapter:

1. **EEG Correlates of Vection**, further subdivided into:
   (a) Rhythms (Power, Frequency)
   (b) Potentials (ERPs, SSEPs)
   (c) Connectivity & Synchronization
   (d) Topography & Source Localization
2. **Stimulus Factors** (e.g., effects of different visual stimuli, field-of-view, motion types, posture).
3. **Individual Differences** (e.g., age, handedness, motion sickness susceptibility).
4. **Task Interaction** (e.g., vection's impact on concurrent tasks/cognition).
5. **Neuromodulation** (e.g., effects of tACS).

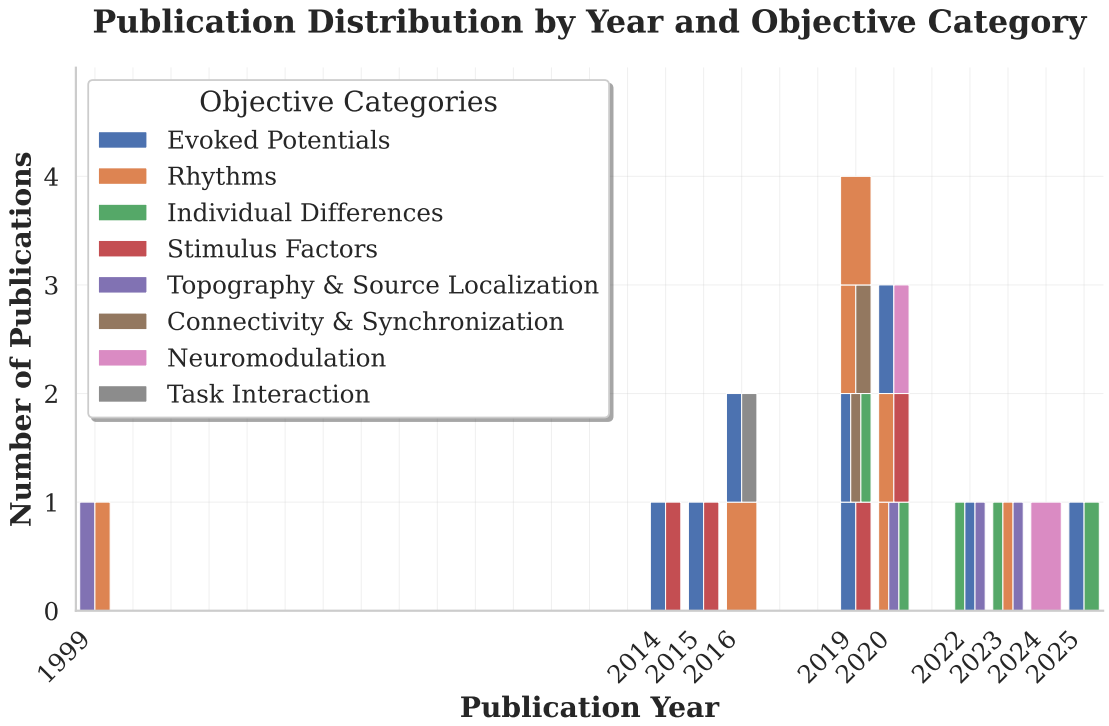

Figure 3.2: *Distribution of the included studies by publication year and research-objective category. Each block represents one study. For studies assigned to multiple categories, the block is divided into colored stripes, each corresponding to one of the assigned categories.*

3.3 Results

3.3.1 Overview of the Included Literature

Sixteen peer-reviewed articles satisfied all eligibility criteria for this chapter. Their temporal distribution (Figure 3.2) confirms a marked growth of electroencephalographic vection research over the past decade, with more than two-thirds of the papers published after 2018, and a recent shift towards studying individual differences and neuromodulation.

Table 3.1: *Experimental parameters of the included EEG–vection studies.*

Study	N	Stimulus / Motion	EEG Ch.	Analysis Focus	Category
(Da-Silva et al. 2015)	29	Tunnel flow (±)	12	M-VEP	Potentials, Stimulus
(Zhou et al. 2023)	20	Rotating dots	64	TF, source	Rhythms, Topography, IndividualDiff
(McAssey et al. 2020)	50	Coherent roll	64	FFT, TF	Rhythms, Topography, IndividualDiff
(Murovec et al. 2025)	47	Optokinetic stripes	32	ERPs	Potentials, IndividualDiff
(Berti et al. 2019)	13	Central/peripheral bars	35	ERPs	Potentials, Stimulus
(McAssey et al. 2022)	57	Coherent vs incoherent roll	64	ERPs, source	Potentials, Topography, IndividualDiff
(Hao et al. 2019)	6	Rotating circles	20	FFT, topography	Rhythms
(Tokumaru et al. 1999)	5	Rotating star field	12	Topography, FFT	Topography, Rhythms
(Stróżak et al. 2016)	19	Moving bars + oddball	64	ERPs	Potentials, TaskInteraction
(Palmisano et al. 2016)	10	Radial forward flow	28	ERSP, t-f PCA	Rhythms
(Keshavarz et al. 2014)	13	Central/peripheral bars	19	ERPs	Potentials, Stimulus
(Harquel et al. 2020)	21	Roll (upright/supine)	96	TF, cluster	Rhythms, Stimulus
(Todd et al. 2019)	9	Vestibular + OKN	4 cerebellar	Coherence	Connectivity, Rhythms
(Harquel et al. 2024)	22	Optokinetic roll + tACS	8	Behaviour, tACS	Neuromodulation
(Y. Wei et al. 2019)	27	Coherent roll	32	ERPs, PLV	Potentials, Connectivity, IndividualDiff
(Dowsett et al. 2020)	20	Optic-flow flicker 10 Hz	3	SSVEP	Potentials, Neuromodulation

3.3.2 Global Study Characteristics

Participants Sample sizes ranged from $N = 5$ to $N = 57$ (Median $= 20$). All studies recruited healthy adults; one examined younger versus older cohorts (Murovec et al. 2025), two contrasted left- and right-handers (McAssey et al. 2022, 2020), and three separated visually induced motion-sickness (VIMS)–susceptible from resistant participants (Hao et al. 2019; Y. Wei et al. 2019; Zhou et al. 2023).

EEG acquisition Most vection–EEG studies recorded with medium-density caps (32–64 active electrodes, 10/20–10/10 layout, although sparser montages of 19–28 channels (Keshavarz et al. 2014; Palmisano et al. 2016) and very dense 96-channel systems (Harquel et al. 2020) also appear. Signals were usually referenced to linked mastoids or earlobes and often re-referenced offline to the common average. Pre-processing almost always applied a 0.1–30/70 Hz band-pass filter plus a 50 or 60 Hz notch for line noise, followed by ocular/muscle artefact removal with ICA or threshold rejection. Data were then resampled to 250–1000 Hz and epoched to stimulus onset or button-marked vection episodes (Murovec et al. 2025; Y. Wei et al. 2019). Spectral features were extracted with Fast Fourier Transforms (Hao et al. 2019; McAssey et al. 2020; Palmisano et al. 2016), Morlet wavelet time–frequency analyses (Harquel et al. 2020; Y. Wei et al. 2019; Zhou et al. 2023), or ERSP/t-f PCA approaches (Palmisano et al. 2016). Event-related potentials were quantified in fixed windows over occipito-parietal sites (Berti et al. 2019; Keshavarz et al. 2014; Murovec et al. 2025), and some studies also derived connectivity measures such as phase-locking value or cerebro-cerebellar coherence (Todd et al. 2019; Y. Wei et al. 2019).

Visual stimulation All experiments relied on visually induced vection. Eight studies used full-field roll-motion dot patterns (Dowsett et al. 2020; Hao et al. 2019; Harquel et al. 2024, 2020; McAssey et al. 2022, 2020; Y. Wei et al. 2019; Zhou et al. 2023); one presented tunnel flow (Da-Silva et al. 2015) and another simulated constant-velocity forward flow in depth (Palmisano et al. 2016); two manipulated central versus peripheral motion (Berti et al. 2019; Keshavarz et al. 2014). The duration of visual motion stimulation varies substantially, ranging from brief epochs of 250 ms (Da-Silva et al. 2015) to prolonged presentations lasting up to 45 seconds (Berti et al. 2019). Body posture was seated in all but one study that contrasted upright with supine

positions to modulate visuo-vestibular conflict (Harquel et al. 2020).

3.3.3 Research Objective Categories

Category 1: EEG Correlates of Vection

1.1 Rhythms (Power and Frequency) Seven studies quantified oscillatory power, predominantly in the α band (8–13 Hz) (Hao et al. 2019; Harquel et al. 2020; McAssey et al. 2020; Palmisano et al. 2016; Todd et al. 2019; Tokumaru et al. 1999; Zhou et al. 2023). Analytical approaches comprised fast-Fourier transforms, Morlet wavelets, and event-related spectral perturbation (ERSP) maps. Table 3.2 consolidates the principal rhythm findings.

1.2 Potentials (ERPs, SSVEPs) Eight studies examined potentials time-locked to the visual stimuli used for vection induction, comprising seven studies focusing on Event-Related Potentials (ERPs) (Berti et al. 2019; Keshavarz et al. 2014; McAssey et al. 2022; Murovec et al. 2025; Da-Silva et al. 2015; Stróżak et al. 2016; Y. Wei et al. 2019) and one on Steady-State Visually Evoked Potentials (SSVEPs) (Dowsett et al. 2020). Motion-onset ERPs typically included early sensory components like P1 ($\sim$100 ms) and N2 ($\sim$200 ms), followed by later P2/P3 complexes. Table 3.3 summarizes the findings on ERPs, which generally demonstrate differences in characteristics depending on the specific visual motion parameters presented (e.g., coherence, spatial location). Additionally, one study employed steady-state visually evoked potentials (SSVEPs) elicited by 10 Hz flickering stimuli, finding a shift in amplitude and lateralization depending on whether subjects experienced vection (Dowsett et al. 2020).

1.3 Connectivity and Synchronization Two studies computed functional connectivity metrics. One found that phase-locking values revealed increased parieto-temporal theta synchrony preceding vection in VIMS-resistant individuals (Y. Wei et al. 2019). The other found that cerebro-cerebellar coherence in the α band increased during vestibular-driven vection (Todd et al. 2019).

1.4 Topography and Source Localization Scalp distributions were assessed in four papers, with parieto-occipital regions most frequently implicated. Lateralization depended on handedness (McAssey et al. 2020) and on vection state in SSVEP paradigms (Dowsett et al. 2020). Source estimations

Table 3.2: *Summary of rhythm-based findings across studies. ↑ = increase; ↓ = decrease.*

Study	Band(s)	Direction	Time Window	Topography
(Palmisano et al. 2016)	α (10 Hz)	↑	∼14 s after onset	Left fronto-central (diffuse)
	β	↓	8–12 s after onset	Parietal
	δ	↓	Later during motion (16–20 s)	Right fronto-central / diffuse
(McAssey et al. 2020)	α	↓ (onset); ↑ (sustained)	Around vection onset / ongoing	Centro-parietal (left-lateral for LH; midline for RH)
(Harquel et al. 2020)	α	↓ (onset); ↑ (upright)	Onset / during vection	Sensorimotor (onset); parieto-occipital (upright)
(Tokumaru et al. 1999)	High α	↓	During vection	Variable centro-parietal
(Zhou et al. 2023)	$\delta,\ \theta$	↑	During vection	Temporal (sensor-space); superior/middle temporal (source)
	$\alpha,\ \beta$	↑ (resistant group only)	During vection	Widespread (sensor-space)
(Hao et al. 2019)	High α	↑	"Unrecognised" vection period	Right centro-frontal
(Todd et al. 2019)	α (ECeG)	↓	Vestibular vection	Cerebellum (ECeG); cerebro-cerebellar coherence ↑

Table 3.3: *Summary of ERP findings across studies. ↑ = larger amplitude / longer latency for the vection condition relative to its control; ↓ = smaller amplitude / shorter latency.*

Study	Component(s)	Modulation	Latency (ms)	Topography
(Da-Silva et al. 2015)	M-VEP	Direction-dependent difference	∼600+	Occipital → central
(Keshavarz et al. 2014)	P1, N2	N2 ↑ (moving stripes); P1 marginal	120–240	Occipital
(Berti et al. 2019)	P2, N2	Amplitude varies with motion pattern	130–330	Parieto-occipital
(Stróżak et al. 2016)	P1, N2, P3	↓ amplitude, P3 ↑ latency (periphery moving)	P1: 90–130 N2: 150–240 P3: 300–500	Occipital, parietal, frontal
(McAssey et al. 2022)	Early/Late CP	Attenuated for vection-consistent motion	160–300	Central, CSv/retrosplenial
(Y. Wei et al. 2019)	N223, N290	N223 ↑ (susceptible), N290∼vection	N223: 195–250 N290: 250–310	Parietal
(Murovec et al. 2025)	P1, P2	↑ (non-coherent motion)	P1: 100–150 P2: 150–230	Parietal-occipital

(eLORETA / sLORETA) mapped early ERP generators to the cingulate sulcus visual area (CSv) and retrosplenial cortex (McAssey et al. 2022; Zhou et al. 2023). Tokumaru et al. (Tokumaru et al. 1999) observed variable high alpha topography during vection, often showing decreases in centro-parietal or mid-frontal regions.

Category 2: Stimulus Factors

Four studies manipulated properties of the visual stimulus or body posture. Field-of-view restrictions modulated vection strength and ERP magnitude (Berti et al. 2019). Body position (upright vs supine) altered sustained α increases during vection (Harquel et al. 2020). Forward versus backward optic flow produced distinct motion-related VEPs (Da-Silva et al. 2015). Central versus peripheral motion also affected vection strength and N2 amplitude, with peripheral motion being most effective at inducing both subjective vection and larger occipital N2 responses (Keshavarz et al. 2014).

Category 3: Individual Differences

Handedness studies reported topographical shifts of α power and ERP lateralization without behavioural vection differences (McAssey et al. 2022, 2020). Aging did not significantly affect vection ratings or early ERPs to coherent motion (Murovec et al. 2025). VIMS susceptibility was linked to enhanced parietal N2 amplitudes and altered θ connectivity (Y. Wei et al. 2019), as well as differential band-power changes (Zhou et al. 2023).

Category 4: Task Interaction

One study combined a visual oddball task with vection stimulation, showing attenuated sensory (P1, N2) and cognitive (P3) ERPs plus slower reaction times when both central and peripheral fields were moving (Stróżak et al. 2016).

Category 5: Neuromodulation

Two studies have examined neuromodulatory approaches during visually induced self-motion. One experiment applied individualized α-frequency transcranial alternating current stimulation (tACS) over the superior parietal

cortex while inducing vection. Alpha-tACS increased subjective vection intensity compared with θ-tACS and sham conditions (Harquel et al. 2024). Another study combined right-hemisphere alpha-frequency tACS with SSVEP recording and found that tACS enhanced SSVEP amplitudes during optic-flow-induced self-motion perception; the effect depended on frequency specificity and sufficient current intensity (Dowsett et al. 2020).

3.3.4 Synthesis of Core Electrophysiological Findings

Across methodologies, α-band activity and early visual ERPs emerged as the most frequently addressed EEG correlates of visually induced self-motion and visual perception. The majority of rhythm investigations reported transient α reductions near vection onset followed by parieto-occipital α enhancements during sustained vection, whereas ERP studies consistently identified N2 amplitude modulations in response to motion-onset configurations. Connectivity and neuromodulation research is less prevalent but provides preliminary evidence for cerebello-cortical coupling and causal influences of parietal α oscillations on vection experience.

3.4 Discussion

This systematic review synthesized sixteen peer-reviewed studies investigating the electroencephalographic correlates of visually induced self-motion perception, or vection. The growing body of literature, particularly over the last five years, underscores an increasing interest in leveraging EEG to understand the neural mechanisms underlying this phenomenon. Our analysis reveals consistent patterns of brain activity associated with vection, alongside variability introduced by stimulus parameters, individual traits, and task demands.

The most robust finding across studies centers on the modulation of alpha-band (α) oscillations, primarily over parieto-occipital scalp regions. Several investigations report a transient decrease in α power around the onset of the vection percept (Harquel et al. 2020; McAssey et al. 2020), potentially reflecting the initial engagement of cortical resources required to re-evaluate sensory inputs and initiate the re-weighting process favoring vision. This is often followed by, or contrasted with, a sustained increase in α power during established vection (Harquel et al. 2020; McAssey et al. 2020; Palmisano et al.

2016), particularly in upright postures involving visuo-otolithic conflict (Harquel et al. 2020). Such sustained alpha enhancement is frequently interpreted within the framework of cortical inhibition (Klimesch et al. 2007), suggesting a mechanism for actively suppressing conflicting vestibular or proprioceptive signals once the visual dominance is established (Harquel et al. 2020). These later oscillatory changes, particularly in the alpha band, have shown direct correlations with subjective vection intensity ratings (Palmisano et al. 2016; Todd et al. 2019). The topographical distribution of these alpha changes shows some dependence on individual factors, notably handedness, which influences the lateralization of the effect (McAssey et al. 2020). Furthermore, the causal relevance of parietal α oscillations was directly demonstrated through tACS, where driving activity at the individual alpha frequency enhanced vection intensity (Harquel et al. 2024).

Evidence concerning other frequency bands and connectivity measures is emerging but currently less extensive. Decreases in beta (β) power sometimes precede or accompany alpha modulations (Palmisano et al. 2016), while delta (δ) and theta (θ) activity show associations with vection strength (Palmisano et al. 2016) or VIMS susceptibility (Y. Wei et al. 2019; Zhou et al. 2023). Connectivity analyses, though sparse, have pointed towards altered theta-band phase synchronization related to VIMS (Y. Wei et al. 2019) and increased cortico-cerebellar coherence during vection involving vestibular input (Todd et al. 2019), highlighting a potential role for the cerebellum in modulating self-motion perception.

The reviewed studies confirm that stimulus characteristics significantly influence both vection and its EEG correlates. Factors such as the type of optic flow (e.g., radial vs. rotational), field-of-view size, and the specific visual field region stimulated (central vs. peripheral) impact the strength of the illusion and associated neural responses (Berti et al. 2019; Keshavarz et al. 2014; Da-Silva et al. 2015). Similarly, manipulating visuo-vestibular conflict through body posture affects brain oscillations (Harquel et al. 2020). Individual differences beyond handedness and VIMS, such as age, have also been explored, although significant age effects on core vection ERPs were not found in one study (Murovec et al. 2025). The finding that vection-inducing backgrounds modulate ERPs related to a concurrent visual task (Stróżak et al. 2016) indicates that the processing underlying vection consumes attentional resources, impacting performance on other tasks.

Early event-related potentials (ERPs), specifically the visual P1, N2, and

P2 components occurring within approximately 250 ms of motion onset, consistently reflect the differential processing of vection-inducing versus non-inducing visual stimuli (Berti et al. 2019; Keshavarz et al. 2014; McAssey et al. 2022; Murovec et al. 2025). The amplitude modulation of these components, particularly the N2, appears sensitive to the spatial configuration of motion (e.g., central vs. peripheral stimulation (Berti et al. 2019; Keshavarz et al. 2014)) and stimulus coherence (Murovec et al. 2025), suggesting they index pre-perceptual stages of sensory evidence integration relevant for self-motion computation. Notably, the N2 amplitude was also found to be larger in individuals more susceptible to visually induced motion sickness (VIMS) (Y. Wei et al. 2019), hinting at differences in early sensory processing or conflict detection in these populations.

An observation emerging from this chapter is that, while ERPs effectively distinguish between different stimulus conditions designed to elicit varying levels of vection, findings regarding direct, quantitative correlations between raw ERP components (e.g., amplitude, latency) and the subjective intensity of the vection perceived on a trial-by-trial basis are less consistently reported compared to oscillatory power. This contrasts with oscillatory power findings (Palmisano et al. 2016; Todd et al. 2019), which appear to correlate more reliably with vection strength. While changes or differences in ERPs might correlate with individual traits related to vection or VIMS susceptibility (Y. Wei et al. 2019), the current evidence suggests that early ERPs may primarily reflect the brain's initial processing of the potential for vection inherent in the visual stimulus, rather than the strength of the resulting subjective experience itself (Berti et al. 2019; Murovec et al. 2025). Understanding the precise conditions and components under which ERPs might track subjective vection intensity remains an important open question for future research.

Moreover, certain methodological trends present challenges for synthesis. Sample sizes are often small, potentially limiting statistical power and generalizability. The heterogeneity in visual stimuli (displays, motion parameters), vection measurement techniques (subjective scales, onset latencies), and EEG processing pipelines (referencing, filtering, analysis methods) complicates direct comparisons across studies. Although source localization techniques are beginning to be employed (McAssey et al. 2022; Zhou et al. 2023), their application remains limited, leaving the precise cortical and subcortical generators of the observed scalp potentials largely inferred.

EEG provides valuable insights into the neural dynamics of vection. Mod-

ulations in the alpha band and early visual ERP components stand out as relatively consistent markers, reflecting inhibitory control processes and sensory integration, respectively. While oscillatory activity, particularly alpha power, often shows correlations with subjective vection intensity, findings for early EPs are less consistent in directly tracking subjective strength, suggesting they may be more reliably tied to the processing of stimulus properties predictive of vection. Emerging evidence highlights contributions from other frequency bands, connectivity patterns, and the cerebellum. While methodological variability warrants caution, the existing literature strongly supports the utility of EEG for objectively investigating the temporal course and neural underpinnings of illusory self-motion perception.

3.5 Conclusion

This chapter systematically examined the current body of literature employing electroencephalography to investigate the neural correlates of visually induced self-motion (vection). The converging evidence from sixteen studies highlights consistent patterns of brain activity associated with this phenomenon, primarily involving modulations of alpha-band oscillations and early visual event-related potentials. Alpha activity, particularly over posterior scalp regions, appears dynamically regulated, with transient decreases potentially marking the onset of sensory re-weighting and sustained increases reflecting inhibitory processes during established vection. Concurrently, early ERP components such as the P1, N2, and P2 index the initial cortical processing and integration of motion cues critical for triggering the illusion.

The reviewed literature demonstrates that these EEG markers are sensitive to various factors, including the specific characteristics of the visual stimulus, the nature of the induced sensory conflict, task demands, and individual traits like handedness and motion sickness susceptibility. While methodological diversity across studies necessitates careful interpretation, EEG has unequivocally proven to be a valuable tool, offering the temporal resolution required to highlight the rapid neural dynamics underlying the emergence and maintenance of vection.

However, a gap emerges from this synthesis: while vection's neural correlates have been characterized, the mechanisms underlying the perception of visual acceleration, the trigger that initiates vection, remain unexplored. The reviewed studies focus on sustained vection states rather than the processes that

precipitate vection onset. Understanding acceleration perception represents a step toward mechanistic comprehension of vection, as visual acceleration events serve as the stimulus that transitions observers from static to self-motion perception. This knowledge gap necessitates empirical investigation into the neural markers of acceleration perception itself. By identifying the EEG signatures associated with the perception of visual acceleration in virtual environments, we can establish the neurophysiological basis underlying vection initiation and advance toward approaches for detecting and understanding self-motion illusions in virtual reality.

Chapter 4

Experimental EEG-VR Paradigm for Acceleration and Vection Perception

> *I knew exactly what to do; but in a much more real sense, I had no idea what to do*
>
> — Michael Scott

Prelude — *This chapter introduces the experimental paradigm that forms the foundation for the empirical investigations presented in Chapter 5, Chapter 6, and Chapter 7. It presents a comprehensive methodology for studying acceleration and vection perception in virtual reality using electroencephalography. The experiment was conducted with 20 participants for the initial acceleration study (Chapter 5) and extended to 30 participants for the vection and spatial filtering investigations (Chapter 6 and Chapter 7). Additional measures including vection intensity ratings and Simulator Sickness Questionnaire responses were collected throughout but are analyzed specifically in Chapter 6 and Chapter 7. This experimental framework enables a systematic investigation of neural markers for visual acceleration perception and vection using time-locked EEG responses in virtual reality.*

4.1 Introduction

The systematic reviews presented in the previous chapters identified a potential path for research towards the neurophysiological understanding of cybersickness and vection. While the cybersickness literature revealed consistent patterns of increased low-frequency power and decreased alpha-band activity, there remains a frequent absence of ERP studies explicitly time-locked to vection or acceleration events. The vection literature review further highlighted that existing EEG research focuses primarily on sustained vection states rather than the processes that precipitate vection onset. Specifically, the mechanisms underlying the perception of visual acceleration, and how it triggers vection, remain unexplored.

Understanding acceleration perception is relevant to vection because visual acceleration events can sometimes lead to self-motion perception. This motivates empirical investigation into the neural markers of acceleration perception. By identifying EEG signatures associated with the perception of visual acceleration in virtual environments, we aim to characterize signals related to vection initiation and to inform objective approaches for detecting self-motion experiences in virtual reality.

To address these questions, we designed an experimental paradigm that combines virtual reality stimulus presentation with continuous EEG recording to investigate both acceleration perception and subsequent vection responses. This chapter presents the complete methodology that underlies the empirical investigations in the following chapters, providing a detailed reference for the experimental procedures, data collection protocols, and analysis pipelines employed throughout this research.

4.2 Experimental Objectives

This experimental paradigm was designed to achieve several interconnected objectives:

1. **Identify neural markers of visual acceleration perception**: Investigate whether sudden changes in visual motion velocity in virtual reality elicit distinct, time-locked EEG responses that can serve as objective markers of acceleration perception.
2. **Characterize vection-related brain activity**: Examine the relationship between subjective vection experiences and corresponding EEG signatures, extending the literature findings of alpha-band modulations and early visual ERPs.
3. **Establish directional sensitivity**: Determine whether the brain exhibits differential responses to forward versus backward acceleration, providing insight into the neural processing of motion direction.
4. **Validate spatial filtering techniques**: Evaluate the effectiveness of different spatial filtering approaches for enhancing the detection of acceleration and vection-related ERPs in noisy EEG data.
5. **Assess individual variability**: Investigate inter-subject differences in neural responses and their relationship to cybersickness susceptibility and vection sensitivity.

These objectives delineate the analyses conducted in subsequent chapters and specify the event-locked EEG measures evaluated for visual acceleration and vection in VR.

4.3 Participants and Ethics

4.3.1 Participant Recruitment

Two cohorts of healthy adult participants were recruited for this research. The initial acceleration perception study (Chapter 5) included 20 participants (12 men, 8 women; age $\mu = 28.1$, $\sigma = 7.99$, range: 20-56 years). This cohort was subsequently extended to 30 participants (18 men, 12 women; age $\mu = 26.0$, $\sigma = 7.38$, range: 18-56 years) for the vection and spatial filtering investigations (Chapter 6 and Chapter 7). Sample sizes were determined according to the

literature as reported in their respective chapters and are consistent with typical ERP research, where within-subject designs and repeated measures provide statistical power through trial-level analyses. The participant population consisted predominantly of young adults, limiting demographic diversity. While expanding participant pool diversity would be beneficial, it is more critical for studies aiming to generalize findings across populations than for investigations identifying novel neural markers, where the primary objective is to establish the existence and characteristics of the markers rather than to validate their generalizability. All participants reported normal or corrected-to-normal vision and had no history of neurological disorders, vestibular dysfunction, or severe motion sickness.

4.3.2 Ethical Considerations

Ethical approval for this research was obtained from the Ethics Committee of the University of Lille under approval number 2021-526-S97. The study protocol adhered to the principles outlined in the Declaration of Helsinki for research involving human subjects. Written informed consent was obtained from all participants prior to their involvement in the experiment.

Participants were explicitly informed of their unconditional right to withdraw from the experiment at any time without repercussion or need for justification. Special attention was given to informing participants about the potential for cybersickness during VR exposure, with clear instructions that they could immediately discontinue participation should they experience any discomfort, nausea, dizziness, or other adverse symptoms. The experimenter maintained continuous communication with participants throughout sessions to monitor their well-being.

All collected data were anonymized immediately upon acquisition and stored in compliance with the General Data Protection Regulation (GDPR). Each participant was assigned a unique anonymized identifier, and they retained the right to withdraw their consent and request removal of their data from the dataset at any time, both during and after the experimental session.

4.4 Experimental Setup

4.4.1 Virtual Reality System

The virtual environment was displayed using a Valve Index Head-Mounted Display (HMD), chosen for its high refresh rate (144 Hz), wide field of view (130°), and low persistence display technology that minimizes motion blur. The HMD was connected to a DELL PRECISION 3640 personal computer equipped with an NVIDIA RTX 3080 graphics card, ensuring consistent high-frame-rate rendering throughout the experimental sessions.

The virtual environment was developed using the Unity game engine (version 2020.3.11f1), selected for its robust VR development tools and precise control over stimulus timing. Custom scripts were implemented to ensure frame-accurate stimulus presentation and synchronization with the EEG recording system through parallel port triggers.

4.4.2 EEG Recording System

Electroencephalographic data were recorded using OpenVibe 3.1.0 software in conjunction with a g.GAMMAcap2 EEG cap from g.tec medical engineering GmbH (Austria). The system employed 14 active electrodes positioned according to the international 10-20 system at locations: FPz, Fz, F1, F2, FCz, FC1, FC2, Cz, C1, C2, CPz, CP1, CP2, and Pz. An additional reference electrode was placed on the right earlobe, with impedances maintained below 10 kΩ throughout recording sessions. The central distribution of electrodes was chosen based on prior literature indicating that event-related potentials are most prominent over central and parietal regions along the frontal-occipital axis (Berti et al. 2019; Keshavarz et al. 2014). This 14-electrode configuration provides sufficient spatial sampling for detecting time-locked responses at expected scalp locations, while the wet-electrode system (g.GAMMAcap2) offers signal quality advantages over dry EEG systems (R. Liu et al. 2020). The montage aligns with the research objective of detecting event-locked neural signatures rather than mapping distributed networks, as illustrated in Figure 4.1.

The EEG amplifier provided a sampling rate of 512 Hz with 24-bit resolution and a hardware bandpass filter from 0.01 to 100 Hz. Real-time monitoring of signal quality was maintained throughout data acquisition to ensure opti-

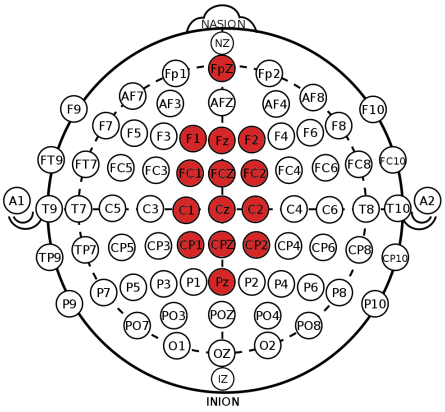

Figure 4.1: *Electrode Placement in the 10–20 International System. The highlighted electrodes (marked in red) indicate the specific sites used in this study: FPz, Fz, F1, F2, FCz, FC1, FC2, Cz, C1, C2, CPz, CP1, CP2, and Pz.*

mal recording conditions.

4.4.3 Synchronization and Timing

Synchronization between the VR stimulus presentation and EEG recording was achieved through hardware triggers sent via parallel port communication using the Lab Streaming Layer (LSL) protocol. Trigger codes were embedded in the EEG data stream to mark the onset of each experimental phase, enabling time-locking of neural responses to specific stimulus events.

4.5 Virtual Environment Design

4.5.1 Visual Stimulus Configuration

The virtual environment consisted of a minimalistic scene designed to maximize vection induction while minimizing visual complexity that could confound EEG analysis. Following established protocols in the vection literature (Keshavarz et al. 2019), the environment featured 2000 stationary white spheres (diameter: 0.20 meters) arranged cylindrically around the participant's virtual position against a black background, illustrated in Figure 4.4.

The spheres were uniformly distributed in terms of angle and depth within a range of 0 to 150 meters, with the distribution centered 1.2 meters above the ground to align with seated participants' eye level. To achieve a homogeneous radial distribution, a Gaussian distribution with a standard deviation of 5

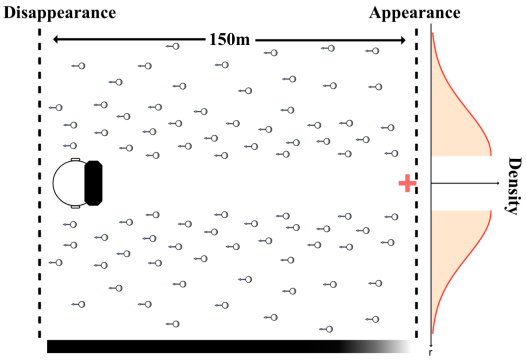

Figure 4.2: *A top-down view of the simulation shows spheres uniformly distributed along the depth axis and arranged radially with a Gaussian distribution. Spheres become increasingly transparent as they approach the depth limit to prevent visual distraction. To avoid participant collisions, spheres are kept away from the radial center.*

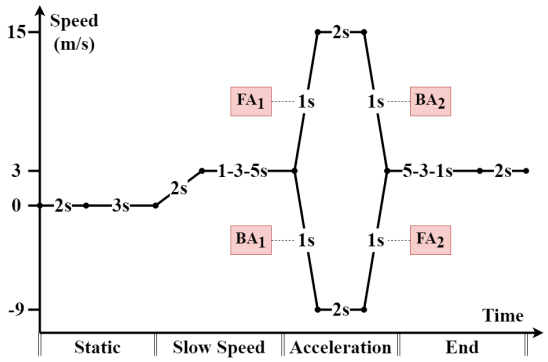

Figure 4.3: *Illustration of a trial: Evolution of speed over time is depicted. Dashed durations represent variable delays, with one of the three delays chosen randomly. The second delay is selected to ensure that the cumulative sum of delays amounts to 6 seconds.*

meters was employed. To prevent collisions, spheres were maintained 1.8 meters away from the radial center. Spheres appeared 150 meters away and gradually became visible over the first 30 meters to avoid distracting appearances, then faded out behind the participant. This configuration provided rich optic flow cues during motion phases while maintaining visual simplicity.

The virtual environment employed a black background to maximize contrast with the white spheres. Ambient lighting was minimal, with sphere visibility determined solely by their proximity to the observer. No additional visual elements, textures, or environmental details were included to avoid potential confounds in the motion perception analysis.

A red fixation crosshair was positioned at the center of the visual field to encourage consistent gaze direction and minimize eye and head movements that could introduce artifacts in the EEG recordings. Participants were explicitly instructed to maintain fixation on this crosshair throughout each trial.

Figure 4.2 illustrates the top-down view of the sphere arrangement, while the participant's view of this environment is shown in Figure 4.4.

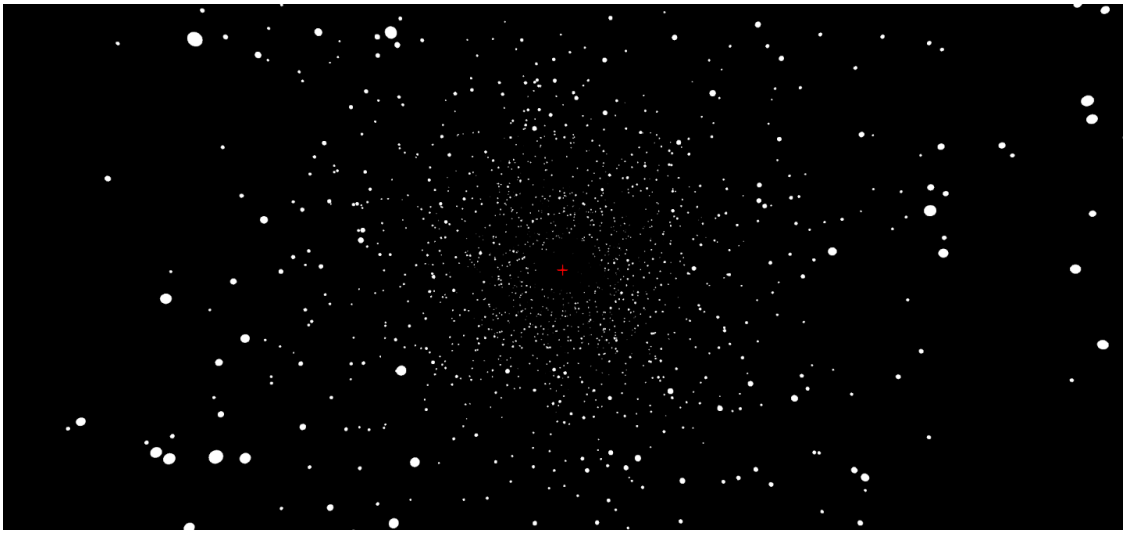

Figure 4.4: *Depiction of the visual experience presented to participants, featuring a virtual scene composed of point clouds and a central crosshair.*

4.6 Experimental Protocol

4.6.1 Trial Structure

Each experimental trial lasted exactly 19 seconds and consisted of four distinct phases designed to elicit specific neural responses while providing appropriate baseline periods for comparison (see Figure 4.3).

1. **Static Phase** (2 seconds): The virtual environment faded in smoothly over the first 2 seconds while remaining completely stationary. This phase allowed participants to acclimate to the visual scene and provided a pre-stimulus baseline for EEG analysis.
2. **Slow Speed Phase** (2-6 seconds): The environment accelerated smoothly from rest to a constant forward velocity of 3 m/s over 2 seconds, then maintained this velocity for a variable duration of 1, 3, or 5 seconds. The constant velocity period (at 3 m/s) served as the baseline condition for acceleration comparisons. This baseline was chosen to provide visual motion stimulation, ensuring that observed differences between conditions reflect acceleration-specific neural responses rather than the mere presence or absence of visual movement. The slower, constant velocity allows direct contrast with the subsequent acceleration events while maintaining visual stimulation throughout the trial.
3. **Acceleration Phase** (4 seconds total): Participants experienced a sud-

den acceleration of 12 m/s^2 for exactly 1 second, either in the forward direction (spheres accelerating backward relative to the observer, creating forward self-motion perception) or backward direction (spheres accelerating forward, creating backward self-motion perception). The resulting higher velocity was maintained for 2 seconds, followed by a return to the initial 3 m/s speed through either forward or backward acceleration lasting 1 second.

4. **End Phase** (2-6 seconds): The environment maintained the 3 m/s velocity for a duration complementing the initial slow speed phase, ensuring that the slow speed and end phase delays always sum to 6 seconds, to keep trial lengths consistent. The environment then faded out smoothly over 2 seconds, returning the display to black.

This design provided multiple comparison conditions within each trial: baseline constant-speed motion (at 3 m/s), initial acceleration events (FA_1 and BA_1), and return-to-baseline acceleration events (FA_2 and BA_2).

The protocol exhibits an asymmetry in the acceleration phase: forward acceleration (FA_1) continues in the same direction as the baseline constant speed, while backward acceleration (BA_1) first decelerates from the forward baseline speed before reversing direction. This asymmetry was intentional and motivated by several design considerations. The constant forward baseline speed was chosen over a backward baseline to ensure that forward acceleration, which corresponds to the more ecologically common vection experience (as encountered in vehicles such as cars and trains), does not pass through zero velocity. If the baseline had been backward and forward acceleration were applied, participants would experience a deceleration to zero followed by acceleration, which could confound the neural response to acceleration onset. By maintaining a forward baseline, forward acceleration events represent a direct continuation of motion, while backward acceleration events represent a clear reversal, allowing both conditions to be analyzed without the confounding factor of velocity sign changes. A fully symmetric design with four conditions (forward baseline with forward or backward acceleration, and backward baseline with forward or backward acceleration) was considered but rejected to avoid halving the number of comparable trials per participant, which would have reduced statistical power for the analyses.

4.6.2 Condition Design and Counterbalancing

The experimental session comprised 78 trials organized into four blocks of approximately 20 trials each, with brief rest periods between blocks to minimize fatigue and maintain attention.

The experimental conditions were fully counterbalanced across several dimensions:

- **Acceleration Direction**: 39 trials featured initial forward acceleration (FA_1), and 39 trials featured initial backward acceleration (BA_1)
- **Pre-acceleration Duration**: 26 trials each included constant-speed periods (at 3 m/s) lasting 1, 3, or 5 seconds before the acceleration event
- **Return Acceleration**: The direction of the return-to-baseline acceleration (FA_2 or BA_2) was determined by the initial acceleration direction: forward acceleration (FA_1) was always followed by backward return acceleration (BA_2), and backward acceleration (BA_1) was always followed by forward return acceleration (FA_2)

To prevent participants from anticipating the timing or direction of acceleration events, trial sequences were generated in advance using a pseudorandom algorithm that determined the initial acceleration direction (FA_1 or BA_1) for each trial. This algorithm ensured balanced presentation of all condition combinations (acceleration direction, pre-acceleration duration, and their interactions) with equal numbers of forward and backward accelerations (39 trials each) and constant speed durations, while avoiding predictable patterns. This predetermined sequence remained the same across all participants to ensure consistency in the experimental protocol. The counterbalancing ensured that any systematic biases related to trial order, adaptation effects, or temporal expectations were distributed equally across experimental conditions.

4.6.3 Session Procedures

Each experimental session followed a standardized protocol to ensure consistency across participants and minimize confounding variables.

Pre-experiment Procedures:

- Participants were briefed on the study's objective: detecting self-motion patterns in EEG data
- Confirmation of absence of epilepsy or implanted electrical devices

- Participants completed informed consent procedures and demographic questionnaires
- Each participant received a unique identification number
- Administration of baseline Simulator Sickness Questionnaire (SSQ)
- The EEG cap was fitted and electrode impedances were optimized
- VR headset calibration was performed, including interpupillary distance adjustment
- Participants completed practice trials to familiarize themselves with the task and environment

During Experiment:

- Rest periods of minimum 5 minutes between blocks during which the HMD was removed, allowing participants to rest and complete the SSQ for the preceding block
- Regular impedance checks between blocks
- Collection of subjective ratings after each trial: participants asked to rate perceived vection intensity on a four-point Likert scale following each 19-second visual simulation (ratings were presented while wearing the HMD through a virtual interface)
- Maintenance of consistent lighting and acoustic conditions
- Participants instructed to minimize head movements and maintain fixation on central crosshair
- Continuous inspection of the EEG signal and VR view by the experimenter to check for anomalies.

Post-experiment Procedures:

- Debriefing regarding the experimental experience
- Monitoring for delayed motion sickness symptoms

4.7 Data Collection

4.7.1 Subjective Measures

Subjective ratings were collected at two different time points during the experimental session, with distinct procedures for each. Following each trial, participants provided vection intensity ratings while still wearing the HMD. During rest periods between blocks, the HMD was removed to facilitate comfortable completion of the SSQ and to mitigate fatigue.

Vection Intensity Rating: Prior to the experimental session, the concept of vection was explained individually to each participant using standardized language to ensure consistent understanding across subjects. Vection was defined as the subjective sensation of self-motion that can occur when viewing moving visual patterns, distinct from simply seeing motion in the environment. Examples were provided, such as the sensation of movement experienced when sitting in a stationary train while an adjacent train departs. Care was taken to use identical explanations for all participants to avoid biasing their subsequent responses. It was crucial to avoid describing either the participant or the spheres as moving, since both interpretations of the stimuli are valid and could bias their responses. Following each trial, participants were asked to rate the perceived vection intensity specifically during the first acceleration event of the acceleration phase (FA_1 or BA_1) using a four-point Likert scale, consistent with the SSQ's scale format:

- **NO VECTION** (`NV`): Subject only perceived object-motion
- **WEAK VECTION** (`WV`): Subject perceived slight self-motion and mostly object-motion
- **MODERATE VECTION** (`MV`): Subject perceived slight object-motion and mostly self-motion
- **STRONG VECTION** (`SV`): Subject only perceived self-motion

This rating specifically targeted the subjective experience of vection rather than the objective perception of visual motion. These self-reports serve as the foundation for comparison with objective EEG measures since vection is a subjective experience.

Motion Sickness Symptoms: Participants indicated their current level of motion sickness symptoms on a scale from 0 ("no symptoms") to 10 ("severe symptoms requiring immediate discontinuation"). This measure served both

as a safety monitoring tool and as data for subsequent analysis of cybersickness correlates.

Simulator Sickness Questionnaire (SSQ): The complete SSQ (Kennedy et al. 1993) was administered once before the experiment to establish a baseline and again after each experimental block. This questionnaire consists of 16 questions, each using a 4-point Likert scale ('None,' 'Slight,' 'Moderate,' or 'Severe') to assess the severity of various symptoms. Originally designed to assess simulator sickness in aviators, the SSQ was selected due to its extensive use in cybersickness research, allowing for comparative analysis with other studies. The instrument categorizes responses into Oculomotor, Nausea, and Disorientation subscales, providing comprehensive assessment of symptoms associated with simulator exposure.

4.7.2 Behavioral Monitoring

Throughout the experiment, participant behavior was monitored through several channels:

- Continuous verbal communication to assess comfort and well-being
- Observation of head movements and postural stability
- Monitoring of trial completion rates and response patterns
- Documentation of any adverse events or early terminations

4.8 Data Processing

The EEG data underwent a three-stage processing pipeline: conversion to standardized format, preprocessing to remove artifacts, and study-specific analysis. All processing was performed using the MNE-python library (Larson et al. 2023) for EEG signal processing, with visualization performed using the seaborn library (L. Waskom 2021).

4.8.1 Raw to BIDS Conversion

Raw EEG recordings were converted to Brain Imaging Data Structure (BIDS) format (Gorgolewski et al. 2016; Pernet et al. 2019) to ensure compatibility with standard analysis tools and facilitate data sharing. GDF files were loaded and enriched with metadata extracted from filenames and dedicated metadata files. Annotations were corrected to replace numeric event codes with descriptive event names and to assign appropriate durations to events (e.g., constant speed periods lasting until the next acceleration event). Manual corrections were applied to vection ratings when participants had indicated errors or changes in their responses during debriefing.

4.8.2 Preprocessing

Preprocessing was applied independently to each run (four runs per participant), following established practices in ERP research (Ditz et al. 2020).

Initial Quality Assessment: Raw EEG data were visually inspected to identify channels with excessive noise, persistent artifacts, or technical malfunctions. Channels exhibiting abnormally high variance compared to neighboring channels were manually marked as bad on a participant-by-participant basis.

Filtering and Resampling: A notch filter at 50 Hz was applied to eliminate power line interference. Data were then bandpass filtered using a 4th order IIR Butterworth filter applied in both forward and backward directions to eliminate phase distortions. Filter settings varied by study: 0.3 to 10 Hz for the acceleration study, and 0.3 to 35 Hz for the vection study. Following filtering, data were downsampled to 128 Hz to reduce computational load while maintaining adequate temporal resolution for ERP analysis. The spatial filtering study maintained the original sampling rate through preprocessing to preserve high-frequency information.

Epoching: Continuous EEG data were segmented into epochs time-locked to experimental events of interest. Epochs extended from 0.5 seconds before event onset to 1.0 seconds after event onset. Relevant events included acceleration onsets, constant speed periods, and other experimental markers. Each epoch was tagged with associated metadata, including subjective vection ratings when applicable.

Epoch-Level Quality Control: Following epoching, data underwent a second stage of quality assessment. Visual inspection identified bad channels

and bad epochs with finer granularity than the initial raw data inspection. Epochs and channels showing clear artifacts were manually marked for exclusion.

Re-referencing: Common average referencing (CAR) was applied using projection to minimize the influence of reference electrode artifacts and enhance spatial specificity of the recorded signals. The projection approach preserved the underlying data structure while allowing reversible application of the reference.

Independent Component Analysis: ICA (Jutten et al. 1991) was computed on each run to identify stereotypical artifacts. Components were manually inspected to identify those corresponding to muscular artifacts or eye blinks. Selected ICA components were then removed from the EEG data. This process resulted in relatively few components being removed, typically between 0 and 3 components per block.

Baseline Correction: Baseline correction was applied to each epoch using the pre-stimulus interval (before 0 seconds relative to event onset) to remove slow drifts and DC offsets.

Data Storage: Preprocessed runs were saved to file in BIDS-compatible format, preserving all preprocessing parameters and marked bad channels, bad epochs, and ICA components.

4.8.3 Study-Specific Analysis

Following preprocessing, data underwent additional study-specific processing steps before statistical analysis.

Acceleration and Vection Studies: Preprocessed runs were loaded and combined across sessions. Relevant epochs were selected based on experimental conditions. The FPz channel was marked as bad across all participants due to consistent contamination by muscular artifacts. Epochs with voltage deflections exceeding ± 125 μV were automatically rejected to eliminate remaining artifacts from muscle activity, electrode movements, or amplifier saturation. Visualization and statistical analyses were then performed on the cleaned epoch sets.

Spatial Filtering Study: Preprocessed runs were loaded and resampled to 128 Hz at the analysis stage. Relevant epochs were selected based on experimental conditions. A stricter artifact rejection criterion was applied: epochs containing two or more bad channels were excluded, and channels

marked as bad in one or more epochs were removed from all epochs. This approach ensured consistent channel configurations across epochs for spatial filtering comparisons.

4.9 Data Utilization Across Studies

The comprehensive dataset collected through this experimental paradigm supports multiple complementary analyses presented in the subsequent chapters:

Chapter 5 - Acceleration ERPs: Analysis focuses on the 20-participant initial cohort, examining time-locked neural responses to sudden acceleration events.

Chapter 6 - Vection Detection: Utilizes the extended 30-participant dataset, incorporating subjective vection ratings to identify neural correlates of self-motion perception.

Chapter 7 - Spatial Filtering: Employs the full dataset to systematically compare spatial filtering techniques for enhancing ERP detection.

This dataset supports several related analyses across chapters, each addressing a specific research question about event-locked EEG responses in virtual reality.

4.10 Conclusion

This chapter described an experimental methodology to investigate event-locked EEG responses to acceleration and vection in virtual reality. The paradigm combines controlled stimulus presentation with continuous EEG recording and predefined analysis procedures linked to the aims of subsequent chapters. The design provides datasets suitable for analyses at both the trial and participant levels, with standardized procedures and quality control measures that support reproducibility.

Chapter 5

Evoked Potentials of Acceleration

> *A complex system that works is invariably found to have evolved from a simple system that worked*
>
> Gall's law

Prelude — *This chapter, except for the abstract, redundant VR / BCI definitions (covered in the Introduction), and detailed methodology sections (covered in Chapter 4), was published as "EEG markers of acceleration perception in virtual reality" at the 2024 Graz BCI conference. Paragraphs in italics were added to improve readability.*

Following the systematic literature reviews of cybersickness and vection EEG correlates, this chapter presents the first empirical investigation of neural markers for visual acceleration perception in virtual reality. Using the experimental methodology established in Chapter 4, this investigation analyzes EEG data from 20 participants to identify time-locked neural responses to sudden acceleration events. The analysis evaluates how the brain processes visual acceleration, hypothesized to precede the emergence of self-motion perception (vection).

5.1 Introduction

The systematic reviews presented in the previous chapters identified gaps in the neurophysiological understanding of cybersickness and vection, specifically highlighting the absence of ERP studies explicitly time-locked to acceleration events. This investigation addresses this gap by analyzing EEG data from the 20-participant cohort described in the experimental methods chapter, focusing specifically on neural responses to sudden acceleration events.

This chapter investigates brain responses to acceleration in VR to identify potential markers of acceleration perception. Our experimental setup involved the simultaneous use of a 14-electrode EEG headset and a VR headset. Participants were presented with stimuli consisting of moving white spheres within the VR environment. These spheres initially moved at a slow constant speed before undergoing a sudden acceleration, either forward or backward, followed by a return to the initial speed. This experimental paradigm allowed us to examine the neural responses associated with the perception of acceleration in different directions.

Thus, studying the perception of acceleration serves as a foundational step in investigating vection and its associated neural correlates.

We identify two potential neuromarkers:

1. A frontal marker of visual acceleration characterized by a positive potential between 300ms and 700ms after the start of the acceleration.
2. A signal differentiating the direction of the acceleration, whether it was forward or backward in the central region.

To the best of our knowledge, these findings have not been previously reported in the literature. They entail two potential meanings for the fields of neuroscience and BCIs. Firstly, they highlight fundamental cortical responses associated with acceleration perception. Secondly, they pave the way for passive BCIs that utilize this neuromarker to tailor the user experience accordingly. By identifying markers of acceleration perception, we can develop algorithms capable of discerning user attention towards acceleration events. Aligning detected accelerations with corresponding neuromarkers offers insight into user engagement with such stimuli.

In summary, this study contributes to the growing body of literature on BCIs and VR by hinting at the neural basis of acceleration perception and its potential applications in human-computer interaction and immersive technol-

ogy.

5.2 Materials and methods

The experimental methodology, participant recruitment, apparatus setup, and data processing procedures are comprehensively described in Chapter 4. This section focuses on the specific aspects relevant to acceleration perception analysis, utilizing the 20-participant cohort from the initial study phase.

We collected 39 trials per condition, exceeding the approximately 14–20 trials required to obtain stable internal consistency for cognitive ERP components as established by (Rietdijk et al. 2014). Prioritizing trial count maximizes statistical power here, as increasing trials is particularly effective for detecting significant effects in within-participant designs (Boudewyn et al. 2018).

5.2.1 Objective

This protocol aims to generate acceleration perception responses using Virtual Reality (VR). To achieve this goal, a user study was designed to trigger a potential through two types of trials: (1) sudden forward acceleration FA_1 and (2) sudden backward acceleration BA_1 (see Figure 4.3). Following this event, the participant slowed back down to their initial speed by either a forward (FA_2) or a backward (BA_2) acceleration.

5.3 Results

In our subjects, we split the EEG data between different conditions:

- Baseline: This is taken during the slow speed phase, as shown in Figure 4.3. Where the subject is going at a constant speed of $3m/s$.
- FA_1, BA_1, FA_2, BA_2 *as defined in Chapter 4.*

In this study, we evaluate the significance of observed differences using a non-parametric bootstrapping approach. First we perform 10,000 resamples on our data with replacement. Then we compute the 95% confidence intervals which correspond to the range between the 2.5th and 97.5th percentiles of the resampled data distribution. These confidence intervals are represented as shaded areas in the figures. Additionally, we utilize topographic maps to

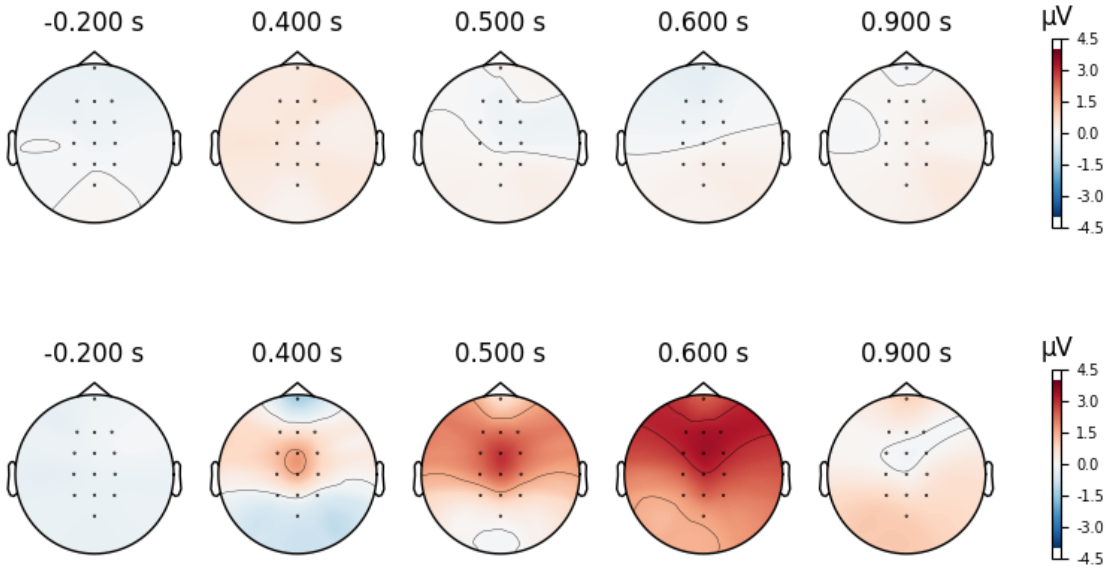

Figure 5.1: *Topographic map comparison of the average response for all subjects to baseline (top) and the first acceleration, FA_1 and BA_1, averaged (bottom)*

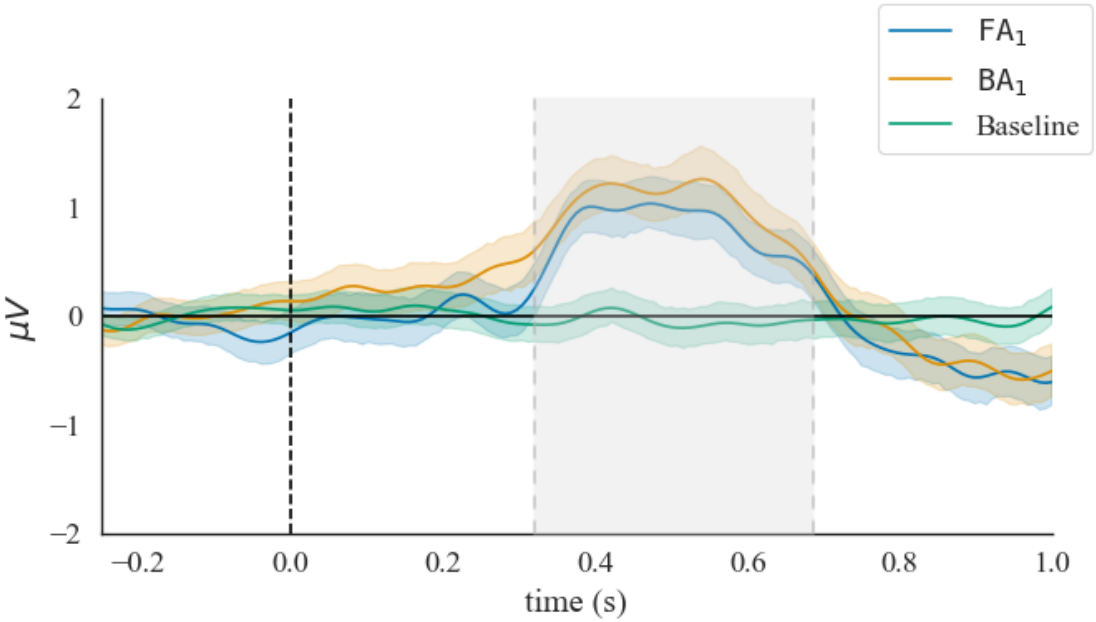

Figure 5.2: *Mean values of the FCz electrode for FA_1 (blue), BA_1 (orange), and baseline (green). The 95% confidence interval is shown for each event. The shaded gray area corresponds to the time period where there was a statistically significant difference between the signals. FA_1 And BA_1 present similar patterns distinguishable from the baseline.*

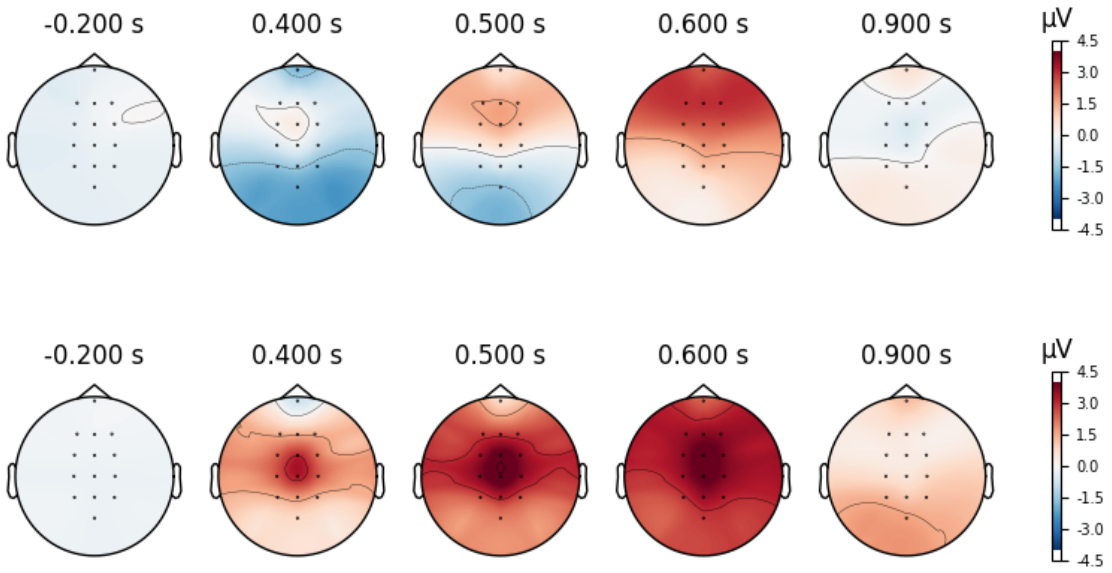

Figure 5.3: *A comparison of the average topographic map across all subjects for FA_1 (top) and BA_1 (bottom)*

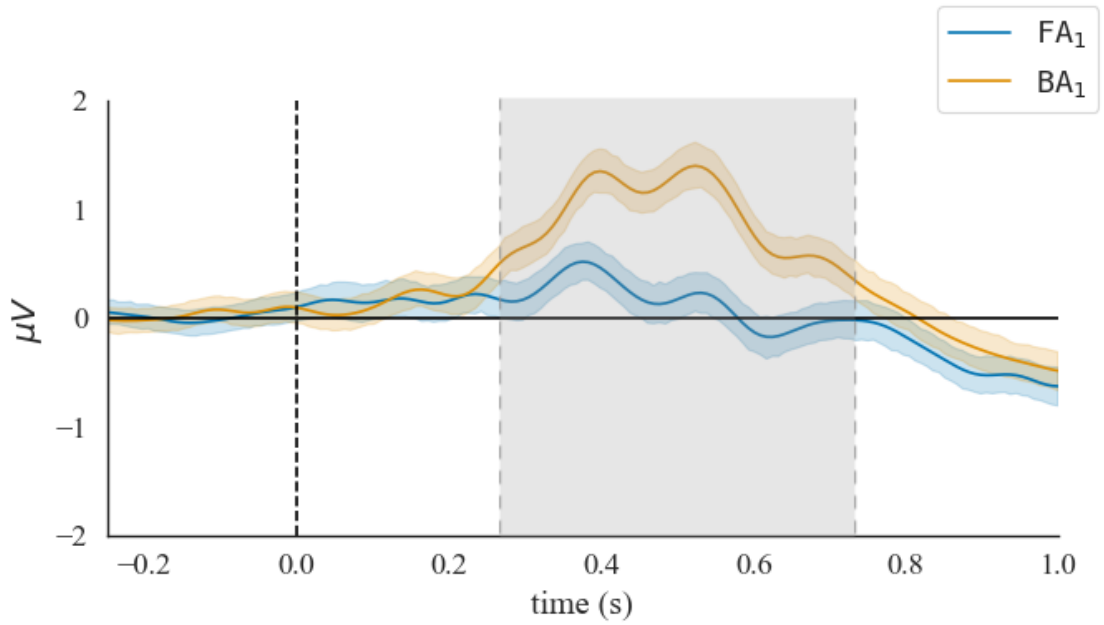

Figure 5.4: *Mean values of the Cz electrode for FA_1 (blue) and BA_1 (orange). The 95% confidence interval is shown for each event. The shaded gray area corresponds to the time period where there was a statistically significant difference between the signals. The Cz presents a significant difference between FA_1 and BA_1.*

underscore spatial differences between conditions, with cubic interpolation applied to obtain values between electrodes.

5.3.1 Marker of acceleration

The spatial response shows differences between the baseline and the acceleration condition as shown in Figure 5.1 which presents a much higher positive peak along the central regions and especially the fronto-central region peaking at 600ms. A better temporal representation can be found in Figure 5.2, which shows a significant difference at electrode FCz between periods of strong acceleration (FA_1 or BA_1) compared to slow speed ($3m/s$), regardless of acceleration direction. We see the characteristic strong positive potential between 300 and 700ms after acceleration onset. Both FA_1 and BA_1 follow a similar pattern in this region. This particular pattern in the region could represent a marker of acceleration, regardless of direction.

5.3.2 Marker of direction

The spatial response to the direction of acceleration also shows differences. Comparing the topographic maps in Figure 5.3, we find a stronger negativity in the parietal region for the FA_1 condition around 400ms, that becomes a frontal and positive over the course of the next 200ms. The BA_1 condition shows a much stronger negativity, especially around the central electrodes, that increases until 600ms. Looking at the Cz electrode, a significant difference was found between forward and backward acceleration, as seen in Figure 5.4. The BA_1 condition differentiates from the FA_1 condition by showing a higher peak around 400ms and keeping a stronger positive potential until 700ms after acceleration onset.

5.3.3 Return to slow speed

Responses when returning to the slower speed were not as pronounced as the responses we found in the initial acceleration condition. We did find a distinct marker for the return to slow speed section during the Acceleration phase, as seen in Figure 5.5. First we observe a small difference in conditions around 350–500ms, which is followed by a more pronounced late marker. This late marker showed a significant difference between the FA_2 and BA_2 conditions between 750–1000ms after acceleration onset. *The mechanism underlying the distinct response to deceleration and the reason for the distinctly different signature remains incomplete and is left for future work. Two working, non multually exclusive hypotheses are considered. First, participants know both*

the timing and the direction of the return-to-baseline segment, which likely reduces surprise and could attenuate or alter the evoked response relative to the initial acceleration because of an anticipation effect. Second, the deceleration corresponds to a return toward the slow-speed baseline, re-establishing the preceding sensory context rather than introducing a novel motion state, which may produce a qualitatively different neural pattern from the initial acceleration away from baseline.

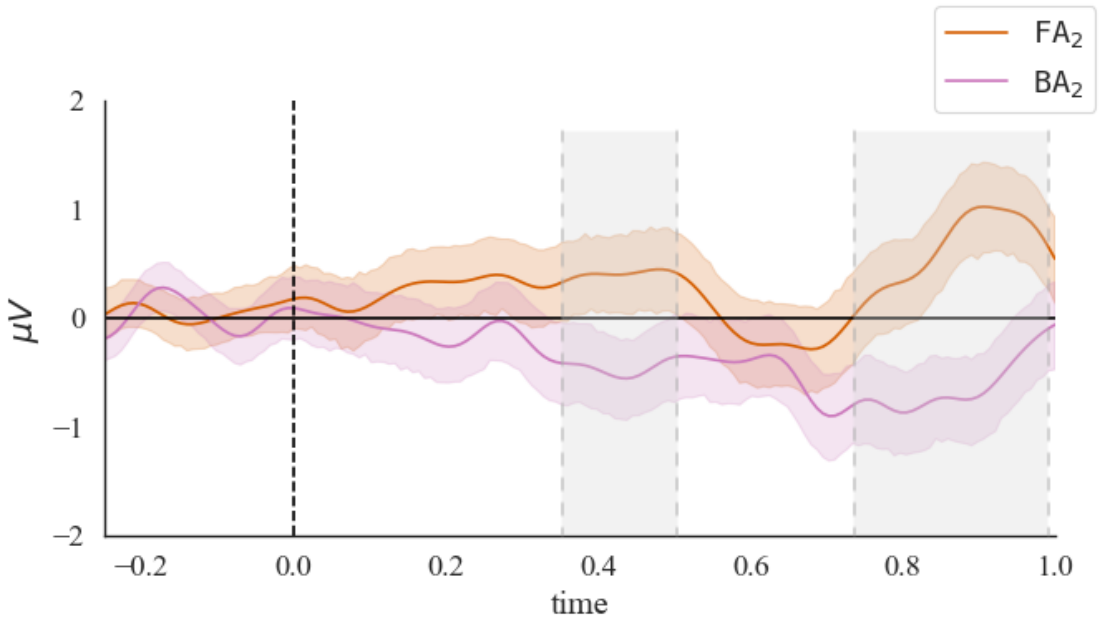

Figure 5.5: *Mean values of the Pz electrode for FA_2 (brown) and BA_2 (purple). The 95% confidence interval is shown for each event. The shaded gray area corresponds to the time period where there was a statistically significant difference between the signals. The Pz presents a significant difference between FA_2 and BA_2.*

5.4 Discussion

5.4.1 Interpretation

The identification of distinct neural activation patterns in response to acceleration stimuli opens the door for a deeper understanding of acceleration perception circuits in the brain. Further understanding of the neural mechanisms underlying acceleration perception may reveal insights into motor control processes. Some of these responses, notably the one exhibited in Figure 5.4 bears resemblance to P300 responses from the literature in its

timing and location (Polich 2007). As the P300 is associated with surprise and decision-making, the perception of a sudden acceleration could trigger a decision-making process in the brain.

Importantly, these findings lay the foundation for future research on passive BCIs that use acceleration perception as a neural signal. Acceleration perception could be used in a similar manner to established passive BCI signals such as mental workload (Luong et al. 2020; Roy et al. 2013) or changes in error-related potentials (Dehais et al. 2019). Such systems could adapt a user's environment and inputs, knowing if the user perceived an acceleration and in which direction they perceived it. For example, a passive BCI could detect if a driver in a vehicle is paying attention to the road by using the markers of acceleration perception along with an accelerometer.

5.4.2 Limitations and future work

In this study, we find patterns when going from a slow speed to a high speed (FA_1 and BA_1), but very different patterns when starting from a high speed and going back to normal (FA_2 and BA_2). All four patterns are unique, we do not explain this difference, and it warrants further study to be better understood. Moreover, while this study shows a signal specific to acceleration perception and direction, these findings are limited to specific conditions: the subject is sitting, in VR, with a stimulation consisting of white spheres.

Continued research in this direction could uncover how the response evolves as we add sensory indicators of acceleration such as sounds. One could also compare this signal to those exhibited ecological experiences of acceleration in VR as well as in real-world scenarios. Beyond the perception of motion, this opens the door to understanding how the brain perceives self-motion induced by visual stimuli, or vection, which bears importance for the field of VR and cybersickness. Thus, another direction could be correlating this signal with the subjective perception of the participant.

5.5 Conclusion

In this study, we find neural responses associated with perceptual changes induced by sudden accelerations in VR. We find different spatial responses characteristic of both acceleration and acceleration direction. We also uncover differences in EEG signals at electrodes FCz and Cz during acceleration perception, suggesting the existence of distinct neural markers for acceleration direction. These findings have implications for the development of passive BCIs and the enhancement of virtual reality experiences. By leveraging these neural markers, future research can design adaptive BCIs and create more immersive and interactive VR environments. Overall, this study contributes to advancing our understanding of the neural mechanisms underlying acceleration perception and paves the way for innovative applications in brain computer interfaces.

These findings establish EEG responses time-locked to visual acceleration and identify event-level markers of motion onset and direction. In the experimental paradigm, sudden visual acceleration often triggers the subjective experience of self-motion, or vection. Whether acceleration-locked neural activity relates to the emergence and strength of vection represents a natural extension of these findings. The relationship between acceleration perception and subsequent vection experiences merits investigation to understand the relationship between motion detection and self-motion illusions.

Chapter 6

Evoked potentials of Vection

> إن دامت الشمس أقفرت
>
> *A lasting sun makes a desert*
>
> Arab proverb

Prelude — *This chapter, except for the removed abstract, the complete related works section (covered in the Introduction), and the complete methodology section (covered in Chapter 4), was published as "Towards the Automatic Detection of Vection in Virtual Reality Using EEG" and is currently accepted at the IEEE Transactions on Visualization and Computer Graphics journal. Paragraphs in italics were added to improve readability.*

This chapter extends the analysis of the acceleration ERP findings presented in Chapter 5 to examine vection-related neural responses using the same experimental paradigm and an expanded participant cohort. While the acceleration chapter focused on time-locked neural responses to sudden motion changes, this investigation evaluates whether an event-related potential associated with perceived vection can be observed. The experimental methodology follows the paradigm described in Chapter 4, with analysis focusing on the relationship between acceleration events and subjective vection experiences. We report a vection-related potential around 600 ms (P600-like) characterized by parietal positivity with concurrent frontal negativity following acceleration onset.

6.1 Introduction

Cybersickness frequently co-occurs with vection and can exacerbate symptoms, yet the precise mechanisms underlying this relationship remain poorly understood. Current vection assessment relies primarily on subjective reports that suffer from reliability issues, temporal imprecision, and susceptibility to bias. The need for objective, real-time measures of vection has been consistently highlighted in the literature, as such measures would enable more accurate cross-subject comparisons and real-time VR system adaptations. EEG offers a promising approach for objective vection assessment through the identification of characteristic neural signatures, particularly evoked potentials that provide high temporal resolution and may reveal consistent brain responses across subjects.

Our objective is to identify potential neuromarkers of vection through EEG. To the best of our knowledge, no evoked potential of perceived vection has been reported in the literature. In pursuit of this objective, we conducted an experiment that exposed participants to moving white spheres in VR, while recording EEG. The participant either experienced a forward acceleration (with the spheres accelerating in the backward direction) or a backward acceleration (with the spheres accelerating in the forward direction). We then asked participants to rate the intensity of their perceived vection and analyzed how their self-reports correlated with their brain signals. Our analysis yields the following key contributions:

- We identify an evoked potential of vection. A bilateral pattern shows in both the frontal and centro-parietal regions that is distinct between vection conditions approximately 600ms after stimulus onset.
- We uncover significant differences in subject susceptibility to vection and acceleration direction.
- We replicate literature results finding bespoke signals of acceleration and showing an effect of vection on alpha power.
- We find a link between vection and Simulator Sickness Questionnaire answers, with subjects reporting strong vection having higher Simulator sickness scores.

6.2 Related Work

Research on vection highlights its relevance for sensory integration, VR user experience, and cybersickness.

Building upon the importance of this research, several studies have investigated specific factors influencing vection. A study by Seno et al. demonstrated a significant positive correlation between the duration of exposure to optic flow stimuli and the perceived strength of vection. Vection magnitude systematically increases with longer exposure durations, supporting the influence of exposure duration on vection strength (Seno et al. 2018). Kim et al. found that adding simulated visual movement, regardless of whether it was synchronized with head movements or viewed while stationary, consistently increased the strength and perceived speed of self-motion. This suggests that visual processing plays a dominant role in the perception of self-motion, particularly when low-frequency sensory stimuli are involved (J. Kim et al. 2008). Furthermore, correlations between dizziness and vection duration have been found, as well as between general discomfort and sway (Pöhlmann et al. 2021). Moreover, unexpected vection significantly exacerbates cybersickness during HMD-based virtual reality, suggesting that unanticipated sensations of self-motion are a key predictor of cybersickness (Teixeira et al. 2022). In many studies, a pivotal question remains: How to accurately measure vection?

To answer this question, we investigate the existing literature on vection assessment. In the subsequent sections, we look into publications relating to the two primary categories of vection assessment: subjective and objective measurements.

6.2.1 Subjective measures

Subjective self-reports of vection have traditionally played an important role in vection research (Kooijman et al. 2023; Palmisano et al. 2016), where vection is commonly defined as the visual illusion of self-motion (Palmisano et al. 2015). Questionnaire methods typically include binary choice responses, where participants indicate whether they experience vection, and onset time determination, which records when vection is first perceived. Intensity rating scales ask participants to rate the strength of their vection experience, while magnitude estimation involves quantifying the perceived intensity relative to a reference (Kooijman et al. 2023). These methods have been used to assess

vection's occurrence, timing, and strength in various contexts, including in VR. This enabled the investigation of various aspects of vection, including its correlation with simulator sickness (Hettinger et al. 1990) and its role in controlling self-motion and navigation(Palmisano et al. 2015).

The limitations of subjective reports, as detailed in the Introduction, motivate the need for objective, real-time measures to enable more robust cross-subject comparisons and adaptive VR systems.

6.2.2 Objective measures

Notably, postural sway analysis has been successfully employed to estimate the impact of vection on postural balance (Nooij et al. 2017; Pöhlmann et al. 2021). This method provides valuable insights into the physical consequences of vection. Such methods can be useful for understanding vection parameters. For example, Palmisano et al. (2014)(Palmisano et al. 2014) found that individuals who rely more on vision for postural stability tend to experience stronger vection. However, it is hard to distinguish visually induced postural sway from visually induced vection (Palmisano et al. 2015). This is due to the fact that visually induced postural sway shares similarities with visually induced vection, but it can occur without vection. Recently, Padmanaban et al. (Padmanaban et al. 2018) have initiated efforts towards predicting vection directly from stereoscopic video. They employed a convolutional neural network-based optical flow algorithm, to compute features that are directly linked to the user's vection experience.

While such approaches advance our ability to predict vection based on visual input, understanding the neurophysiological underpinnings remains crucial. These approaches lay the groundwork for understanding the neural mechanisms underlying vection. Berti and Keshavarz (Berti et al. 2020) review EEG and fMRI studies on visually induced vection, identifying key brain areas involved in vection processing. Their review emphasizes the involvement of a network in the neo-cortex in vection processing as well as a decrease in the alpha band.

Electroencephalography (EEG) has emerged as a promising tool for objective vection assessment (Berti et al. 2019, 2020; Keshavarz et al. 2015a). EEG allows for the investigation of neural correlates during vection experiences. By exploring how vection is processed in the brain, VR developers can better control the environments, reduce cybersickness, and predict overall user

experience.

There are several ways to investigate vection using EEG. Looking at Evoked Potentials, Thilo et al. found a negative occipital response 70ms after optokinetic stimulation (Thilo et al. 2003), but did not link this neuromarker to vection. Some studies looking into brain rhythms during vection confirmed that alpha suppression is correlated with vection (Berti et al. 2020; Harquel et al. 2020). It is important to note that, to investigate robust markers of vection in EEG, one still needs to rely on subjective measures, as there is no other ground truth measurement. Since vection is fundamentally a subjective experience, any objective measure of vection must be measured in conjunction with traditional self-measures reports (Palmisano et al. 2015). Moreover, current EEG methods of studying vection still suffer shortcomings that prevent from using them as a ground truth for vection detection. Many methods struggle to generalize across subjects. Moreover, techniques capable of isolating lower frequencies, as often reported in the literature, may require longer time windows for effective analysis. In this study, we focus on evoked potentials, as they provide a high temporal resolution and may reveal characteristic brain responses that are consistent across subjects, offering a potential objective measure of vection. This chapter proposes a path for objective measurement of vection using EEG by leveraging the established field of Evoked Potentials. Our proposition utilizes acceleration as a stimulus to explore EPs specific to the phenomenon of vection.

The experimental methodology follows the paradigm described in Chapter 4, with specific focus on vection-related subjective measures and analysis approaches. While trial counts remain above the minimums necessary for waveform reliability (Rietdijk et al. 2014), we increased the sample size (N=30) relative to the acceleration study because vection is a subjective response prone to high individual susceptibility. When the primary source of variance is stable individual differences rather than trial-to-trial noise, increasing the number of participants is necessary to achieve adequate statistical power (Boudewyn et al. 2018). We also increased the subject pool because the distribution of vection responses was not evenly distributed and we wanted enough responses for each category.

Using this experimental paradigm, EEG data were collected from 30 participants during vection-inducing trials. The analysis focused on identifying neural correlates of subjective vection experiences through both evoked potential analysis and spectral power investigations.

6.3 Results

The data acquired in this study underwent analysis through two approaches. Initially, we examined which factors influenced subject ratings. We then conducted an aggregate analysis across all subjects, focusing on EEG patterns related to vection. Furthermore, we extend our previous results (Van der Lee et al. 2024) concerning responses to acceleration.

6.3.1 Subjective Results

We combined the subject's responses to our questionnaires and analyze the results.

The distribution of responses to the vection questionnaire can be found in Table 6.1. The results show that some participants exhibited greater sensitivity to vection than others, reinforcing the need for VR systems that can adapt to individual user responses in real time to improve comfort and reduce cybersickness. As seen in Figure 6.1, there are relatively fewer trials where a subject experienced `NV`. A Kruskal-Wallis test revealed a significant difference in reported vection between subjects ($H = 184.78$, $p < 0.001$, $\epsilon^2 = 0.406$), emphasizing the variability in vection reporting across individuals. Similar results are reported in the literature (Berti et al. 2019; Palmisano et al. 2015). Figure 6.1 shows the distribution of reported vection for FA_1 and BA_1. Chi-squared testing reveals that acceleration direction (FA_1 versus BA_1) has a strong influence on reported vection ($\chi^2 = 82.06$, $p < 0.001$, $df = 3$), with forward acceleration (FA_1) correlating with stronger reported vection.

Our objective is to examine the neural markers of vection and how they relate to subjective vection reports. We also analyze the differences between conditions where vection was reported and those where it was absent. The four-point vection scale provides valuable granularity; however, for the purpose of distinguishing the presence or absence of vection, a binary categorization is more appropriate. The goal is to clearly separate trials where participants did not feel substantial self-motion from those where they reported strong self-motion. This approach helps to draw a more distinctive boundary between object-motion perception and vection, reducing ambiguity in the analysis.

The examination revealed variability in the perception threshold across subjects, with the `NV` category being notably underrepresented in the FA_1 condition, as evident in Figure 6.1. The low frequency of `NV` responses limited statistical

Table 6.1: *Totals for reports of vection for each subject across all trials. Each row is a subject, the last row represents the average for each column.*

No Vection	Weak Vection	Moderate Vection	Strong Vection
8	19	22	28
1	11	35	30
16	25	15	22
10	40	24	1
14	27	28	9
0	25	39	14
38	28	10	1
0	4	33	41
3	32	8	33
0	1	14	65
0	6	38	36
1	11	24	42
4	14	35	24
0	30	31	17
57	21	0	0
0	12	24	42
1	28	31	18
3	21	36	18
0	0	52	26
36	42	0	0
14	31	27	6
1	19	40	20
0	23	37	18
13	27	27	10
3	19	31	25
0	39	39	0
0	3	19	56
0	13	48	17
52	26	0	0
1	8	26	43
9	20	26	22

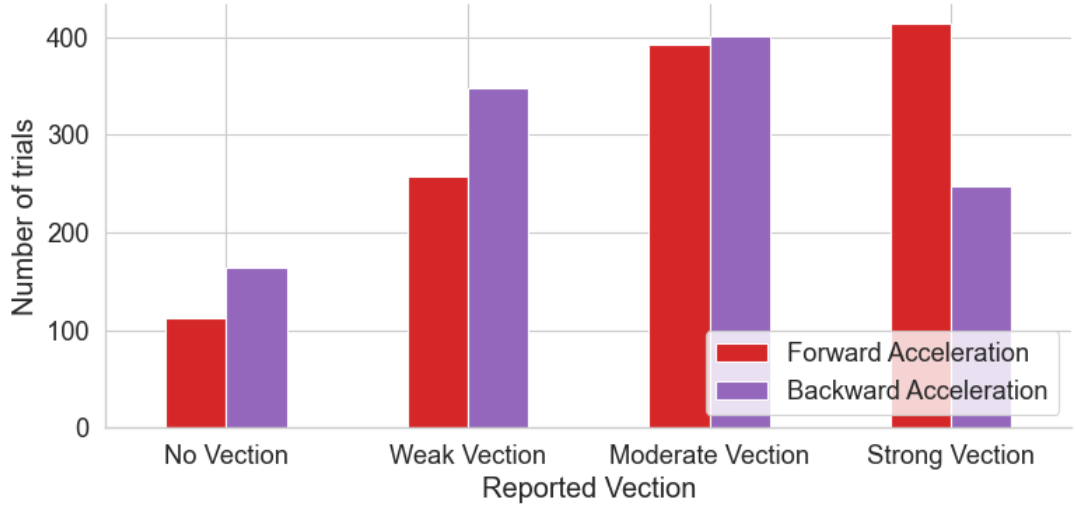

Figure 6.1: *Distribution of reported vection per trial for FA_1 (red) and BA_1 (purple).*

power for this category in isolation. To address this limitation, we combined `NV` and `WV` responses into a single category for comparative analysis. This grouping is methodologically justified because both categories represent predominantly object-motion perception: `NV` corresponds to exclusive object-motion perception, while `WV` corresponds to predominantly object-motion perception with minimal self-motion sensation. The substantially higher frequency of `SV` responses relative to `NV` and `WV` responses enabled balanced class sizes when excluding `MV` from the analysis. Exclusion of the boundary category `MV` accounts for the inherent variability in subjective reporting, where participants may categorize equivalent perceptual experiences differently due to individual variation of the responses. Given these considerations, we merged the `NV` and `WV` categories for comparative analysis against the `SV` category. `MV` was excluded and served as a demarcator to differentiate between the two classes.

6.3.2 Correlates of Acceleration

In this study, we divided the EEG data into different conditions. We set the baseline condition as the slow-speed phase, where the subject moved at a constant speed of 3 m/s, as shown in Figure 4.3. This ensures that some visual stimulus is also present in the baseline condition. Additionally, the conditions labeled FA_1, BA_1, FA_2, and BA_2 were defined as described in the *Trial Design* subsection.

To highlight the difference in EEG responses when vection occurs, we

compare the median responses around accelerations and a baseline. We selected the median over the mean due to its greater robustness against outliers and because some artifacts bypassed the artifact rejection process, potentially distorting the mean. A Shapiro–Wilk test confirmed that the data is not normally distributed with a W statistic of 0.0247 and $P < 0.0001$.

We assess the significance of observed differences using a non-parametric bootstrapping method. We generate 10,000 resamples of our data with replacement, and then calculate 95% confidence intervals, defined as the range between the 2.5th and 97.5th percentiles of the resampled data. These confidence intervals are displayed as shaded areas around the median curves in the figures.

Our findings on acceleration reinforce previous results reported in the literature (Van der Lee et al. 2024) by expanding the subject cohort and finding similar patterns of acceleration perception. *Figure 6.2 and Figure 6.3 reproduce the acceleration ERP results from Chapter 5 and are shown across all vection conditions.*

Figure 6.2 shows EEG signals that present statistically significant differences when the subject is experiencing FA_1 or BA_1 compared to baseline on the FCz electrode. This signal is identical in both the FA_1 and BA_1 conditions, but it differs significantly from baseline. It represents a marker of visual acceleration. Figure 6.3 shows a significant difference between FA_1 and BA_1 on Cz. This presents a characteristic signal of the acceleration direction.

6.3.3 Correlates of vection

Additionally, we find novel results concerning correlates of self-motion perception. The data shows significant differences in EEG signals between trials where participants reported self-motion and those where they reported object-motion. Figure 6.4 shows the difference between the runs where subjects reported `SV` versus the ones where subjects reported `WV` & `NV`. However, we also observed that vection events induce high signal variance.

The vection signal was subtle, and inherent EEG noise resulted in high signal variance, increasing the confidence intervals. We observed that signals displayed similar patterns along the lateral axes, with symmetrical response patterns on both sides. Electrodes recorded similar source signals as they are centrally distributed. Since the signal displays similar patterns along the lateral axes and in order to mitigate the impact of noise across different

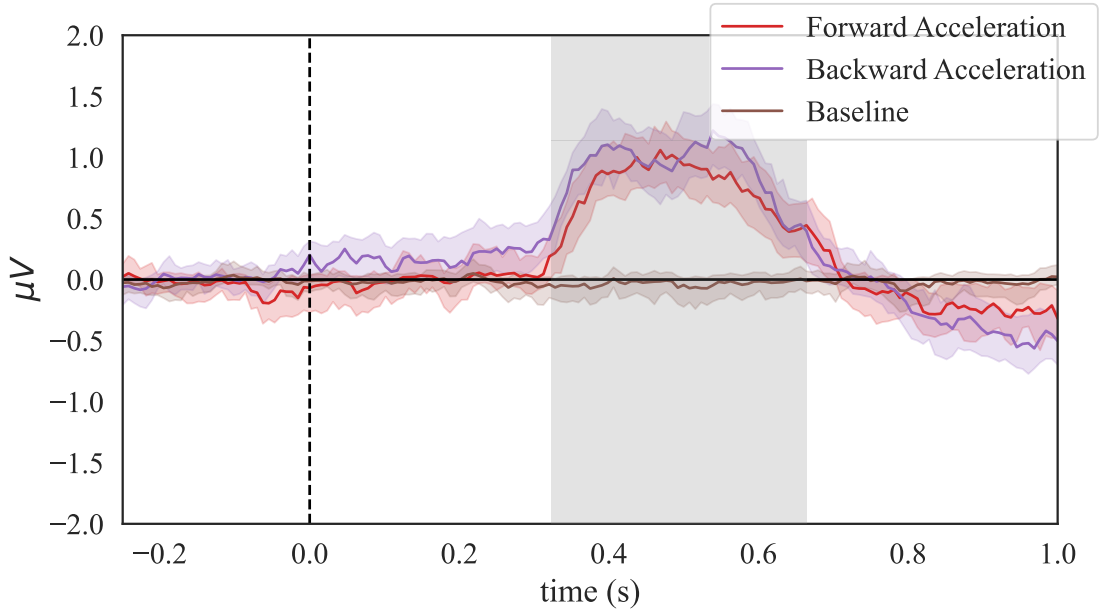

Figure 6.2: *Comparison of the median of the FCz electrode for FA_1 (red), BA_1 (purple) and baseline (brown). The dotted line at 0 seconds represents the start of the acceleration. The y axis represents the median voltage for FCz at that time point. The 95% confidence interval is displayed around each event's line, in its corresponding color. The shaded gray area corresponds to the time period where there was a statistically significant difference between the signals. FA_1 and BA_1 present similar patterns distinguishable from the baseline.*

subjects, we chose to first aggregate electrodes. Lateral averaging improved the signal-to-noise ratio, thereby enhancing the differences between vection conditions. We first calculate the median for each row of electrodes for every subject. We then take the median of these values across all subjects to reduce additive noise.

We plot the spatial differences using topographic maps between the vection conditions in Figure 6.5. The topographic maps highlight the stronger frontal positivity in the `WV` & `NV` condition 600ms after acceleration onset, as well as the lingering parietal negativity in the `SV` condition.

Additionally, Figure 6.6 shows EEG rhythms associated with `SV` compared to `WV` & `NV`. Patterns consistent with the literature (Berti et al. 2020; Harquel et al. 2020) are found, with alpha rhythm suppression during perceived self-motion.

Finally, we observe a link between reported vection and subject responses to the SSQ. Responses from each subject's pre-experiment questionnaire were subtracted from subsequent questionnaires for baseline correction. There is a strong positive correlation between `SV` and the SSQ total score as evidenced by

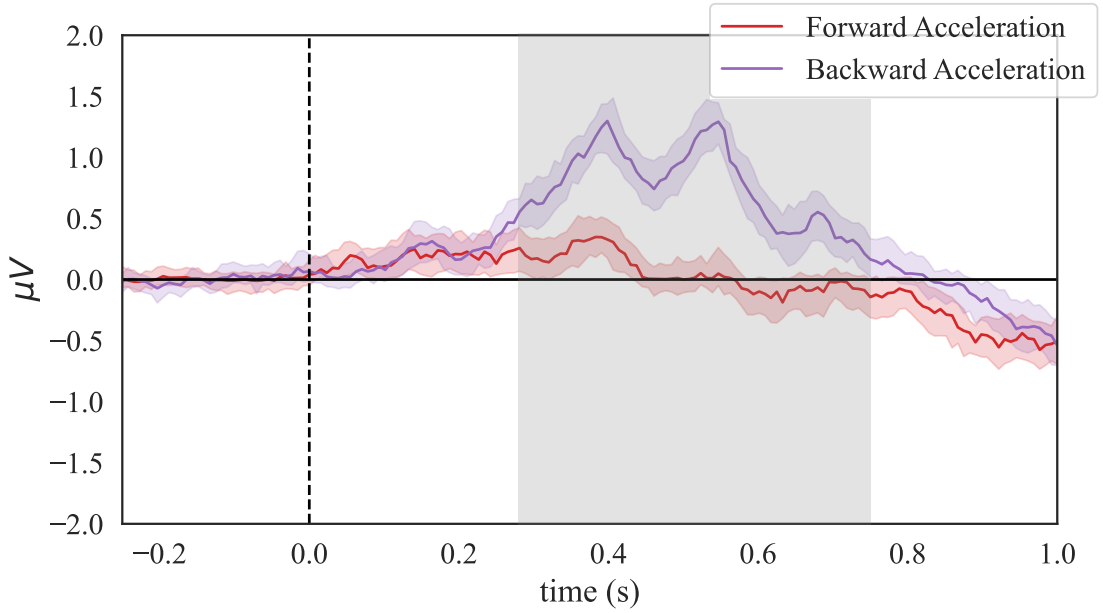

Figure 6.3: *Comparison of the median of the Cz electrode for FA_1 (red), BA_1 (purple). The dotted line at 0 seconds represents the start of the acceleration. The y axis represents the median voltage for Cz at that time point. The 95% confidence interval is displayed around each event's line, in its corresponding color. The shaded gray area corresponds to the time period where there was a statistically significant difference between the signals. Cz presents a significant difference between FA_1 and BA_1.*

the Pearson correlation ($r = 0.55$, $P < 0.01$). More precisely, this correlation can be broken down in the SSQ subcategories: Oculomotor ($r = 0.45$, $P < 0.04$), Disorientation ($r = 0.51$, $P < 0.02$) and Nausea ($r = 0.62$, $P < 0.003$). Thus, we observe that vection correlates the strongest with Nausea and Disorientation, which is consistent with the symptoms of cybersickness (Rebenitsch et al. 2016).

6.4 Discussion

Our findings confirm previous results that identified distinct EEG markers associated with acceleration in VR. Specifically, we observed significant signal differences between forward and backward motion in the Cz electrode, consistent with earlier studies. By analyzing EEG signals, we not only discerned the presence of acceleration but also identified the direction, with statistically distinct signals for forward versus backward motion.

For self-motion, we identified a notable neuromarker approximately 600 ms after the onset of acceleration, distinguishing strong vection experiences from

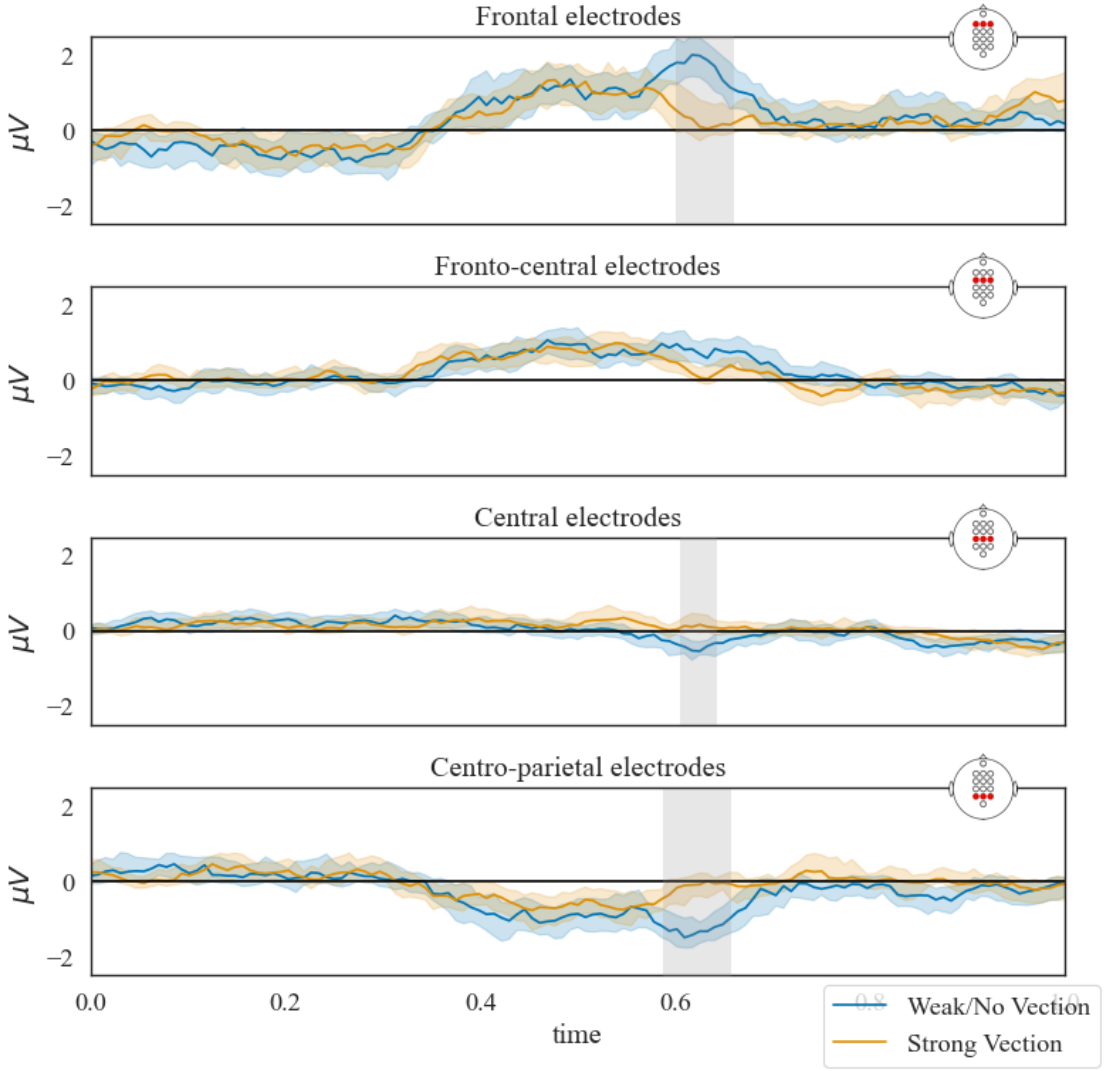

Figure 6.4: *Comparison of the EEG signals between* `WV` *&* `NV` *(blue) and* `SV` *(orange) during* FA_1*. The x axis represents the time since the acceleration started. The y axis represents the median voltage of the electrodes at that time point. The 95% confidence interval is shown around the line of each vection condition, in its corresponding color. The shaded gray area corresponds to the time period where there was a statistically significant difference between the signals. The* `SV` *signal has a significant positive deviation from baseline around 600ms after acceleration onset compared to a negative deviation for* `WV` *&* `NV`*. This trends reverses as the signal travels from the parietal to the frontal region, with a negative deviation for* `SV` *at 600ms compared to a positive deviation for* `WV` *&* `NV`*.*

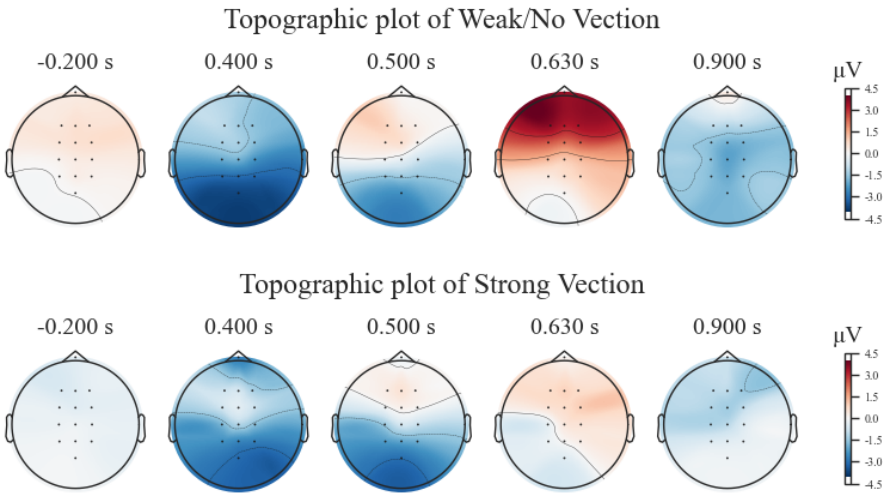

Figure 6.5: *Topographic map comparison of the average response for all subjects during FA_1 to* `WV` *&* `NV` *(top) and* `SV` *(bottom).* `SV` *displays a lingering parietal negativity until 600ms while* `WV` *&* `NV` *displays a stronger frontal positivity around 600ms*

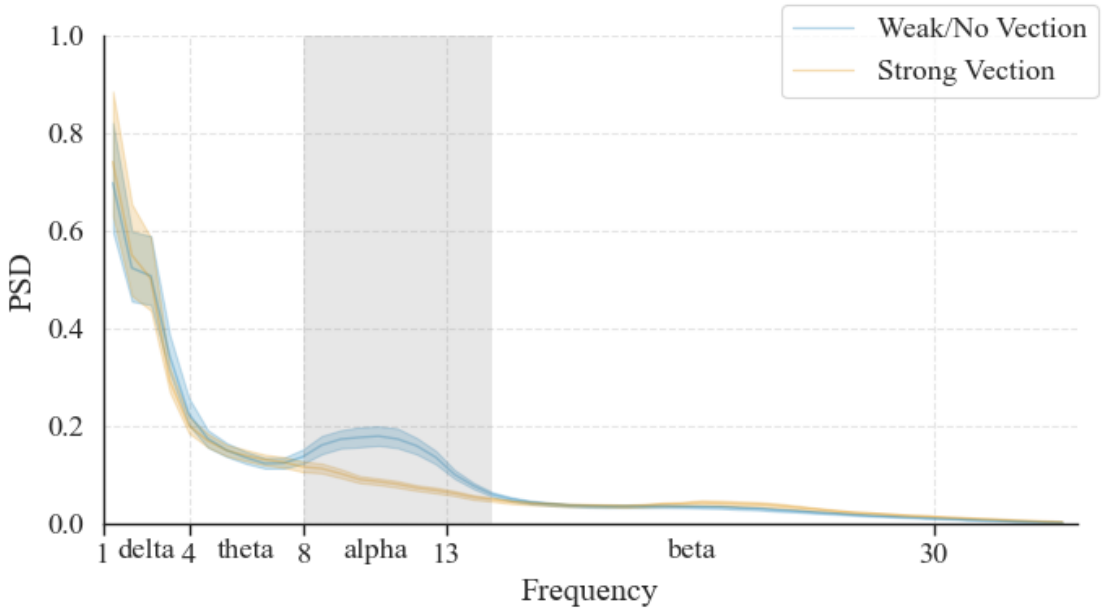

Figure 6.6: *Power spectral density plot comparing* `WV` *&* `NV` *(blue) to* `SV` *(orange) during FA_1 before filtering. The power of the frequencies during the acceleration event is shown, split between the vection conditions. The 95% confidence interval is shown around the line of vection condition. The shaded gray area corresponds to the frequency interval where there was a statistically significant difference between the signals. FA_1 elicits a strong increase of the alpha rhythm, which is suppressed when the subject is experiencing self-motion.*

weak or no vection experiences. We notice a pattern during sudden changes in speed that varies depending on whether the subject experiences vection. As illustrated in Figure 6.4, a robust positive deviation 600ms after stimulus onset in the parietal region during strong vection gradually transitions into a negative deviation towards the frontal region, whereas the reverse pattern is observed for weak or no vection.

Our patterns resemble those observed in vestibular oddball paradigms by Nolan et al. (2012). They investigated brain responses using a high-density EEG setup to an expected yet unpredictable event, also known as an oddball stimulus. In this case, the stimulus was a movement of the chair the participant is sitting in. The study found a robust P3 and P6 component, typical of oddball paradigms, indicating that vestibular changes in heading are processed similarly to oddball stimuli in other sensory modalities, with potential clinical relevance for assessing vestibular function. In their paper, Figure 2 shows a similar P600 to the one shown in this chapter's Figure 6.4, we argue that the similarity in neural patterns hints to identical underlying cognitive processes. Note that their paper induced vection using actual movements of the chair, thus inducing motion perception through visual and vestibular stimulations. Consequently, we hypothesize that unpredictable vection in VR triggers cognitive processes similar to those seen by unpredictable real-world motion.

A similar pattern was also found in the resolution of incongruity in the existing literature (Du et al. 2013; Tu et al. 2014; Wang et al. 2017). Given that the sensation of vection originates from the brain interpreting the VR environment's acceleration as the participant's acceleration, we hypothesize that an incongruity arises due to sensory conflict. This effect, we argue, is meaningfully detectable, as it pertains to the active resolution of this conflict. Notably, the incongruity is absent when participants do not experience vection, as they accurately perceive the environment, not their body, as moving. The absence of such signals in this context can be attributed to the absence of such incongruity.

This interpretation aligns to the sensory conflict theory of cybersickness. Cybersickness is a major problem for widespread VR adoption, with 60–95% of users affected and 6–42% unable to finish their experiment (Caserman et al. 2021; Nesbitt et al. 2017). Understanding the nature of cybersickness is crucial to improving the VR experience and increasing its adoption. Sensory conflict theory is the most common theory of motion sickness and cybersickness (Davis

et al. 2014; Palmisano et al. 2020). This theory posits the discrepancy between the visual, vestibular and proprioceptive senses as expectation and experiences cause cybersickness (Davis et al. 2014). This includes scenarios like perceiving self-motion in VR while remaining physically stationary. Neural activation patterns found in this study may be indicative of the brain's active resolution of such sensory conflicts during vection experiences. They provide valuable insights into the neurophysiological mechanisms underlying cybersickness.

We also found a correlation between vection and Simulator Sickness Questionnaire (SSQ) scores, particularly with Nausea and Disorientation scores. Studies have highlighted the strong relationship between cybersickness and the Nausea and Disorientation scores (Kourtesis et al. 2023; Nesbitt et al. 2017). Therefore, the neuromarker associated with vection may serve as a precursor to cybersickness in VR participants. As vection has often been associated with motion sickness (Nooij et al. 2017), a better understanding of vection will allow for a deeper comprehension of motion sickness, its causes and mechanisms, and help VR designers create experiences that are more comfortable and less likely to cause sickness. Moreover, detecting it in real time can help VR systems reduce motion sickness by adjusting content based on user experience.

This research also opens avenues for future exploration. A promising direction lies in investigating the specific neuromarkers associated with other types of motion. Using a similar setup, studies could also explore if such signals can also be found in the case of backward vection, sideways motion or rotations. Additionally, the discovery of this neuromarker presents an exciting opportunity for the development of a classifier capable of determining whether a user is experiencing vection following an acceleration event. Finally, this new paradigm can help study the neural mechanisms of vection in the brain.

6.5 Conclusion

In this chapter we studied if and how electroencephalography (EEG) could be used to detect vection in VR. We conducted a VR experiment exposing participants to strong forward or backward acceleration while recording reported vection and EEG signals. Our results revealed substantial variability among individuals and a notable influence of the acceleration direction on reported vection. Replicating prior research, we observed a significant effect of vection on alpha power in EEG brain waves. Moreover, the recorded EEG

signals exhibited distinguishable patterns for both acceleration and direction of motion. Finally, we identified a novel event related potential of vection occurring 600ms after forward acceleration. These findings offer insights into vection's neural correlates, and pave the way to automatic techniques for measuring vection and self-motion sensations in VR using EEG recordings.

The identification of acceleration and vection ERPs establishes neural markers for motion perception and self-motion illusion. However, the choice of channels was done through manual evaluation. A more robust approach would consist in mathematically choosing the channels that best separate our conditions of interest. Spatial filtering techniques offer potential solutions for improving the separability and consistency of these neural signatures in real-world applications.

Chapter 7

Spatial filtering techniques for improving Evoked Potentials

> *The advantage of the emotions is that they lead us astray, and the advantage of science is that it is not emotional.*
>
> Oscar Wilde

Prelude — *This chapter, except for the abstract, the first three sentences of the Introduction section (covered in the Introduction), the paper structure outline, the complete experimental setup and preprocessing subsections of the original methodology section (covered in Chapter 4), and the last paragraph of section 7.4, was published as "Enhancing Detection of Acceleration-Related ERPs in VR using Spatial Filtering Techniques" at the EUSIPCO 2025 conference. Paragraphs in italics were added to improve readability. The removed experimental methodology content is comprehensively covered in Chapter 4.*

Following the ERP markers identified previously, this chapter tests linear spatial filtering methods to enhance condition separability and reliability. We evaluate CSP, EMS, and xDAWN on the same dataset to derive channel projections that maximize discrimination of acceleration direction and vection-related responses. The objective is to determine which method yields the most reproducible improvement suitable for integration into passive BCI pipelines.

7.1 Introduction

In our preceding work (Van der Lee et al. 2024), we found novel neural markers associated with acceleration and its direction by analyzing specific electrodes.

Notably, we discovered a significant difference between perceived forward and backward acceleration at the Cz electrode signal, as well as through manual combinations of multiple signals at neighboring electrodes. Motivated by these findings, this study investigates whether linear spatial filtering methods can effectively discriminate acceleration-related EEG signals. To this end, we employ a pipeline combining Independent Component Analysis (ICA) (Jutten et al. 1991) with established linear spatial filtering techniques: Common Spatial Patterns (CSP) (Fukunaga 1990), Effect-Matched Spatial filtering (EMS) (Schurger et al. 2013), and xDAWN (Rivet et al. 2009). By leveraging these filters, we seek to gain deeper insights into the brain's activation patterns during acceleration.

To achieve this goal, we first explore Common Spatial Patterns (CSP), a technique widely used for extracting discriminative spatial filters that maximize variance differences between two conditions in multi-sensor neural data (Fukunaga 1990). CSP optimally decomposes EEG signals into spatial components that best separate experimental conditions by enhancing specific signal variance in one condition while minimizing variance in the other. It has been widely used in motor imagery classification, cognitive state decoding, and clinical applications such as seizure detection (Akuthota et al. 2023). It is particularly effective in motor imagery tasks but is sensitive to inter-trial variability and noise.

Next, we consider Effect-Matched Spatial (EMS) filtering, a technique that extracts a single representative time course from multi-sensor neural recordings by dynamically adjusting a spatial filter at each time point (Schurger et al. 2013). This approach maximizes the signal-to-noise ratio (SNR) while preserving interpretability. Using leave-one-out cross-validation, EMS filtering prevents circularity and ensures unbiased extraction of experimental effects. Unlike PCA or ICA, which capture fixed spatial patterns, EMS filtering directly tracks evolving neural responses. It has been shown to improve single-trial detection and has been applied successfully in cognitive and motor studies.

Finally, we examine the xDAWN algorithm, a spatial filtering technique developed to enhance ERPs, particularly the P300 component, in EEG data

(Rivet et al. 2009). In Brain-Computer Interface (BCI) applications, such as the P300 speller paradigm introduced by Farwell and Donchin (Farwell et al. 1988), users focus on target stimuli that elicit P300 responses, enabling communication without muscular activity. However, P300 signals are often obscured by background EEG activity and noise. The xDAWN algorithm addresses this challenge by estimating spatial filters that maximize the signal-to-signal-plus-noise ratio, effectively enhancing the ERP component.

Despite the widespread adoption of these techniques in different EEG contexts, their relative performance in the context of VR-induced ERPs remains unexplored. This is particularly relevant given the challenges of EEG in VR, such as increased motion artifacts, nonstationary signal properties, and the need for feature extraction methods that generalize across varying stimulus conditions. Understanding how these spatial filtering techniques compare in enhancing EEG features during VR experiences is crucial for optimizing ERP-based VR research and applications. Therefore, this study aims to directly compare these filters in the context of EEG-based VR acceleration perception. We evaluate their performance by assessing (1) filter output separability via bootstrapping and (2) multi-dimensional discriminability using Linear Discriminant Analysis.

7.2 Methodology

This investigation employs the experimental paradigm described in Chapter 4, utilizing the 30-participant dataset. As we only analyze the first acceleration events, denoted FA_1 and BA_1 in Chapter 4, those conditions are refered to in the equations as `FA` *and* `BA`*.*

In the following, tensors are denoted by underlined bold uppercase letters ($\underline{\boldsymbol{V}}$), matrices by bold uppercase letters ($\boldsymbol{X}$), column vectors by bold lowercase letters ($\boldsymbol{w}$), fixed scalars by cursive uppercase letters (C), variable scalars by cursive lowercase letters (f) and methods or conditions in typewriter font (`CSP`, `FA`).

Let $\underline{\boldsymbol{X}} \in \mathbb{R}^{E \times S \times C}$ denote the EEG data tensor, where E is the number of epochs, S the number of samples per epoch, and C the number of channels. Each observation is a channel vector $\boldsymbol{x}_{e,s} \in \mathbb{R}^C$ in an epoch $e \in [0..E-1]$ for a sample $s \in [0..S-1]$. We denote $E_{\texttt{FA}}$ and $E_{\texttt{BA}}$ the number of epochs associated with conditions `FA` and `BA`, respectively ($E = E_{\texttt{FA}} + E_{\texttt{BA}}$). After preprocessing, we have $E_{\texttt{FA}} = 1127$ corresponding to $\underline{\boldsymbol{X}}_{\texttt{FA}}$ and $E_{\texttt{BA}} = 1113$ corresponding to

$\underline{\boldsymbol{X}}_{\texttt{BA}}$, i.e. $\underline{\boldsymbol{X}}_{\texttt{FA}} \in \mathbb{R}^{E_{\texttt{FA}} \times S \times C}$ and $\underline{\boldsymbol{X}}_{\texttt{BA}} \in \mathbb{R}^{E_{\texttt{BA}} \times S \times C}$.

7.2.1 Spatial filtering and analysis

A spatial filter is defined as $\boldsymbol{w} \in \mathbb{R}^C$, implementing a linear mapping $\mathbb{R}^C \to \mathbb{R}$, yielding the virtual electrode output $v_{e,s} = \boldsymbol{x}_{e,s}^\top \boldsymbol{w}$. A set of F spatial filters forms a matrix $\boldsymbol{W} \in \mathbb{R}^{C \times F}$, yielding the virtual electrode vector $\boldsymbol{v}_{e,s} = \boldsymbol{x}_{e,s}^\top \boldsymbol{W} \in \mathbb{R}^F$. We denote the f-th spatial filter from method $\texttt{M}$ as $\boldsymbol{w}_{\texttt{M},f} = (\boldsymbol{W}_{\texttt{M}})_{:,f}$, where $f \in [1..F]$ and $\texttt{M} \in \{\texttt{AVG}, \texttt{CSP}, \texttt{EMS}, \texttt{xDAWN}\}$. The virtual electrode signal for a given method $\texttt{M}$ is then denoted as:

$$\begin{cases} \boldsymbol{V}_{\texttt{M}} = \underline{\boldsymbol{X}} \boldsymbol{w}_{\texttt{M}} \in \mathbb{R}^{E \times S} & \text{if } F = 1 \\ \underline{\boldsymbol{V}}_{\texttt{M}} = \underline{\boldsymbol{X}} \boldsymbol{W}_{\texttt{M}} \in \mathbb{R}^{E \times S \times F} & \text{if } F > 1 \end{cases}$$

We denote the virtual electrode corresponding to the f-th spatial filter from method $\texttt{M}$ as $\boldsymbol{V}_{\texttt{M},f} = (\underline{\boldsymbol{V}}_{\texttt{M}})_{:,f}$. The average spatial filter is defined as $\boldsymbol{w}_{\text{AVG}} = \frac{1}{C}\mathbf{1}$, where $\mathbf{1} \in \mathbb{R}^C$ is the vector of ones. Applied to each observation $\boldsymbol{x}_{e,s}$, it computes the mean across all channels. We apply the average and each of the 3 following filters separately on the data.

Common Spatial Pattern

For our two-condition problem with data $\underline{\boldsymbol{X}}_{\texttt{FA}}$ and $\underline{\boldsymbol{X}}_{\texttt{BA}}$, CSP seeks to find F spatial filters, with $F \in \{1, 2, 4\}$ in our implementation, which are a subset in $\mathbb{R}^{C \times F}$ of the full filter matrix $\boldsymbol{W}_{\texttt{CSP}} \in \mathbb{R}^{C \times C}$, that maximizes the objective function J:

$$J(\boldsymbol{W}_{\texttt{CSP}}) = \frac{\boldsymbol{W}_{\texttt{CSP}}^\top \boldsymbol{\Sigma}_{\texttt{FA}} \boldsymbol{W}_{\texttt{CSP}}}{\boldsymbol{W}_{\texttt{CSP}}^\top \boldsymbol{\Sigma}_{\texttt{BA}} \boldsymbol{W}_{\texttt{CSP}}} \tag{7.1}$$

where $\boldsymbol{\Sigma}_{\texttt{FA}}$ and $\boldsymbol{\Sigma}_{\texttt{BA}}$ are the spatial covariance matrices for the $\texttt{FA}$ and $\texttt{BA}$ conditions (Fukunaga 1990). This objective function is solved as a generalized eigenvalue problem. We keep the top and bottom eigenvectors because the largest and smallest eigenvalues correspond to spatial filters that maximize variance for one condition while minimizing it for the other, capturing the most discriminative information. More CSP components are selected by alternating between the first and last eigenvectors as the number of filters, F, increases.

The projection of the EEG data onto these spatial filters yields virtual electrodes with maximal discriminability between the two conditions. For visualization in Figure 7.1, we use $F = 1$ to highlight the primary spatial pattern. For signal discrimination in Figure 7.3, we evaluate separability

using $F \in \{1, 2, 4\}$ to assess the impact of additional filters. It is important to note that CSP is optimally suited for oscillatory or sustained power differences between conditions, rather than short, phase-locked ERP differences.

Effect-Matched-Spatial Filtering

Unlike other spatial filtering methods that focus on maximizing variance or specific frequency components, EMS is designed to optimize the extraction of experimental effects. The core principle of EMS filtering is to project data, at every sampling time, onto a single spatial filter that maximizes a specific objective function, most commonly the difference between two experimental conditions. EMS computes a separate spatial filter for each sample of the data, denoted $\boldsymbol{w}_{\texttt{EMS},s}$. The optimization problem is solved as follows:

$$\boldsymbol{w}_{\texttt{EMS},s} = \frac{\sum_{e=0}^{E-1} y_e \boldsymbol{x}_{e,s}}{\| \sum_{e=0}^{E-1} y_e \boldsymbol{x}_{e,s} \|} \tag{7.2}$$

where y_e is the label for epoch e, taking $1/E_{\texttt{FA}}$ if epoch e belongs to condition `FA`, and $-1/E_{\texttt{BA}}$ if it belongs to condition `BA`. $\boldsymbol{w}_{\texttt{EMS},s} \in \mathbb{R}^C$ is equivalent to the normalized difference between the mean response in condition `FA` and the mean response in condition `BA` at each sample (Schurger et al. 2013). To obtain a single filter for comparative visualization of all methods, we compute the mean $\boldsymbol{w}_{\texttt{EMS}} = \frac{1}{S} \sum_{s=0}^{S-1} \boldsymbol{w}_{\texttt{EMS},s} \in \mathbb{R}^C$. For evaluating separability, we use both the average filter $\boldsymbol{w}_{\texttt{EMS}}$ and one filter per sample using $\boldsymbol{w}_{\texttt{EMS},s}$.

xDAWN Spatial Filter

xDAWN utilizes the occurrence of the stimuli to enhance the signal-to-noise ratio. Here we apply xDAWN and create filters for each of the two conditions (`FA` and `BA`) separately. xDAWN first estimates the ERP responses, using least squares: $\hat{\mathbf{A}} = (\mathbf{D}^\top \mathbf{D})^{-1} \mathbf{D}^\top \underline{\boldsymbol{X}}$ with $\mathbf{D} \in \mathbb{R}^{S \times 2}$ a Toeplitz matrix encoding the stimulus onsets corresponding to the two conditions. Then, it designs spatial filters $\mathbf{U}$ that maximize the signal to signal-plus-noise ratio where $\mathbf{U} \in \mathbb{R}^{C \times C}$ is the matrix of all spatial filters, of which we keep a reduced filter matrix of size $\mathbb{R}^{C \times F}$.

Finally, the xDawn filter, $\boldsymbol{W}_{\texttt{xDAWN}}$, is estimated as:

$$\boldsymbol{W}_{\texttt{xDAWN}} = \arg\max_{\mathbf{U}} \frac{\mathbf{Tr}(\mathbf{U}^\top \hat{\mathbf{A}}^\top \mathbf{D}^\top \mathbf{D} \hat{\mathbf{A}} \mathbf{U})}{\mathbf{Tr}(\mathbf{U}^\top \underline{\boldsymbol{X}}^\top \underline{\boldsymbol{X}} \mathbf{U})} \tag{7.3}$$

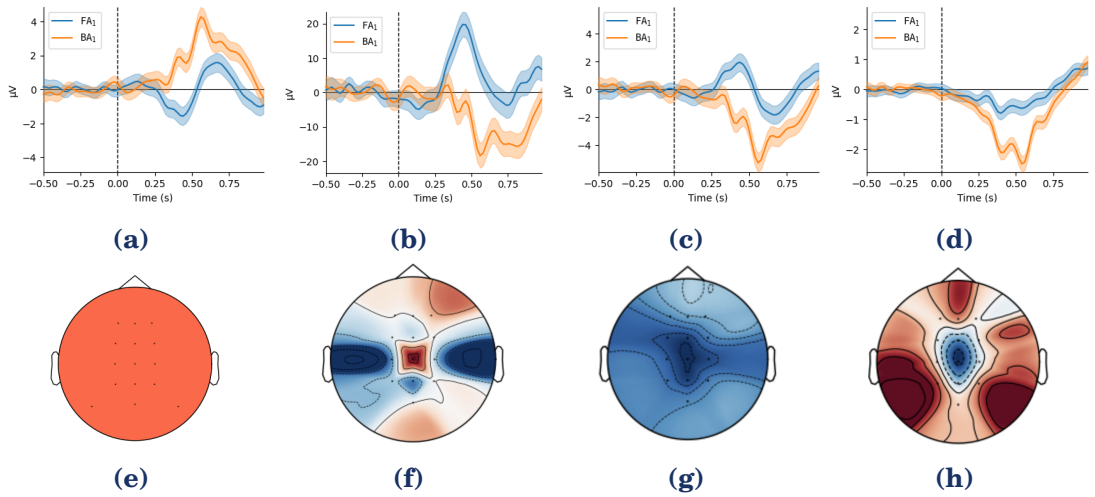

Figure 7.1: *First line: average evoked responses in the two conditions* `FA` *and* `BA` *for signals filtered by (a) the mean filter yielding* $\mathbf{V}_{AVG}$*, (b) the first CSP filter yielding* $\mathbf{V}_{CSP,1}$*, (c) the average EMS filter yielding* $\mathbf{V}_{EMS}$*, and (d) the first xDAWN filter yielding* $\mathbf{V}_{xDAWN,1}$*. Shaded areas indicate the 95% confidence interval over all epochs (*$E_{FA} = 1127$*,* $E_{BA} = 1113$*). Second line: spatial representation of the filters for (e) The average filter* $\mathbf{w}_{AVG}$ *yielding responses in (a), (f) the first filter for CSP* $\mathbf{w}_{CSP,1}$*, (g) the average EMS filter* $\mathbf{w}_{EMS}$*, (h) the first xDAWN filter* $\mathbf{w}_{xDAWN,1}$*.*

where $\mathrm{Tr}(\cdot)$ is the trace operator (Rivet et al. 2009). This optimization problem can be efficiently solved through QR decomposition and singular value decomposition. Separability is computed using $F \in \{1, 2, 4\}$ and visualization using $F = 1$.

7.3 Results & Discussion

7.3.1 Evoked potentials

We analyze the impact of individual spatial filters on the temporal evolution of signal amplitudes. When several filters can be determined, we just keep the most significant ($F = 1$), and compute the 95% confidence interval across epochs. 95% confidence intervals are shown around the response for each condition `FA` and `BA` using a non-parametric bootstrapping approach on 10,000 resamples on our data with replacement. Looking at the average of all electrodes for both conditions Figure 7.1 (a), we find a distinct signal consistent with the results found in (Van der Lee et al. 2024). There is a different signal when looking at the average of all electrodes in each condition `FA` and `BA`.

The CSP algorithm highlights only the component that encodes the most

variance (first component) and effectively modulates the variance of the time series data, increasing variance for the FA condition and decreasing it for the BA condition, as seen in Figure 7.1 (b). However, this variance maximization approach did not optimize ERP separability because, in our paradigm, the main discriminative information is a polarity difference in the phase-locked ERP around Cz, not a sustained change in variance. CSP is designed to maximize variance differences, and is thus suboptimal for brief, phase-locked ERP components where opposite-polarity deflections result in similar variances across conditions. The resulting spatial filter predominantly isolated the signal from the Cz electrode (Figure 7.1 (f)). This observation aligns with our previous findings (Van der Lee et al. 2024), where the Cz electrode was manually found to represent the most pronounced amplitude difference between the FA and BA conditions, suggesting that CSP, in this instance, effectively and automatically identified the electrode with the greatest discriminatory power, albeit not necessarily leading to optimal ERP separability in terms of signal difference.

The CSP-induced modulation of signal variance, specifically the increase in variance for one condition and the decrease for the other, manifests as a discernible difference in the time-frequency representation (TFR). This suggests that CSP effectively alters the frequency content of the signal in a condition-dependent manner. Figure 7.2 shows the significant clusters when looking at the difference of the TFR representation of FA and BA, with a stronger low frequency response (under 6Hz) between 200ms to 600ms after stimulus onset for FA. Time-frequency representations were computed using Morlet wavelets across a logarithmically-spaced frequency range from 1 to 10 Hz (50 frequency points), with the number of cycles adaptively scaled to optimize temporal and frequency resolution. The data were baseline-corrected using a log-ratio transformation relative to the pre-stimulus interval (-0.45 to -0.05 seconds).

To identify statistically significant differences between conditions, we employ a cluster-based permutation approach with 100 permutations and a threshold value of 6.0 from the literature (Maris et al. 2007). This non-parametric statistical method effectively controls for multiple comparisons while taking into account the temporal and spectral adjacency of the time-frequency points. The analysis yields clusters of significant differences ($p \leq 0.05$) between conditions, visualized in Figure 7.2 using a bidirectional color map overlaid on the raw F-statistics, providing a comprehensive view of both statistical significance and effect directionality across the time-frequency

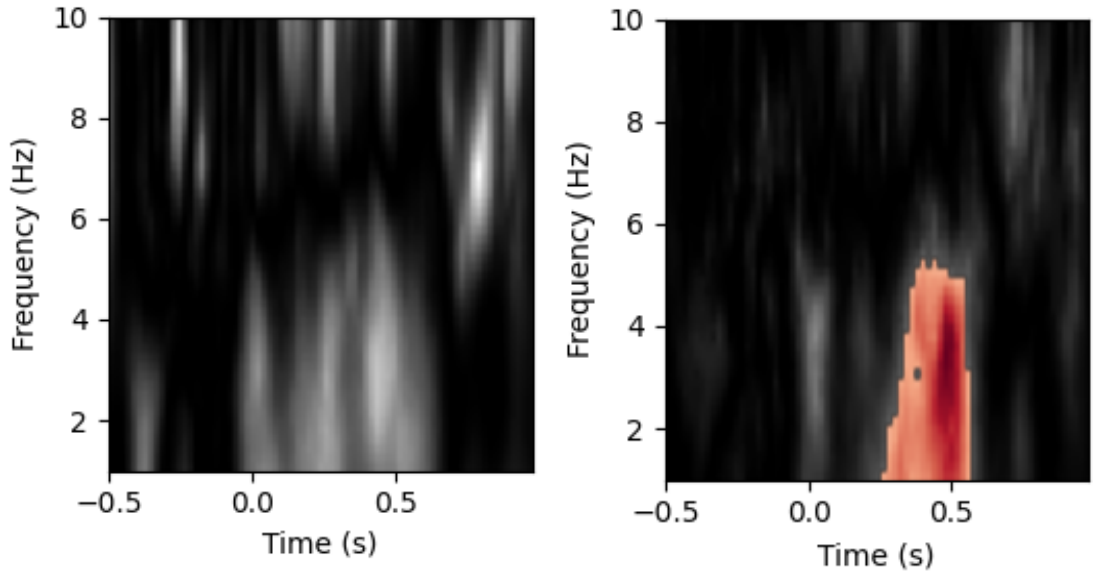

(a) *Original data TFR significant clusters* **(b)** *CSP significant clusters*

Figure 7.2: *(a) Difference (FA vs. BA) of the average time frequency representation (TFR) of each condition. Significant ($p < 0.05$) clusters are only present in (b), with red representing a stronger signal in that band for the FA condition.*

space.

Looking at the result of the average EMS filter $\boldsymbol{V}_{\text{EMS}}$ shown in Figure 7.1(c), EMS appears to primarily invert the original signal, maintaining a near-uniform negative value across all electrodes, as shown in its filter in Figure 7.1 (g). It seems that the EMS filter does not enhance condition separation by differentially weighting electrodes, and assigns nearly equal weight across channels and samples, resulting in a global inversion. A likely explanation is that the unfiltered data already exhibits a difference between conditions, the EMS filter did not succeed in making this difference more pronounced. Because $\boldsymbol{w}_{\text{EMS},s}$ is estimated independently at every sample, the method does not enforce any relationship between successive filters. When looking into individual time series, we observed that small fluctuations can flip the sign of $\boldsymbol{w}_{\text{EMS},s}$ from one sample to the next, yielding an erratic sequence of spatial patterns. This "sign-flipping" may cancel out slower ERP components that can only be seen when the whole epoch is considered jointly. Moreover, even when examining the sample-resolved EMS filters, the spatial filter remains relatively uniform and constant with negative values after $t = 0.2s$.

Finally, the xDAWN seems to yield superior separability between the FA and BA events compared to CSP and EMS (Figure 7.1 (d)). The selected filter maximizes the SNR for BA. The resulting signal exhibits a strong negative peak

throughout the observed epoch, and effectively minimizes the FA amplitude. The spatial patterns associated with xDAWN reveal a specific topographical weighting (Figure 7.1 (h)). The selected filter is strongly weighted by a negative component centered on the Cz electrode, with the surrounding electrodes having positive weights, isolating the signal of interest and effectively minimizing the other condition. This improved performance is likely attributable to xDAWN's design, which is specifically tailored to enhance the signal-to-noise ratio of ERPs and maximize the discriminability between different ERP conditions, unlike CSP and EMS which optimize for variance or reconstruction error, respectively.

7.3.2 Condition-Separability Analysis

Filter performance is also assessed via a quantitative metric of condition separability. We employ Linear Discriminant Analysis (LDA) not to maximize absolute accuracy, but to provide a standardized, interpretable metric for comparing the separability achieved by each filtering method across different numbers of filters and training epochs. This approach enables quantitative evaluation of filter performance beyond visual inspection, allowing comparison in higher-dimensional feature spaces. We use a stratified k-fold cross-validation procedure (k=5) to ensure robust and unbiased assessment. For each spatial filter method (Average, CSP, xDAWN, and EMS), a two-stage pipeline is implemented: first, the spatial filter is fit to the training data and applied to the training set. A LDA model is then fitted on this output. Then the testing set is used for evaluating the filter. The stratification in the cross-validation procedure preserved the proportion of samples for each condition across folds, ensuring balanced evaluation. Curves of class separability were generated by incrementally increasing the number of epochs used for model fitting in ten equal steps, while maintaining the complete test set for evaluation. Each filter is evaluated across multiple settings as described in subsection 7.2.1. Namely 1, 2 and $F = 4$ filters for xDAWN and CSP, and 1 or S filters for EMS. Class separability results can be found in Figure 7.3.

The separability of features extracted by CSP yields significantly lower accuracy compared to EMS, xDAWN, and the average. Among the tested methods, xDAWN achieved the highest condition separability, a finding that corroborates the enhanced ERP separability observed in the evoked potential plots in Figure 7.1. xDAWN performance improved significantly when fitting

more than one filter. This allows the method to fit one filter per condition, and maximize the SNR for each condition independently, resulting in more distinguishable features. These results provide further quantitative evidence that xDAWN effectively enhances the discriminability of event-related potential signals, leading to improved separation between the `FA` and `BA` conditions. EMS exhibited strong performance, particularly with a lower number of epochs, matching xDAWN and surpassing it for $F = 1$. However, it did not scale as effectively and plateaued as the filter is applied to larger datasets.

CSP did not perform as well as the other filters. This might be due to the fact that the effectiveness of CSP relies on the assumption that the discriminative information between conditions is primarily contained in the variance of the signals rather than in their temporal patterns or phase relationships. This makes CSP particularly well-suited for analyzing oscillatory neural activity but potentially less effective for event-related potentials where temporal dynamics are critical.

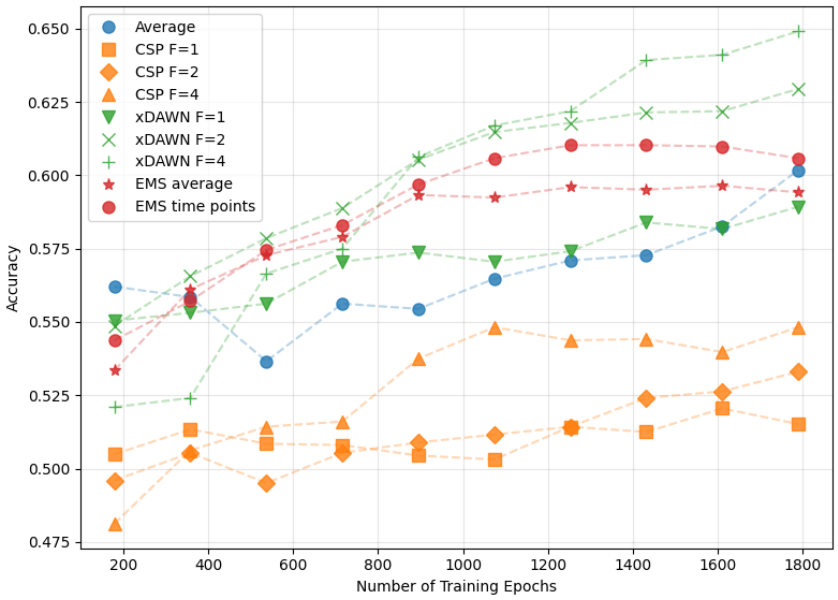

Figure 7.3: *Condition separability (measured by LDA accuracy) over number of training epochs for each spatial filter. The Average filter is compared to CSP with $F \in \{1, 2, 4\}$, to xDAWN with $F \in \{1, 2, 4\}$ and to EMS with one filter per sample or the average filter of all samples applied to the whole time series (w_{EMS} or $w_{EMS,s}$).*

All three spatial filtering techniques demonstrate high computational efficiency, with inference requiring only a matrix-vector multiplication, making them highly suitable for real-time applications. Furthermore, training these filters is also feasible for online scenarios: processing all 2240 epochs on an

Apple M1 processor took 1.03 s for xDAWN, 1.10 s for CSP, and 1.55 s for EMS.

7.4 Conclusion

This study performed a systematic comparison of spatial filtering techniques for enhancing acceleration-related ERPs from EEG data in VR. xDAWN outperformed CSP and EMS in ERP class separability. While EMS was not the most efficient method, future work could explore time smoothing techniques to improve its temporal consistency. CSP isolated the Cz electrode and modulated time-frequency representations, revealing enhanced low-frequency activity. xDAWN, designed for ERP enhancement, yielded distinct spatial filters and the best performance among all tested filters for our use case. Future work could (i) evaluate non-linear methods to improve performance and (ii) adapt the filters on a per-subject and single-trial basis for online use.

The methods compared here, together with the neural markers reported in previous chapters, inform the analysis of motion-related ERPs in VR. The following discussion synthesizes these empirical findings in the context of cybersickness research and potential applications to adaptive VR systems.

Chapter 8

Discussion

> *I began to realize how important it was to be an enthusiast in life. He taught me that if you are interested in something, no matter what it is, go at it at full speed ahead. Embrace it with both arms, hug it, love it and above all become passionate about it. Lukewarm is no good. Hot is no good either. White hot and passionate is the only thing to be.*
>
> Roald Dahl

8.1 Revisiting Research Objectives

This dissertation addressed three overarching objectives derived from gaps in the literature on cybersickness, vection, and brain-computer interfaces.

Objective 1: Map the research landscape of BCIs, cybersickness, and vection, including neural markers, algorithms, and methodologies. The Introduction reviewed the broader landscape, and the systematic reviews presented in Chapter 2 and Chapter 3 revealed both promising results and substantial heterogeneity in stimuli, hardware, protocols, and reporting practices. This fragmentation limits cumulative understanding of neural correlates of motion perception and cybersickness. It also highlighted the need for a more fundamental understanding of how cybersickness and vection arise.

Objective 2: Explore potential neuromarkers for understudied aspects of cybersickness and acceleration perception. Previous studies primarily

relied on retrospective self-report measures and correlation-based analyses, which lack temporal resolution and cross-subject comparability. Our investigation characterized acceleration-related ERPs (Chapter 5) and vection-specific neural responses (Chapter 6), addressing these methodological gaps. However, a low signal-to-noise ratio especially for the vection ERP encouraged us to improve signal quality.

Objective 3: Contribute to better identification of VR user experience markers suitable for adaptive applications. The spatial filtering evaluation (Chapter 7) demonstrated that xDAWN outperforms Common Spatial Patterns (CSP) and Effect-Matched Spatial (EMS) filtering for enhancing acceleration ERPs, providing a practical foundation for real-time passive BCI implementations.

8.2 Novel Contributions

8.2.1 Neurophysiological Understanding of Motion Processing in VR

First Characterization of Neural Responses to Sudden Acceleration

The acceleration ERP provides the first systematic characterization of neural responses to sudden visual acceleration in virtual reality, establishing a causal, time-locked link between stimulus onset and neural response. Emerging 300–700 ms post-stimulus with a fronto-central positivity, this component represents the neural encoding of sudden changes in optic flow velocity. Direction-sensitive activity at the Cz electrode indicates parallel processing streams for forward and backward acceleration, suggesting that the brain differentiates motion direction at early perceptual stages.

This finding situates acceleration processing within established multisensory and self-motion ERP literature (Nakul et al. 2021; Nolan et al. 2012). The temporal characteristics align with visual motion processing and vestibular integration pathways documented in studies of heading detection and self-motion perception (Dichgans et al. 1978; Harquel et al. 2020).

First Evoked Potential Linked to Subjective Vection

The vection P600 is the first evoked potential reliably linked to the subjective perception of self-motion in VR (Chapter 6). Characterized by a positive peak in the parietal region and a simultaneous negative peak in the frontal region approximately 600 ms post-stimulus, this component bridges stimulus-locked neural responses with subjective perceptual experience.

The bipolar parietal-frontal topography resembles cognitive conflict and incongruity resolution components documented in ERP literature (Du et al. 2013; Nolan et al. 2012; Tu et al. 2014; Wang et al. 2017). Its temporal and spatial profile aligns with late positive complexes associated with context updating and conflict monitoring (Polich 2007), as well as vestibular oddball paradigms (Nolan et al. 2012). This pattern suggests that the vection P600 could reflect active resolution of sensory conflict during visually induced self-motion.

Objective Neuromarker of Subjective Experience

A central contribution of this work is the identification of an objective, inter-subject neuromarker corresponding to the subjective experience of vection. Finding a reliable ERP marker for a subjective perceptual state enables cross-subject comparisons and demonstrates common neural processes underlying individual variability in vection susceptibility. This approach complements established self-report instruments used to assess sickness in VR, such as the SSQ and VRSQ (Kennedy et al. 1993; H. K. Kim et al. 2018).

Beyond VR, identifying an inter-subject ERP marker of a subjective state contributes to a wider neuroscience goal of robust, comparable biomarkers across individuals and contexts. Positioned within the broader biomarker literature, such cross-subject ERP markers provide a practical bridge between laboratory neuroscience and deployable neuroadaptive systems.

8.2.2 Temporal Relationship of Motion Processing

The experimental findings reveal a temporal relationship in motion processing that unfolds sequentially from sensory encoding to subjective perception.

Hierarchical processing sequence:

- **Acceleration perception** (300–700 ms, fronto-central positivity): initial neural response to sudden changes in visual motion, with direction-sensitive activity at Cz.
- **Subjective vection experience** (600 ms, parietal positivity / frontal negativity): reflects higher-order processing associated with the conscious perception of self-motion.

This temporal sequence suggests that initial sensory encoding of acceleration precedes the neural processes underlying vection. The hierarchical picture integrates with predictive-processing accounts of perception, where early prediction-error signals precede higher-order model updating during multisensory conflict (Nürnberger et al. 2021).

8.2.3 Methodological Innovations

Spatial filtering evaluations demonstrated that xDAWN outperforms Common Spatial Patterns (CSP) and Effect-Matched Spatial (EMS) filtering for enhancing ERPs in VR (Chapter 7). xDAWN's design for time-locked responses makes it particularly suitable for ERP-based VR research. Computational efficiency permits real-time application in passive BCIs, though single-trial detection remains challenging due to inter-subject variability.

Evaluating xDAWN against CSP and EMS situates this work within established ERP enhancement methods in brain-computer interfacing (Mason et al. 2003; Wolpaw et al. 2012). That xDAWN performs best for time-locked responses reinforces its role in real-time neurotechnology, where computational efficiency and latency bounds are critical for safe, closed-loop adaptation.

Methodologically, the time-locked, low-channel ERP approach used here complements large-scale initiatives advocating standardized acquisition and sharing (e.g., BIDS-style practices, (Pernet et al. 2019)), facilitating reproducible, cross-lab comparisons. This aligns with community movements toward standardized, reproducible pipelines for time-locked neural signals in naturalistic tasks, enabling cross-lab benchmarking.

8.3 Theoretical Implications

8.3.1 Evidence for Sensory Conflict Theory

The vection P600 provides measurable evidence of neural processes consistent with sensory conflict theory, historically foundational to understanding visually induced motion sickness (Dichgans et al. 1978; LaViola 2000; McCauley et al. 1992; Stanney et al. 1997). Its topography aligns with alpha-band inhibitory control mechanisms and cognitive conflict processing (Harquel et al. 2020; Klimesch et al. 2007), suggesting that the neural response to visually induced motion involves both sensory integration and conflict monitoring processes. The vection P600 could constitute a reflection of active sensory conflict resolution, bridging subjective perception with objective neural measures.

Critically, stronger vection correlates with higher nausea and disorientation, suggesting that individual differences in conflict resolution efficiency may modulate susceptibility to cybersickness. Taken together, the acceleration ERP and its timing relative to the vection-related P600 could provide a time-resolved neural correlate of visually induced sensory conflict underlying vection, in line with the **vection conflict hypothesis** (Hettinger et al. 1990). This hierarchical sequence is further supported by the observed symptom-linked variability: as detailed in Chapter 6, increases in reported vection were significantly correlated with increases in SSQ scores, particularly in nausea and disorientation subscales. Figure 8.1 demonstrates this relationship across all SSQ subscales, showing that higher vection intensity ratings are systematically associated with increased simulator sickness symptoms. This convergence of neural and behavioral evidence strengthens the case for the vection conflict hypothesis in VR, highlighting both objective and subjective markers of sensory conflict.

The theoretical insights extend beyond VR to other contexts where visual–vestibular conflicts arise, including simulators, automotive, and maritime/aviation environments (Caserman et al. 2021; Min et al. 2004). However, transferability of the specific ERPs identified here remains to be established empirically. Future research could systematically disentangle competing theories of cybersickness by:

- Attempting to induce sickness without vection to test the vection-conflict hypothesis.

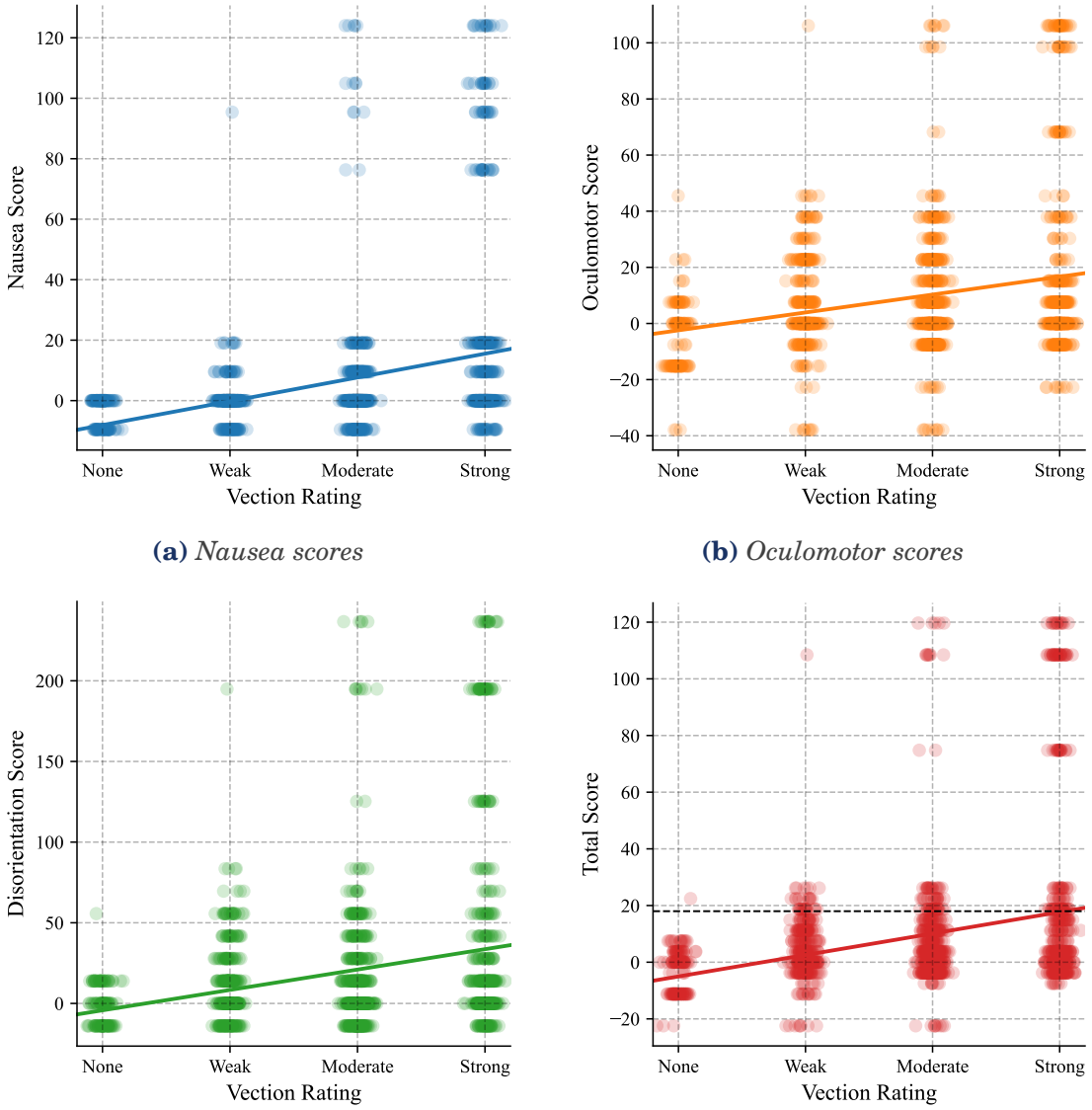

(a) *Nausea scores*

(b) *Oculomotor scores*

(c) *Disorientation scores*

(d) *Total SSQ scores*

Figure 8.1: *Relationship between vection intensity and simulator sickness symptoms across experimental blocks from the Chapter 4 experiment. (a) Nausea scores, (b) Oculomotor scores, (c) Disorientation scores, and (d) Total SSQ scores plotted against vection intensity ratings. Data points represent individual vection responses within each block, with scores adjusted by subtracting baseline values. Solid lines indicate linear regression fits. Usually, a Total Score above 18 is considered "sick" (Cortes et al. 2023b). This threshold is represented as a dotted line in (d). Higher vection intensity ratings are associated with increased simulator sickness symptoms across all measured dimensions.*

- Testing alternative mismatches (visual-auditory conflicts, reversed Doppler effects) to examine the Subjective Vertical Mismatch Theory or predictive coding hypothesis.
- Designing experiments that directly contrast vection conflict, predictive coding, and postural instability theories.
- Isolating sensory conflict variables. For example, reversing the vection situation, with vestibular motion but no matching visual motion.

8.3.2 Predictive Coding Framework

The acceleration ERP may represent detection of prediction errors when visual motion violates the observer's internal model, while the vection P600 corresponds to model updating (Nürnberger et al. 2021). This framework complements sensory conflict theory by providing a mechanistic account for how the brain resolves discrepancies between expected and observed sensory input.

Participants with rapid vection onset may possess more flexible predictive models, whereas resistant participants maintain rigid priors, consistent with individual differences in neural processing efficiency (Gevins et al. 2000). The hierarchical sequence of acceleration processing followed by vection experience fits naturally within Bayesian accounts of multisensory integration, where early error signals trigger subsequent model revision.

8.4 Integration Across Studies

8.4.1 Cross-Study Synthesis and Robustness

Acceleration ERP characteristics remained stable across the initial 20-participant cohort and the expanded 30-participant dataset, supporting the replicability of these neural markers. Vection P600 findings extend the acceleration ERP foundation, supporting systematic hierarchical investigation of motion perception in VR.

Replication across cohorts supports current field-wide priorities on robustness and generalizability. Framing the analyses with sharable, time-locked pipelines encourages adoption in comparative studies and meta-analyses across laboratories.

8.4.2 Individual Differences and Systematic Variability

Significant inter-subject variability in acceleration sensitivity and vection susceptibility demonstrates that individual differences are systematic rather than noise (Park et al. 2008). These differences can predict cybersickness risk and inform the development of personalized adaptive VR interventions.

The neuromarker enables objective comparison across participants, overcoming limitations of subjective reporting and providing a foundation for understanding why some users experience stronger vection and cybersickness than others.

8.5 Practical Implications for Neuroadaptive VR

8.5.1 Real-Time VR Applications and Latency Constraints

As Vection has been linked to cybersickness, rapid detection during known sudden acceleration events using xDAWN may permit interventions such as field-of-view reduction, velocity modulation, or stabilizing visual cues (Uyan et al. 2024; Zander et al. 2011). However, single-trial variability remains a challenge; algorithms must account for inter-subject differences while maintaining temporal precision.

Adaptive strategies must balance cybersickness mitigation with preservation of immersion. Excessive adaptation may reduce user engagement, while insufficient adaptation may fail to prevent symptoms. Fine-grained, ERP-guided adjustments offer a quantitative approach for optimizing this balance. The findings contribute to neuroadaptive VR, where user-state estimates drive real-time content changes (Yadav et al. 2020). Predictive models can extend these reactive adjustments by anticipating sickness onset and triggering preventive interventions before symptoms emerge. Combining acceleration and vection ERP markers with kinematic signals, headset telemetry, and recent symptom history enables short-horizon forecasts of discomfort. Such forecasts can drive proactive mitigation techniques such as field-of-view reduction, transient visual anchors, or subtle velocity smoothing during high-risk segments, then restore full immersion once risk subsides. Evaluating these strategies requires quantifying latency, signal trial noise, false-alarm costs, and user acceptance to ensure that preventive adaptations reduce symptoms without

degrading presence.

8.6 Critical Evaluation and Limitations

8.6.1 Methodological Constraints

The 14-electrode EEG montage limits source localization and network-level interpretation. Low-density EEG and controlled stimuli reflect a broader neuroergonomics trade-off between ecological validity and measurement fidelity; acknowledging this situates the work alongside field-ready neuroscience that prioritizes deployability.

Controlled visual stimuli (white spheres on dark background), though necessary to isolate ERPs, may not generalize to complex, naturalistic VR environments. The participant sample consisted of young, healthy adults, limiting the generalizability of results to older adults or individuals with vestibular or visual impairments. These trade-offs mirror wider challenges in field-deployable neuroscience, balancing measurement precision with ecological validity and scalability.

8.6.2 Technical Constraints

Variability in ERP morphology, amplitude, and latency complicates single-trial classification. Real-time detection requires balancing signal quality, artifact rejection, and processing speed. Inter-subject variability in ERP morphology challenges generalized classification algorithms.

Factors such as fatigue, engagement, demographic factors and environmental conditions may influence neural responses, potentially reducing ecological validity. Temporal precision is critical; sustained attention and stable context are necessary for reliable neuromarker detection in practical applications. Crucially, the robustness of the results would be greatly enhanced by a bigger and more varied participant pool for the vection experiment.

8.7 Future Research Directions

8.7.1 Short-Term and Immediately Feasible Objectives

The immediate research priorities focus on consolidating and extending the methodological foundations established in this dissertation. Applying the xDAWN spatial filtering technique to vection data will improve signal-to-noise ratio and classification accuracy for the vection P600, enabling more robust single-trial detection. This represents a natural extension of the spatial filtering work presented in Chapter 7 and will directly inform the development of real-time classification algorithms.

Developing classification algorithms for acceleration and vection ERPs suitable for online, real-time detection constitutes a critical step toward practical neuroadaptive applications. These algorithms must balance temporal precision with inter-subject variability, incorporating adaptive thresholds and personalized calibration procedures. Success in this objective will determine the feasibility of deploying ERP-based interventions in consumer VR systems.

A logical next step would be to investigate vestibular and visual stimulation separately to improve our understanding of the sensory processing mechanisms underlying the identified ERPs. To this end, we designed the PECS (Potentiels Evoqués par des Conflits Sensoriels) experimental protocol, outlined in detail in Appendix A, which decouples physical and visual motion to examine how the brain processes congruent, incongruent, and absent multisensory signals. Participants experienced forward or backward physical motion in a motorized wheelchair while visual motion in VR was either congruent (same direction in VR and in real life), incongruent (inverted direction), or absent (immobile in VR). Analyzing pilot data from the PECS experimental protocol will provide initial insights into sensory integration when physical motion and visual motion are decoupled. This paradigm extends the dissertation's findings by examining whether acceleration and vection ERPs persist, reverse, or exhibit novel patterns when vestibular input contradicts or complements visual input, offering a critical test of the sensory conflict framework.

8.7.2 Medium-Term Objectives

Expanding the PECS dataset with additional participants will enable robust statistical analysis of neural correlates when physical and visual motion are systematically decoupled. Understanding how the brain integrates congruent, incongruent, and absent multisensory motion signals will clarify the neural mechanisms underlying both vection and cybersickness, potentially identifying distinct ERP signatures for different types of sensory conflict. This work has direct implications for motion simulator design, autonomous vehicle interfaces, and rehabilitation protocols involving virtual environments.

Investigating neuromarkers specifically linked to cybersickness-inducing vection is essential for distinguishing benign self-motion perception from pathogenic responses that trigger symptoms. Not all vection leads to cybersickness; identifying the neural signatures that differentiate symptom-free from symptom-inducing vection will enable targeted interventions. This may involve comparing ERP characteristics between participants who report strong vection with minimal symptoms versus those who develop nausea and disorientation, potentially revealing differences in conflict resolution efficiency or predictive model updating.

Increasing participant diversity and sample size for the vection study will strengthen the generalizability and statistical power of the findings. Recruiting participants across a broader age range, and diverse prior VR experience will clarify whether the identified ERPs represent universal neural responses or are modulated by individual traits and expertise. This is particularly important for translating findings to a more diverse population, who may exhibit different susceptibility profiles, depending on origin, sex etc.

Source localization and connectivity analysis using high-density EEG or combined EEG-fMRI will map the cortical and subcortical networks underlying acceleration perception, vection, and sensory conflict resolution. Identifying whether the acceleration ERP originates from early visual motion areas or multisensory integration hubs, and whether the vection P600 reflects parietal-frontal network interactions, will provide mechanistic insights into the hierarchical processing sequence. Connectivity analyses can reveal how information flows between sensory encoding, conflict monitoring, and predictive model updating stages.

8.7.3 Long-Term Objectives and Real-World Applications

Long-term research directions aim to validate and extend the identified neuromarkers to naturalistic contexts and diverse populations, while translating findings into practical applications that benefit both scientific understanding and public health.

Ecological validity and expanded motion paradigms. Validating ERP markers across naturalistic VR environments, including navigation, gaming, and training simulations, will establish whether the controlled, linear acceleration paradigm generalizes to complex, interactive scenarios with multiple motion directions (sideways, backward, rotations, and combined translations). Ecological validity is critical for consumer VR adoption, as most applications involve rich, unpredictable motion rather than simple linear vection. Testing whether the acceleration ERP and vection P600 remain detectable amid complex visual scenes, user-driven motion, and cognitive load will determine the robustness of these markers for real-world deployment.

Multisensory integration with vestibular stimulation. Incorporating physical vestibular stimulation through motion platforms or galvanic vestibular stimulation will examine how congruent vestibular input modulates or suppresses the visual acceleration and vection ERPs. This addresses a fundamental question: do these ERPs reflect purely visual processing, or do they represent multisensory prediction errors that diminish when vestibular signals align with visual motion? Understanding this will inform the design of motion simulators for training (e.g., flight, driving) and rehabilitation (e.g., vestibular therapy), where matching or deliberately mismatching sensory cues can optimize learning or therapeutic outcomes.

Demographic and clinical generalizability. Expanding the demographic scope to include older adults, individuals with vestibular dysfunction, and clinical populations (e.g., patients with migraine, motion sickness susceptibility, or anxiety disorders) will assess whether acceleration and vection ERPs are modulated by age, sensory impairments, or comorbidities. For example, individuals with vestibular hypofunction may rely more heavily on visual motion cues, potentially exhibiting different vection ERPs. Conversely, older adults with reduced neural plasticity may show attenuated or delayed ERPs. Identifying these patterns can guide personalized VR interventions and inform clinical assessments of vestibular integrity and sensory integration.

Closed-loop BCI systems for adaptive VR. Developing closed-loop BCI

systems that adapt VR content in real time based on detected acceleration and vection ERPs represents the ultimate translational goal of this research. Such systems could dynamically adjust field-of-view, velocity profiles, or stabilizing visual anchors within the critical 600 ms window to prevent vection onset or mitigate cybersickness before symptoms escalate. Real-time neuromarker classification across participants remains challenging due to inter-subject variability, but advances in machine learning and personalized calibration may enable practical implementations. Applications extend beyond entertainment to training (reducing simulator sickness in pilots, drivers, surgeons), accessibility (customizing VR experiences for individuals with sensory sensitivities), and therapeutic contexts (gradual exposure therapy for phobias or vestibular rehabilitation).

Real-world safety and monitoring applications. Beyond VR, real-time detection of acceleration perception has potential applications in automotive safety and attention monitoring. For instance, detecting whether a driver's brain is processing visual acceleration cues from the road ahead, versus showing attenuated responses indicative of distraction or drowsiness, could inform advanced driver-assistance systems. Similarly, monitoring vection-related neural responses in pilots or operators of heavy machinery could provide objective indicators of spatial disorientation or fatigue, complementing behavioral measures. While such applications require extensive validation and miniaturized, unobtrusive EEG systems, the foundational neuromarkers identified here provide a starting point.

Understanding individual differences and susceptibility. Investigating how individual differences in acceleration sensitivity and vection susceptibility relate to health, cognitive traits, and lifestyle factors will clarify the sources of inter-subject variability. For example, vection responses may differ systematically between individuals with high versus low motion sickness susceptibility, those with vestibular training (e.g., dancers, athletes), or those with neurological conditions affecting multisensory integration. Linking ERP characteristics to personality traits (e.g., field dependence), cognitive flexibility, or neurophysiological measures (e.g., resting-state EEG) could enable predictive screening for VR compatibility and personalized content recommendations.

Interactions between vection, presence, immersion, and cybersickness. Examining how motion perception, vection, presence, and immersion interact will provide a holistic understanding of the VR user experience. Vec-

tion enhances presence, but also increases cybersickness risk. Investigating whether acceleration and vection ERPs correlate with presence ratings, and whether interventions that reduce cybersickness inadvertently diminish immersion, will inform design trade-offs.

Additionally, it would be valuable to understand anticipatory effects. Investigations could present a predictable vection stimulus and investigate whether there is a neuromarker of anticipation prior to the stimulus, how it affects vection and cybersickness, and if it modulates the observed vection neuromarker once the stimulus starts.

Disentangling cybersickness theories. Designing experiments that systematically contrast competing theories (sensory conflict, predictive coding, and postural instability) will advance theoretical understanding. For instance, inducing cybersickness without vection (e.g., through postural perturbations or visual flicker) and comparing neural signatures to vection-induced sickness can test whether the vection P600 is specific to conflict-based mechanisms. Testing visual-auditory conflicts (e.g., Doppler shifts incongruent with visual motion) or manipulating predictive model priors (e.g., through training) can isolate prediction-error signaling from sensory mismatch. Such mechanistic studies could refine theoretical models and inform targeted interventions tailored to specific etiologies.

The PECS protocol can also contribute to this area of study through separation of the vestibular and visual stimuli. It will allow us to investigate if cybersickness occurs in the same way when the subject is mobile vs immobile, across visual stimuli.

8.8 Positioning Within the Broader Scientific Landscape

This work connects accounts of multisensory perception with deployable BCIs. By identifying inter-subject ERP markers of acceleration and vection, evaluating real-time capable spatial filters, and articulating latency constraints for adaptation, the dissertation contributes to ongoing agendas in predictive processing (Nürnberger et al. 2021), neuroergonomics (Wolpaw et al. 2012), and human-computer interaction (Mason et al. 2003; Yadav et al. 2020).

Related domains such as simulators have established measurement frameworks for sickness and user state (Kennedy et al. 1993; Stanney et al. 1997).

While our methods motivate exploration beyond VR, their applicability must be validated. This work also underscores open, standardized (Pernet et al. 2019) practices. Standardizing VR/EEG reporting and datasets will enable cross-site benchmarking and challenge tasks, facilitating sensor-fusion models consistent with predictive processing. Translational studies in training, rehabilitation, and accessibility can leverage objective motion-perception markers to personalize content and improve user experience.

8.9 Concluding Remarks

This dissertation demonstrates that EEG can provide objective, inter-subject markers of subjective motion perception in virtual reality. The identification of acceleration and vection ERPs establishes temporal and hierarchical neural pathways underlying motion perception, linking early sensory encoding to conscious perceptual experience.

While these findings do not resolve all questions regarding cybersickness, they provide a framework for future investigations, integrating sensory conflict, predictive coding, and adaptive VR applications. The results situate vection and cybersickness within general principles of multisensory inference and neuroadaptive control, contributing transferable methods and markers to the broader scientific landscape of human neuroscience, neuroergonomics, and immersive technologies.

Chapter 9

Conclusion

> *Reality is that which, when you stop believing in it, doesn't go away.*
>
> Philip K. Dick

9.1 Summary of Principal Achievements

This dissertation established the first objective, inter-subject neural markers linking visual motion perception to subjective vection experience in virtual reality. By characterizing the acceleration-related ERP (300–700 ms, fronto-central positivity) and the vection-specific P600 component (600 ms, parietal positivity with frontal negativity), this work provides time-locked neural measures that complement established self-report instruments.

These findings reveal a temporal processing hierarchy: early sensory encoding of visual acceleration precedes higher-order neural correlates of subjective vection, with both showing significant correlations to cybersickness symptoms. The demonstration that xDAWN spatial filtering outperforms alternative methods for ERP enhancement provides a computationally efficient foundation for real-time passive BCI applications.

9.2 Significance and Impact

9.2.1 Theoretical Contributions

The vection P600 provides measurable evidence consistent with sensory conflict theory, historically foundational to understanding visually induced motion sickness. Its bipolar parietal-frontal topography aligns with cognitive conflict processing, suggesting active sensory conflict resolution during visually induced self-motion. The hierarchical temporal sequence, from acceleration perception (300–700 ms) to subjective vection experience (600 ms), integrates naturally with predictive-processing frameworks, where early prediction-error signals precede higher-order model updating during multisensory conflict.

Importantly, stronger vection correlated with higher nausea and disorientation, supporting the vection conflict hypothesis and suggesting that individual differences in conflict resolution efficiency may modulate cybersickness susceptibility.

9.2.2 Methodological and Practical Impact

Identifying an objective, inter-subject neuromarker of subjective vection experience contributes to the broader neuroscience goal of robust, comparable biomarkers across individuals and contexts. This complements established self-report instruments (SSQ, VRSQ) with time-locked neural measures suitable for real-time detection.

The xDAWN spatial filtering evaluation situates this work within established ERP enhancement methods for brain-computer interfacing, demonstrating computational efficiency suitable for latency-constrained, closed-loop neuroadaptive VR systems. Rapid ERP detection enables interventions such as field-of-view reduction, velocity modulation, or stabilizing visual cues to mitigate cybersickness while preserving immersion.

9.3 Evolution of the Field and Future Vision

9.3.1 A Field in Transformation

The landscape of VR neuroscience has transformed substantially during the course of this doctoral research. When this work began, the field focused primarily on detecting cybersickness after it occurred, treating it as an unavoidable side effect to be measured and reported. The research questions centered on whether neural correlates of cybersickness could be identified at all, with limited consideration of what those correlates might reveal about underlying mechanisms.

The field has since matured considerably. Research objectives have broadened from simple detection to encompass mitigation strategies, mechanistic understanding, and source localization of neural processes. Contemporary investigations increasingly ask not just *whether* we can detect cybersickness, but *why* it occurs, *how* sensory conflicts propagate through neural hierarchies, and *when* interventions can prevent symptoms before they manifest. This shift from reactive measurement to proactive understanding represents a fundamental reorientation of the research agenda.

The volume and sophistication of research in this domain has accelerated markedly. The systematic reviews presented in Chapter 2 and Chapter 3 documented rapid growth in publication rates, with increasing methodological rigor and reproducibility standards. Cross-laboratory collaborations, standardized protocols, and open datasets are increasing in occurence. This growing momentum suggests the field is transitioning from exploratory investigations to systematic theory building.

Perhaps most promising is the convergence of hardware and methodology. Integrated systems combining VR, EEG, and multimodal biometrics are emerging from research prototypes into commercially available platforms. The Galea headset[1], exemplifies this convergence: a consumer-ready device providing synchronized EEG, eye tracking, physiological monitoring, and high-fidelity VR within a single system. Such platforms eliminate technical barriers that previously limited neuroadaptive VR research to specialized laboratories with cumbersome and hard to obtain equipment. When objective neural markers can be recorded seamlessly during ordinary VR experiences, the path from scientific discovery to deployed application shortens dramatically.

[1] https://galea.co/

This technological maturation arrives at a critical juncture. The neuromarkers identified in this dissertation, validated through traditional research-grade EEG systems, can now be tested and refined using integrated consumer platforms. What was previously feasible only in controlled laboratory settings becomes possible in homes, clinics, schools, and training facilities.

9.3.2 Toward Brain-Aware Immersive Experiences

The confluence of identified neuromarkers, validated spatial filtering methods, and emerging integrated hardware enables a vision of immersive systems that understand users at a neurophysiological level.

Future VR systems could continuously monitor acceleration and vection ERPs, adjusting content within the critical 600 ms temporal window to prevent cybersickness onset while preserving immersion. Rather than applying uniform motion profiles to all users, these systems would personalize experiences based on individual neural responses, accommodating wide variation in vection susceptibility and conflict resolution efficiency. Users particularly sensitive to visual motion could receive stabilizing cues or reduced optic flow velocity, while resistant users could experience unrestricted motion, maximizing engagement without compromising comfort.

Such adaptive systems extend beyond entertainment. Training applications in aviation, maritime navigation, surgical simulation, and autonomous vehicle operation currently face a fundamental limitation: trainees who develop cybersickness cannot complete training protocols, regardless of the simulation's instructional quality. Real-time neural monitoring could adjust simulator fidelity dynamically, maintaining immersion at the threshold of each individual's tolerance, gradually expanding their comfort envelope through controlled exposure. Over time, this could enable systematic acclimatization, reducing motion sensitivity through neuroadaptive training regimens.

Therapeutic contexts present similarly compelling opportunities. Exposure therapy for phobias, vestibular rehabilitation following injury, and spatial orientation training for individuals with sensory impairments all involve carefully controlled sensory experiences. Objective neural markers of sensory conflict and self-motion perception could guide clinicians in optimizing exposure intensity, ensuring therapeutic challenge without overwhelming patients. The temporal precision afforded by ERPs allows interventions calibrated not to subjective self-report, which may be delayed or inaccurate, but to direct

neural signatures of perceptual state.

9.3.3 Broader Horizons: Beyond Virtual Reality

The principles established here generalize to any context where humans process visually mediated motion. Augmented reality navigation systems, teleoperation interfaces for robotics, and automotive displays presenting heads-up information all induce visual motion perception that may conflict with vestibular input. As these technologies proliferate, understanding and monitoring neural responses to visual-vestibular conflicts becomes increasingly relevant to safety, usability, and user acceptance.

Autonomous vehicles, in particular, represent a near-term application domain. Passengers in self-driving cars experience visual motion from windows and displays while physically accelerating, often with unpredictable timing and direction changes they do not control. This situation closely parallels VR-induced sensory conflict. Detecting neural markers of motion processing in automotive contexts could inform interface design, seat orientation, display placement, and even vehicle motion planning to minimize passenger discomfort during autonomous travel.

More fundamentally, this work contributes to broader neuroscience efforts to develop objective biomarkers for subjective perceptual states. Consciousness studies, presence research, and investigations of embodied cognition all grapple with the challenge of measuring internal experience. Demonstrating that vection, a paradigmatically subjective phenomenon, exhibits reliable inter-subject neural signatures provides methodological precedent for similar investigations across perceptual domains. The approach established here, combining controlled stimulation, time-locked neural measurement, and systematic subjective reporting, offers a template for bridging first-person phenomenology and third-person neuroscience.

9.3.4 What comes next

The immediate research priorities are detailed in section 8.7 (Chapter 8). These include applying spatial filtering to vection data, developing real-time classification algorithms, analyzing the PECS protocol dataset, and expanding participant diversity. Each represents a necessary step toward validating and deploying the foundational discoveries presented here.

In the longer term, the field must address questions that transcend individual studies: How do neural responses to sensory conflict evolve with repeated exposure? Can individuals be systematically trained to resolve conflicts more efficiently, reducing cybersickness susceptibility? What individual differences (cognitive, neurophysiological, demographic) predict vection and cybersickness responses, and can we identify them prospectively? How do the identified ERPs interact with attentional state, fatigue, and motivation?

Answering these questions requires not just additional experiments, but sustained community coordination. Standardized protocols, shared datasets, open-source analysis tools, and cross-laboratory validation studies will determine whether findings generalize or remain laboratory-specific artifacts. The field's recent shift toward reproducibility and open science practices positions it well for this transition, but intentional effort is required to maintain momentum.

The ultimate goal extends beyond cybersickness mitigation to a comprehensive understanding of how humans perceive and navigate immersive environments. As virtual, augmented, and mixed reality systems see wider usage in work, education, healthcare, and leisure, ensuring these technologies are accessible, comfortable, and safe for diverse populations becomes a societal imperative. Objective neural markers provide the grounds for inclusive design: identifying who experiences difficulties, understanding why, and developing targeted solutions that accommodate rather than exclude.

The work presented in this dissertation represents one step toward that future. By establishing that subjective motion perception has objective, measurable, and inter-subject neural correlates, it demonstrates the feasibility of brain-aware immersive systems. The challenges ahead are substantial, but the convergence of scientific understanding, methodological tools, and enabling technology suggests they are surmountable. The next generation of immersive experiences may be characterized not by the discomfort they occasionally cause, but by their ability to understand and adapt to the humans who use them.

9.4 Final Remarks

This dissertation demonstrates that EEG can provide objective, inter-subject markers of subjective motion perception in virtual reality. The identification of acceleration and vection ERPs establishes temporal and hierarchical neural pathways underlying motion perception, linking early sensory encoding to conscious perceptual experience.

These findings situate vection and cybersickness within general principles of multisensory inference and neuroadaptive control, connecting accounts of predictive processing with deployable brain-computer interfaces. By identifying reliable neural markers, evaluating real-time capable spatial filters, and articulating technical constraints for adaptation, this work contributes to ongoing agendas in neuroergonomics, human-computer interaction, and immersive technologies.

While these findings do not resolve all questions regarding cybersickness, they provide a framework for future investigations that integrates sensory conflict theory, predictive coding mechanisms, and adaptive VR applications. The results contribute transferable methods and markers to the broader scientific landscape, supporting standardized, reproducible practices that enable cross-laboratory benchmarking and translational studies in training, rehabilitation, and accessibility.

Ultimately, this research advances the vision of brain-state-aware virtual reality systems that objectively detect user state and adapt content to enhance comfort, safety, and immersive experience.

List of Publications

- **The Neurophysiology of Cybersickness: A Review of BCI-based Characterization and Prediction.**
  Gaël Van der Lee; François Cabestaing; Hakim Si–Mohammed
  (Under review at IEEE Transactions on Visualization and Computer Graphics)
- **EEG Correlates of Vection: A Systematic Literature Review.**
  Gaël Van der Lee; François Cabestaing; Hakim Si–Mohammed
  (Published at MetroXRAINE)
- **EEG markers of acceleration perception in virtual reality.**
  Gaël Van der Lee; François Cabestaing; Anatole Lécuyer; Reinhold Scherer; Hakim Si–Mohammed.
  Proceedings of the Graz BCI Conference 2024. DOI: 10.3217/978-3-99161-014-4-044
- **Towards the Automatic Detection of Vection in Virtual Reality Using EEG.**
  Gaël Van der Lee; Anatole Lécuyer; Maxence Naud; Reinhold Scherer; François Cabestaing; Hakim Si–Mohammed.
  (Under review at IEEE Transactions on Visualization and Computer Graphics)
- **Enhancing Detection of Acceleration-Related ERPs in VR using Spatial Filtering Techniques.**
  Gaël Van der Lee; François Cabestaing; Hakim Si–Mohammed
  (Published at EUSIPCO 2025)

Appendix

Appendix A

PECS protocol: A framework for sensory incongruence analysis

> “
>
> این نیز بگذرد
>
> *This too shall pass*
>
> Persian Proverb ”

Prelude — *We have previously established neural markers for visual acceleration perception and vection in stationary participants exposed to moving visual stimuli. This paradigm, while revealing important insights into visual motion processing, represents only one aspect of the sensorimotor integration challenges encountered in virtual reality. This appendix presents the PECS (Potentiels Evoqués par des Conflits Sensoriels) protocol, which investigates the complementary scenario: neural responses to physical motion in the absence of congruent visual motion. By reversing the traditional experimental paradigm, this work addresses fundamental questions about bidirectional sensorimotor processing and extends our understanding of motion perception in virtual environments. The findings contribute to a comprehensive theoretical framework for sensorimotor integration and inform the development of adaptive VR systems.*

A.1 Theoretical Framework and Research Questions

The neural mechanisms underlying motion perception in virtual reality involve complex interactions between visual, vestibular, and proprioceptive systems. The thesis work demonstrated that visual motion processing generates distinct neural signatures, including acceleration-related ERPs and vection-specific responses. However, these findings represent only one direction of sensorimotor integration: the processing of visual motion cues in the absence of physical movement.

Virtual reality applications frequently involve scenarios where physical and visual motion information are incongruent or entirely dissociated. Understanding the neural processing of such sensorimotor conflicts is crucial for both theoretical neuroscience and practical VR system development. The PECS protocol addresses this gap by investigating the complementary paradigm: neural responses to physical motion in the absence of congruent visual motion.

This approach enables investigation of several fundamental research questions:

- Do physical motion events generate distinct, time-locked neural responses analogous to those observed for visual motion?
- How does the brain process conflicts between physical motion and absent or incongruent visual environments?
- Are there directional-specific neural signatures for physical motion that complement those identified for visual motion?
- What neural mechanisms underlie the integration of incongruent sensorimotor information in virtual environments?

These questions are essential for developing a comprehensive theoretical framework of sensorimotor integration in virtual reality and for creating adaptive systems that can detect and respond to sensorimotor conflicts in real-time.

A.2 Experimental Hypotheses

Based on the theoretical framework and findings from visual motion studies, the PECS protocol tests several specific hypotheses:

1. **Physical Motion ERP Hypothesis**: Physical acceleration events will elicit distinct, time-locked event-related potentials analogous to those observed for visual acceleration, but with potentially different topographical distributions reflecting vestibular and proprioceptive processing pathways.
2. **Sensorimotor Conflict Hypothesis**: Absent and incongruent sensorimotor conditions will generate enhanced neural responses in regions associated with conflict monitoring and multisensory integration, compared to congruent conditions.
3. **Directional Specificity Hypothesis**: The brain will exhibit differential neural responses to forward versus backward physical motion, potentially complementing the directional sensitivity observed for visual motion processing.
4. **Integration Network Hypothesis**: Neural responses to sensorimotor incongruence will engage brain networks involved in vestibular processing, spatial orientation, and cognitive control, distinct from those primarily activated by visual motion alone.

These hypotheses provide testable predictions that advance our understanding of bidirectional sensorimotor processing and contribute to the broader theoretical framework of motion perception in virtual environments.

A.3 Experimental Design

A.3.1 Overview

The PECS protocol employs a within-subjects experimental design where participants experience controlled physical motion while viewing virtual environments with varying degrees of visual-vestibular congruence. This approach enables direct comparison of neural responses across different sensorimotor integration conditions while controlling for individual differences in motion sensitivity and neural baseline activity.

A.3.2 Motion Control System

Physical motion is delivered through a motorized wheelchair system providing precise, reproducible movement profiles. The system generates smooth acceleration and deceleration phases along a 5-meter linear trajectory, with automatic bidirectional movement capabilities. This configuration ensures consistent physical motion parameters across participants and experimental conditions, enabling reliable neural response comparisons.

A.3.3 Neural Recording and Analysis

Neural activity is recorded using a 64-electrode wireless EEG system, providing comprehensive scalp coverage and enabling unrestricted participant movement during physical motion. The wireless configuration eliminates movement artifacts associated with traditional wired systems while maintaining high temporal resolution necessary for event-related potential analysis. This technical advancement is crucial for investigating neural responses to dynamic sensorimotor experiences.

Physiological monitoring includes galvanic skin response measurement to assess autonomic responses to sensorimotor conflicts, providing complementary information about the broader physiological impact of sensorimotor incongruence beyond neural activity alone.

The full setup is visualized in Figure A.1

A.4 Experimental Conditions and Protocol

A.4.1 Sensorimotor Congruence Conditions

The experimental design manipulates the relationship between physical motion and visual motion to create three distinct sensorimotor integration conditions:

1. **Congruent Condition**: Physical and visual motion occur in the same direction, representing normal sensorimotor integration and serving as a baseline for comparison.
2. **Absent Condition**: Physical motion occurs while the virtual environment remains stationary, creating a direct sensorimotor conflict analogous to common VR scenarios.

(a) *ANT Neuro Waveguard Net EEG cap with 64 electrodes* [1]

(b) *Valve Index VR headset with tracking cameras and controllers* [2]

(c) *Shimmer3 GSR sensor for physiological monitoring* [3]

(d) *Motorized wheelchair for controlled physical movement*

Figure A.1: *Equipment used in the PECS protocol for investigating sensorimotor incongruence in virtual reality. The setup combines wireless EEG recording, immersive VR display, physiological monitoring, and controlled physical motion to study neural correlates of sensorimotor conflicts.*

3. **Incongruent Condition**: Physical and visual motion occur in opposite directions, generating maximal sensorimotor conflict and testing the limits of sensorimotor integration mechanisms.

These conditions enable systematic investigation of how varying degrees of sensorimotor incongruence affect neural processing and provide insights into the neural mechanisms underlying conflict detection and resolution.

[1] Image source: `https://www.medicalexpo.com`
[2] Image source: `https://store.steampowered.com/valveindex`
[3] Image source: `https://www.shimmersensing.com/product/shimmer3-gsr-unit/`

A.4.2 Data Collection Protocol

Participants experience multiple movement cycles in each condition while neural activity is continuously recorded. Each movement cycle consists of controlled acceleration, constant velocity motion, and deceleration phases, enabling analysis of neural responses to different motion dynamics. The protocol includes sufficient trials per condition to enable robust statistical analysis of event-related potentials and other neural measures.

A.5 Expected Contributions and Implications

The PECS protocol addresses several critical gaps in our understanding of sensorimotor integration in virtual reality. By investigating neural responses to physical motion in the absence of congruent visual motion, this work provides complementary insights to the visual motion studies presented in this thesis.

A.5.1 Theoretical Contributions

The findings are expected to contribute to several theoretical domains:

- **Bidirectional Sensorimotor Processing**: Establishing whether neural mechanisms for processing visual motion conflicts exhibit symmetry with those for processing physical motion conflicts.
- **Conflict Detection and Resolution**: Identifying neural signatures of sensorimotor conflict detection and the mechanisms by which the brain attempts to resolve incongruent sensory information.
- **Adaptive Neural Responses**: Understanding how neural responses adapt to different degrees of sensorimotor incongruence and whether these adaptations follow predictable patterns.
- **Individual Differences**: Characterizing individual variability in sensorimotor integration capabilities and its neural correlates.

A.5.2 Practical Applications

The research has direct implications for virtual reality system development:

- **Adaptive VR Systems**: Neural markers of sensorimotor conflict could enable real-time detection and mitigation of uncomfortable VR experiences.
- **Motion Platform Integration**: Understanding neural responses to physical motion could inform the design of motion platforms and haptic feedback systems.
- **Cybersickness Prevention**: Insights into sensorimotor conflict processing could contribute to strategies for preventing and reducing cybersickness symptoms.

A.6 Current Status and Preliminary Findings

A.6.1 Data Collection Progress

Initial data collection has been completed with five participants, demonstrating the feasibility of the experimental approach. The wireless EEG system has proven effective for recording neural activity during physical movement, with data quality comparable to stationary recording conditions. Participant responses indicate that the experimental conditions successfully generate the intended sensorimotor conflicts while remaining tolerable for research participation.

A.6.2 Methodological Validation

The protocol has successfully demonstrated several key methodological advances:

- **Wireless EEG Efficacy**: High-quality neural recordings during dynamic physical movement with minimal motion artifacts.
- **Precise Synchronization**: Accurate time-locking of neural responses to physical motion events through hardware trigger systems.
- **Controlled Motion Delivery**: Reproducible physical motion profiles enabling reliable cross-participant and cross-condition comparisons.

- **Sensorimotor Manipulation**: Successful creation of distinct sensorimotor congruence conditions that participants can clearly differentiate.

These methodological achievements establish the foundation for comprehensive analysis of sensorimotor integration mechanisms in virtual reality.

A.7 Methodological Innovations

The PECS protocol introduces several methodological innovations that advance the field of sensorimotor integration research:

A.7.1 Bidirectional Paradigm

Unlike traditional vection studies that focus exclusively on visual motion processing, the PECS protocol enables investigation of both directions of sensorimotor integration. This bidirectional approach provides a more complete understanding of how the brain processes conflicts between different sensory modalities and offers insights into the symmetry or asymmetry of sensorimotor processing mechanisms.

A.7.2 Ecological Validity

The experimental conditions closely mirror real-world virtual reality scenarios where users experience physical motion while viewing virtual environments. This ecological validity enhances the translational potential of the findings and their applicability to practical VR system development.

A.7.3 Wireless Neural Recording

The successful implementation of wireless EEG recording during dynamic physical movement represents a significant technical achievement. This capability opens new possibilities for investigating neural responses in naturalistic, dynamic environments that were previously inaccessible to traditional laboratory-based neuroscience methods.

A.8 Future Research Directions

The PECS protocol establishes a foundation for several important research directions:

A.8.1 Comprehensive Neural Analysis

Future work will focus on detailed analysis of the collected neural data to identify specific event-related potentials associated with physical motion and sensorimotor conflicts. This analysis will compare findings with the visual motion studies presented in this thesis to establish whether sensorimotor integration exhibits symmetrical or asymmetrical neural processing patterns.

A.8.2 Individual Differences Investigation

The protocol provides a framework for investigating individual differences in sensorimotor integration capabilities. Understanding how neural responses to sensorimotor conflicts vary across individuals could inform personalized approaches to VR system design and cybersickness prevention strategies.

A.8.3 Real-time Application Development

The neural markers identified through the PECS protocol could be integrated into real-time brain-computer interface systems for adaptive VR applications. Such systems could detect sensorimotor conflicts as they occur and automatically adjust virtual environment parameters to maintain user comfort and immersion.

A.9 Conclusion

This appendix presented the PECS protocol, an innovative experimental paradigm that addresses fundamental questions about sensorimotor integration in virtual reality. By investigating neural responses to physical motion in the absence of congruent visual motion, this work provides essential complementary insights to the visual motion studies presented in the research conducted in this thesis.

The protocol represents a significant methodological advancement in sensorimotor integration research, demonstrating the feasibility of wireless neural recording during dynamic physical movement. The research addresses critical theoretical questions about bidirectional sensorimotor processing while providing practical insights for virtual reality system development.

The PECS protocol contributes to a comprehensive understanding of motion perception in virtual reality and establishes methodological foundations for future research in adaptive VR systems. The ongoing analysis of collected data promises to reveal important insights into the neural mechanisms underlying sensorimotor integration and their implications for improving user experiences in virtual environments.

Acronyms

ANOVA Analysis of Variance.

BCI Brain-Computer Interface.

BIDS Brain Imaging Data Structure.

BOLD Blood-Oxygen-Level Dependent.

BVP Blood Volume Pulse.

CAVE Cave Automatic Virtual Environment.

CNN Convolutional Neural Network.

CS Cybersickness.

CSP Common Spatial Patterns.

CSv Cingulate Sulcus visual area.

ECeG Electrocerebellogram.

ECG Electrocardiography.

ECoG Electrocorticography.

EEG Electroencephalography.

EGG Electrogastrography.

EMG Electromyography.

EMS Effect-Matched Spatial filtering.

EOG Electrooculography.

ERP Event-Related Potential.

ErrP Error-Related Potential.

fMRI functional Magnetic Resonance Imaging.

fNIRS functional Near-Infrared Spectroscopy.

FoR Field of Regard.

FOV Field of View.

GRU Gated Recurrent Unit.

GSR Galvanic Skin Response.

HEP Heartbeat-Evoked Potential.

HMD Head-Mounted Display.

HRV Heart Rate Variability.

ICA Independent Component Analysis.

kNN k-Nearest Neighbors.

LDA Linear Discriminant Analysis.

LSTM Long Short-Term Memory.

MEG Magnetoencephalography.

MS Motion Sickness.

NF Neurofeedback.

OKN Optokinetic Nystagmus.

PC Personal Computer.

PCA Principal Component Analysis.

PLCC Pearson Linear Correlation Coefficient.

PLV Phase-Locked Value.

PPG Photoplethysmography.

PRISMA Preferred Reporting Items for Systematic Reviews and Meta-Analyses.

PSD Power Spectral Density.

RMSE Root Mean Square Error.

RNN Recurrent Neural Network.

SNR Signal-to-Noise Ratio.

SQUID Superconducting Quantum Interference Device.

SROCC Spearman Rank-Order Correlation Coefficient.

SS Simulator Sickness.

SSQ Simulator Sickness Questionnaire.

SSVEP Steady-State Visually Evoked Potential.

SVM Support Vector Machine.

SVR Support Vector Regression.

tACS transcranial Alternating Current Stimulation.

taVNS transcutaneous auricular Vagus Nerve Stimulation.

tDCS transcranial Direct Current Stimulation.

TFR Time-Frequency Representation.

TR Repetition Time.

TS Total Score (SSQ total score).

VEP Visually Evoked Potential.

VIMS Visually Induced Motion Sickness.

VR Virtual Reality.

VRS Virtual Reality Sickness.

VRT Vibro-motor Reprocessing Therapy.

XAI Explainable Artificial Intelligence.

List of Figures

List of Tables

Bibliography

Ahn Min-Hee, Park Jeong Hye, Jeon Hanjae, Lee Hyo-Jeong, Kim Hyung-Jong, and Hong Sung Kwang (Nov. 2020). “Temporal Dynamics of Visually Induced Motion Perception and Neural Evidence of Alterations in the Motion Perception Process in an Immersive Virtual Reality Environment”. In: *Frontiers in Neuroscience* 14, p. 600839. (Visited on 07/02/2025).

Akuthota Srinath, Kumar K.Raj, and Chander J.Ravi (Sept. 2023). “A Complete Survey on Common Spatial Pattern Techniques in Motor Imagery BCI”. In: *Journal of Scientific and Innovative Research* 12.3, pp. 40–49. (Visited on 03/13/2025).

Andrievskaia Polina, Berti Stefan, Spaniol Julia, and Keshavarz Behrang (Oct. 2023). “Exploring Neurophysiological Correlates of Visually Induced Motion Sickness Using Electroencephalography (EEG)”. In: *Experimental Brain Research* 241.10, pp. 2463–2473. (Visited on 07/02/2025).

Argasiński Jan K., Lipp Natalia, and Mazurek Szymon (2023). “Electroencephalographic (EEG) Correlates of Visually Induced Motion Sickness (VIMS) in the Virtual Reality (VR) Based Simulations”. In: *Human-Computer Interaction – INTERACT 2023*. Ed. by Abdelnour Nocera José, Kristín Lárusdóttir Marta, Petrie Helen, Piccinno Antonio, and Winckler Marco. Vol. 14145. Cham: Springer Nature Switzerland, pp. 59–67. (Visited on 07/02/2025).

Berger Hans (Dec. 1929). “Über das Elektrenkephalogramm des Menschen”. In: *Archiv für Psychiatrie und Nervenkrankheiten* 87.1, pp. 527–570. (Visited on 09/06/2025).

Berger Lisa M, Wood Guilherme, and Kober Silvia E (Apr. 2025). “Manipulating Cybersickness in Virtual Reality-Based Neurofeedback and Its Effects on Training Performance”. In: *Journal of Neural Engineering* 22.2, p. 026014. (Visited on 07/02/2025).

Berger Lisa Maria, Wood Guilherme, and Kober Silvia Erika (May 2024). “Influence of a Placebo tDCS Treatment on Cybersickness and EEG-neurofeedback Success”. In: *Behavioural Brain Research* 465, p. 114917. (Visited on 07/02/2025).

Berti Stefan, Haycock Bruce, Adler Julia, and Keshavarz Behrang (July 2019). “Early Cortical Processing of Vection-Inducing Visual Stimulation as Measured by Event-Related Brain Potentials (ERP)”. In: *Displays*. Special Issue: Visually Induced Motion Sensations 58, pp. 56–65. (Visited on 09/19/2023).

Berti Stefan and Keshavarz Behrang (Aug. 2020). “Neuropsychological Approaches to Visually-Induced Vection: An Overview and Evaluation of Neuroimaging and Neurophysiological Studies”. In: *Multisensory Research* 34.2, pp. 153–186.

Bles Willem, Bos Jelte E., De Graaf Bernd, Groen Eric, and Wertheim Alexander H. (Nov. 1998). “Motion Sickness: Only One Provocative Conflict?” In: *Brain Research Bulletin* 47.5, pp. 481–487. (Visited on 07/09/2025).

Boudewyn Megan A., Luck Steven J., Farrens Jaclyn L., and Kappenman Emily S. (June 2018). “How Many Trials Does It Take to Get a Significant ERP Effect? It Depends”. In: *Psychophysiology* 55.6, e13049.

Bowman Doug A. and McMahan Ryan P. (July 2007). “Virtual Reality: How Much Immersion Is Enough?” In: *Computer* 40.7, pp. 36–43.

Cabestaing François and Derambure Philippe (Aug. 2016). “Physiological Markers for Controlling Active and Reactive BCIs”. In: *Brain-Computer Interfaces*. Ed. by Clerc Maureen, Bougrain Laurent, and Lotte Fabien. Vol. 1. Foundations and Methods. Wiley Online Library. (Visited on 09/06/2025).

Caserman Polona, Garcia-Agundez Augusto, Gámez Zerban Alvar, and Göbel Stefan (Dec. 2021). “Cybersickness in Current-Generation Virtual Reality Head-Mounted Displays: Systematic Review and Outlook”. In: *Virtual Reality* 25.4, pp. 1153–1170. (Visited on 12/15/2022).

Chai Lining, Hua Chengcheng, Zhou Zhanfeng, Chen Xu, and Tao Jianlong (2023). “An EEG Study of Virtual Reality Motion Sickness Based on MVMD Combined with Entropy Asymmetry”. In: *Proceedings of 2023 Chinese Intelligent Automation Conference*. Ed. by Deng Zhidong. Vol. 1082. Singapore: Springer Nature Singapore, pp. 372–377. (Visited on 07/02/2025).

Chang Eunhee, Billinghurst Mark, and Yoo Byounghyun (Sept. 2023). “Brain Activity during Cybersickness: A Scoping Review”. In: *Virtual Reality* 27.3, pp. 2073–2097. (Visited on 07/02/2025).

Chang Eunhee, Kim Hyun Taek, and Yoo Byounghyun (Sept. 2022). “Identifying Physiological Correlates of Cybersickness Using Heartbeat-Evoked Potential Analysis”. In: *Virtual Reality* 26.3, pp. 1193–1205. (Visited on 12/13/2023).

Chatain Julia, Ramp Virginia, Gashaj Venera, Fayolle Violaine, Kapur Manu, Sumner Robert W., and Magnenat Stéphane (June 2022). “Grasping Derivatives: Teaching Mathematics through Embodied Interactions Using Tablets and Virtual Reality”. In: *Proceedings of the 21st Annual ACM Interaction Design and Children Conference*. IDC ’22. New York, NY, USA: Association for Computing Machinery, pp. 98–108. (Visited on 07/09/2025).

Chen Yu-Chieh, Duann Jeng-Ren, Chuang Shang-Wen, Lin Chun-Ling, Ko Li-Wei, Jung Tzyy-Ping, and Lin Chin-Teng (Feb. 2010). “Spatial and Temporal EEG Dynamics of Motion Sickness”. In: *NeuroImage* 49.3, pp. 2862–2870. (Visited on 07/02/2025).

Chen Yu-Chieh, Duann Jeng-Ren, Lin Chun-Ling, Chuang Shang-Wen, Jung Tzyy-Ping, and Lin Chin-Teng (2009). “Motion-Sickness Related Brain Areas and EEG Power Activates”. In: *Foundations of Augmented Cognition. Neuroergonomics and Operational Neuroscience*. Ed. by Schmorrow Dylan D., Estabrooke Ivy V., and Grootjen Marc. Vol. 5638. Berlin, Heidelberg: Springer Berlin Heidelberg, pp. 348–354. (Visited on 07/02/2025).

Cheung B. S., Howard I. P., and Money K. E. (June 1991). “Visually-Induced Sickness in Normal and Bilaterally Labyrinthine-Defective Subjects”. In: *Aviation, Space, and Environmental Medicine* 62.6, pp. 527–531.

Chiappa Keith H. (1997). *Evoked Potentials in Clinical Medicine*. Lippincott Williams & Wilkins.

Cortes Carlos Alfredo Tirado, Lin Chin-Teng, Do Tien-Thong Nguyen, and Chen Hsiang-Ting (Mar. 2023a). “An EEG-based Experiment on VR Sickness and Postural Instability While Walking in Virtual Environments”. In: *2023 IEEE Conference Virtual Reality and 3D User Interfaces (VR)*. Shanghai, China: IEEE, pp. 94–104. (Visited on 07/02/2025).

— (Feb. 2023b). *An EEG-based Experiment on VR Sickness and Postural Instability While Walking in Virtual Environments*. arXiv: 2302.11129 [cs]. (Visited on 03/23/2023).

Cummings James J. and Bailenson Jeremy N. (Apr. 2016). “How Immersive Is Enough? A Meta-Analysis of the Effect of Immersive Technology on User Presence”. In: *Media Psychology* 19.2, pp. 272–309. (Visited on 10/02/2023).

Daşdemir Yaşar (Nov. 2023a). “Classification of Emotional and Immersive Outcomes in the Context of Virtual Reality Scene Interactions”. In: *Diagnostics* 13.22, p. 3437. (Visited on 07/02/2025).

— (Dec. 2023b). “Locomotion Techniques with EEG Signals in a Virtual Reality Environment”. In: *Displays* 80, p. 102538. (Visited on 07/02/2025).

Davis Simon, Nesbitt Keith, and Nalivaiko Eugene (Dec. 2014). “A Systematic Review of Cybersickness”. In: *Proceedings of the 2014 Conference on Interactive Entertainment*. IE2014. New York, NY, USA: Association for Computing Machinery, pp. 1–9. (Visited on 12/15/2022).

Dehais Frédéric, Duprès Alban, Blum Sarah, Drougard Nicolas, Scannella Sébastien, Roy Raphaëlle N., and Lotte Fabien (Jan. 2019). “Monitoring Pilot’s Mental Workload Using ERPs and Spectral Power with a Six-Dry-Electrode EEG System in Real Flight Conditions”. In: *Sensors* 19.6, p. 1324. (Visited on 02/21/2024).

Demirel Berken Utku, Dogan Adnan Harun, Rossie Juliete, Möbus Max, and Holz Christian (May 2025). “Beyond Subjectivity: Continuous Cybersickness Detection Using EEG-based Multitaper Spectrum Estimation”. In: *IEEE Transactions on Visualization and Computer Graphics* 31.5, pp. 2525–2534. (Visited on 07/02/2025).

Dennison Mark S., D’Zmura Mike, Harrison Andre V., Lee Michael, and Raglin Adrienne J. (May 2019). “Improving Motion Sickness Severity Classification through Multi-Modal Data Fusion”. In: *Artificial Intelligence and Machine Learning for Multi-Domain Operations Applications*. Ed. by Pham Tien. Baltimore, United States: SPIE, p. 27. (Visited on 07/02/2025).

Dichgans Johannes and Brandt Thomas (1978). “Visual-Vestibular Interaction: Effects on Self-Motion Perception and Postural Control”. In: *Perception*. Ed. by Anstis S. M., Atkinson J., Blakemore C., Braddick O., Brandt T., Campbell F. W., Coren S., Dichgans J., Dodwell P. C., Eimas P. D., et al. Handbook of Sensory Physiology. Berlin, Heidelberg: Springer, pp. 755–804. (Visited on 09/19/2023).

Ditz Jonas C., Schwarz Andreas, and Müller-Putz Gernot R. (May 2020). “Perturbation-Evoked Potentials Can Be Classified from Single-Trial EEG”. In: *Journal of Neural Engineering* 17.3, p. 036008. (Visited on 05/17/2023).

Dowsett James, Herrmann Christoph S., Dieterich Marianne, and Taylor Paul C.J. (Apr. 2020). “Shift in Lateralization during Illusory Self-motion: EEG Responses to Visual Flicker at 10 Hz and Frequency-specific Modulation by

тACS". In: *European Journal of Neuroscience* 51.7, pp. 1657–1675. (Visited on 05/04/2025).

Du Xue, Qin Yigui, Tu Shen, Yin Huazhan, Wang Ting, Yu Caiyun, and Qiu Jiang (2013). "Differentiation of stages in joke comprehension: Evidence from an ERP study". In: *International Journal of Psychology* 48.2, pp. 149–157. (Visited on 09/24/2023).

Ebenholtz Sheldon M. (Jan. 1992). "Motion Sickness and Oculomotor Systems in Virtual Environments". In: *Presence: Teleoper. Virtual Environ.* 1.3, pp. 302–305.

Farwell L. A. and Donchin E. (Dec. 1988). "Talking off the Top of Your Head: Toward a Mental Prosthesis Utilizing Event-Related Brain Potentials". In: *Electroencephalography and Clinical Neurophysiology* 70.6, pp. 510–523.

Feng Naishi, Zhou Bin, Zhang Qianqian, Hua Chengcheng, and Yuan Yue (June 2025). "A Comprehensive Exploration of Motion Sickness Process Analysis from EEG Signal and Virtual Reality". In: *Computer Methods and Programs in Biomedicine* 264, p. 108714. (Visited on 07/02/2025).

Fukunaga Keinosuke (1990). *Introduction to Statistical Pattern Recognition*. 2nd. Academic Press.

Gavgani Alireza Mazloumi, Wong Rachel H.X., Howe Peter R.C., Hodgson Deborah M., Walker Frederick R., and Nalivaiko Eugene (July 2018). "Cybersickness-Related Changes in Brain Hemodynamics: A Pilot Study Comparing Transcranial Doppler and near-Infrared Spectroscopy Assessments during a Virtual Ride on a Roller Coaster". In: *Physiology & Behavior* 191, pp. 56–64. (Visited on 07/02/2025).

Gevins A. and Smith M. E. (Sept. 2000). "Neurophysiological Measures of Working Memory and Individual Differences in Cognitive Ability and Cognitive Style". In: *Cerebral Cortex (New York, N.Y.: 1991)* 10.9, pp. 829–839.

Gorgolewski Krzysztof J., Auer Tibor, Calhoun Vince D., Craddock R. Cameron, Das Samir, Duff Eugene P., Flandin Guillaume, Ghosh Satrajit S., Glatard Tristan, Halchenko Yaroslav O., Handwerker Daniel A., Hanke Michael, Keator David, Li Xiangrui, Michael Zachary, Maumet Camille, Nichols B. Nolan, Nichols Thomas E., Pellman John, Poline Jean-Baptiste, Rokem Ariel, Schaefer Gunnar, Sochat Vanessa, Triplett William, Turner Jessica A., Varoquaux Gaël, and Poldrack Russell A. (June 2016). "The Brain Imaging Data Structure, a Format for Organizing and Describing Outputs of Neuroimaging Experiments". In: *Scientific Data* 3.1, p. 160044. (Visited on 09/29/2023).

Hao Chenru, Zhao Ruibin, Qiao Lihua, Li Xiuyuan, Zhang Jingjing, Wu Yanru, and Chi Ziqiang (Oct. 2019). “EEG Analysis of Visually Induced Spatial Disorientation”. In: *2019 12th International Congress on Image and Signal Processing, BioMedical Engineering and Informatics (CISP-BMEI)*. Suzhou, China: IEEE, pp. 1–5. (Visited on 05/04/2025).

Harquel Sylvain, Cian Corinne, Torlay Laurent, Cousin Emilie, Barraud Pierre-Alain, Bougerol Thierry, and Guerraz Michel (Jan. 2024). “Modulation of Visually Induced Self-motion Illusions by α Transcranial Electric Stimulation over the Superior Parietal Cortex”. In: *Journal of Cognitive Neuroscience* 36.1, pp. 143–154. (Visited on 05/04/2025).

Harquel Sylvain, Guerraz Michel, Barraud Pierre-Alain, and Cian Corinne (Jan. 2020). “Modulation of Alpha Waves in Sensorimotor Cortical Networks during Self-Motion Perception Evoked by Different Visual-Vestibular Conflicts”. In: *Journal of Neurophysiology* 123.1, pp. 346–355.

Hettinger Lawrence J., Berbaum Kevin S., Kennedy Robert S., Dunlap William P., and Nolan Margaret D. (Sept. 1990). “Vection and Simulator Sickness”. In: *Military Psychology* 2.3, pp. 171–181. (Visited on 09/26/2023).

Hettinger Lawrence J. and Riccio Gary E. (Aug. 1992). “Visually Induced Motion Sickness in Virtual Environments”. In: *Presence: Teleoperators and Virtual Environments* 1.3, pp. 306–310. (Visited on 06/12/2023).

Hua Chengcheng, Chai Lining, Yan Ying, Liu Jia, Wang Qiaoxiu, Fu Rongrong, and Zhou Zhanfeng (Oct. 2023). “Assessment of Virtual Reality Motion Sickness Severity Based on EEG via LSTM/BiLSTM”. In: *IEEE Sensors Journal* 23.20, pp. 24839–24848. (Visited on 07/02/2025).

Hua Chengcheng, Chai Lining, Zhou Zhanfeng, Tao Jianlong, Yan Ying, Chen Xu, Liu Jia, and Fu Rongrong (Oct. 2024a). “Detection of Virtual Reality Motion Sickness Based on EEG Using Asymmetry of Entropy and Cross-Frequency Coupling”. In: *Physiology & Behavior* 284, p. 114626. (Visited on 07/02/2025).

Hua Chengcheng, Chen Yuechi, Tao Jianlong, Dai Zhian, Yang Wenqing, Chen Dapeng, Liu Jia, and Fu Rongrong (June 2025). “Dual-Pathway EEG Model with Channel Attention for Virtual Reality Motion Sickness Detection”. In: *Journal of Neuroscience Methods* 418, p. 110425. (Visited on 07/02/2025).

Hua Chengcheng, Tao Jianlong, Zhou Zhanfeng, Chai Lining, Yan Ying, Liu Jia, and Fu Rongrong (June 2024b). “EEG Classification Model for Virtual Reality Motion Sickness Based on Multi-Scale CNN Feature Correlation”.

In: *Computer Methods and Programs in Biomedicine* 251, p. 108218. (Visited on 07/02/2025).

Hua Chengcheng, Zhou Zhanfeng, Tao Jianlong, Yan Ying, Liu Jia, Fu Rongrong, and Chai Lining (Nov. 2024c). "A Siam-LSTM Model for Multichannel EEG on VR Motion Sickness Recognition". In: *IEEE Sensors Journal* 24.21, pp. 35245–35254. (Visited on 07/02/2025).

Jang Kyoung-Mi, Kwon Moonyoung, Nam Sun Gu, Kim DaMee, and Lim Hyun Kyoon (July 2022). "Estimating Objective (EEG) and Subjective (SSQ) Cybersickness in People with Susceptibility to Motion Sickness". In: *Applied Ergonomics* 102, p. 103731. (Visited on 03/09/2023).

Jeong Daekyo, Yoo Sangbong, and Yun Jang (Mar. 2019). "Cybersickness Analysis with EEG Using Deep Learning Algorithms". In: *2019 IEEE Conference on Virtual Reality and 3D User Interfaces (VR)*. Osaka, Japan: IEEE, pp. 827–835. (Visited on 07/02/2025).

Jutten Christian and Herault Jeanny (July 1991). "Blind Separation of Sources, Part I: An Adaptive Algorithm Based on Neuromimetic Architecture". In: *Signal Processing* 24.1, pp. 1–10. (Visited on 03/13/2025).

Kardong-Edgren Suzan (Suzie), Farra Sharon L., Alinier Guillaume, and Young H. Michael (June 2019). "A Call to Unify Definitions of Virtual Reality". In: *Clinical Simulation in Nursing* 31, pp. 28–34. (Visited on 04/06/2023).

Kennedy Robert S., Lane Norman E., Berbaum Kevin S., and Lilienthal Michael G. (July 1993). "Simulator Sickness Questionnaire: An Enhanced Method for Quantifying Simulator Sickness". In: *International Journal of Aviation Psychology* 3.3, p. 203. (Visited on 03/14/2023).

Keshavarz Behrang and Berti Stefan (Feb. 2014). "Integration of Sensory Information Precedes the Sensation of Vection: A Combined Behavioral and Event-Related Brain Potential (ERP) Study". In: *Behavioural Brain Research* 259, pp. 131–136. (Visited on 12/13/2023).

Keshavarz Behrang, Campos Jennifer L., and Berti Stefan (2015a). "Vection Lies in the Brain of the Beholder: EEG Parameters as an Objective Measurement of Vection". In: *Frontiers in Psychology* 6. (Visited on 09/19/2023).

Keshavarz Behrang and Hecht Heiko (Aug. 2011). "Validating an Efficient Method to Quantify Motion Sickness". In: *Human Factors* 53.4, pp. 415–426.

Keshavarz Behrang, Philipp-Muller Aaron Emile, Hemmerich Wanja, Riecke Bernhard E., and Campos Jennifer L. (July 2019). "The Effect of Visual

Motion Stimulus Characteristics on Vection and Visually Induced Motion Sickness". In: *Displays*. Special Issue: Visually Induced Motion Sensations 58, pp. 71–81. (Visited on 10/02/2023).

Keshavarz Behrang, Riecke Bernhard E., Hettinger Lawrence J., and Campos Jennifer L. (2015b). "Vection and Visually Induced Motion Sickness: How Are They Related?" In: *Frontiers in Psychology* 6. (Visited on 04/02/2023).

Khoirunnisaa Alfi Zuhriya, Pane Evi Septiana, Wibawa Adhi Dharma, and Purnomo Mauridhi Hery (July 2018). "Channel Selection of EEG-Based Cybersickness Recognition during Playing Video Game Using Correlation Feature Selection (CFS)". In: *2018 2nd International Conference on Biomedical Engineering (IBIOMED)*, pp. 48–53. (Visited on 07/02/2025).

Kim Hyun K., Park Jaehyun, Choi Yeongcheol, and Choe Mungyeong (May 2018). "Virtual Reality Sickness Questionnaire (VRSQ): Motion Sickness Measurement Index in a Virtual Reality Environment". In: *Applied Ergonomics* 69, pp. 66–73. (Visited on 03/13/2023).

Kim Jinwoo, Kim Woojae, Oh Heeseok, Lee Seongmin, and Lee Sanghoon (Oct. 2019). "A Deep Cybersickness Predictor Based on Brain Signal Analysis for Virtual Reality Contents". In: *2019 IEEE/CVF International Conference on Computer Vision (ICCV)*. Seoul, Korea (South): IEEE, pp. 10579–10588. (Visited on 07/02/2025).

Kim Juno and Palmisano Stephen (Dec. 2008). "Effects of Active and Passive Viewpoint Jitter on Vection in Depth". In: *Brain Research Bulletin* 77.6, pp. 335–342.

Kim Y.Y., Kim H.J., Ko H.D., and Kim H.T. (Oct. 2001). "Psychophysiological Changes by Navigation in a Virtual Reality". In: *2001 Conference Proceedings of the 23rd Annual International Conference of the IEEE Engineering in Medicine and Biology Society*. Vol. 4, 3773–3776 vol.4. (Visited on 07/02/2025).

Kim Young Youn, Kim Hyun Ju, Kim Eun Nam, Ko Hee Dong, and Kim Hyun Taek (2005). "Characteristic Changes in the Physiological Components of Cybersickness". In: *Psychophysiology* 42.5, pp. 616–625. (Visited on 04/03/2023).

Klimesch Wolfgang, Sauseng Paul, and Hanslmayr Simon (Jan. 2007). "EEG Alpha Oscillations: The Inhibition-Timing Hypothesis". In: *Brain Research Reviews* 53.1, pp. 63–88.

Ko Li-Wei, Wei Chun-Shu, Jung Tzyy-Ping, and Lin Chin-Teng (2011). "Estimating the Level of Motion Sickness Based on EEG Spectra". In: *Founda-*

tions of Augmented Cognition. Directing the Future of Adaptive Systems. Ed. by Schmorrow Dylan D. and Fidopiastis Cali M. Vol. 6780. Berlin, Heidelberg: Springer Berlin Heidelberg, pp. 169–176. (Visited on 07/02/2025).

Kooijman Lars, Asadi Houshyar, Mohamed Shady, and Nahavandi Saeid (July 2022). "A Virtual Reality Study Investigating the Effect of Cybersickness on the Relationship Between Vection and Presence Across Environments with Varying Levels of Ecological Relevance". In: *2022 15th International Conference on Human System Interaction (HSI)*, pp. 1–8. (Visited on 09/26/2023).

Kooijman Lars, Berti Stefan, Asadi Houshyar, Nahavandi Saeid, and Keshavarz Behrang (June 2023). "Measuring Vection: A Review and Critical Evaluation of Different Methods for Quantifying Illusory Self-Motion". In: *Behavior Research Methods*. (Visited on 09/19/2023).

Kourtesis Panagiotis, Linnell Josie, Amir Rayaan, Argelaguet Ferran, and MacPherson Sarah E. (Mar. 2023). "Cybersickness in Virtual Reality Questionnaire (CSQ-VR): A Validation and Comparison against SSQ and VRSQ". In: *Virtual Worlds* 2.1, pp. 16–35. (Visited on 07/08/2024).

Kramida Gregory (July 2016). "Resolving the Vergence-Accommodation Conflict in Head-Mounted Displays". In: *IEEE Transactions on Visualization and Computer Graphics* 22.7, pp. 1912–1931. (Visited on 07/09/2025).

Krokos Eric and Varshney Amitabh (Mar. 2022). "Quantifying VR Cybersickness Using EEG". In: *Virtual Reality* 26.1, pp. 77–89. (Visited on 12/15/2022).

L. Waskom Michael (2021). "Seaborn: Statistical Data Visualization". In: *The Open Journal* 6.60, p. 3021.

Larson Eric, Gramfort Alexandre, Engemann Denis A, Leppakangas Jaakko, Brodbeck Christian, Jas Mainak, Brooks Teon, Sassenhagen Jona, Luessi Martin, McCloy Daniel, et al. (Sept. 2023). *MNE-Python*. Zenodo. (Visited on 09/24/2023).

LaViola Joseph J. (Jan. 2000). "A Discussion of Cybersickness in Virtual Environments". In: *ACM SIGCHI Bulletin* 32.1, pp. 47–56. (Visited on 05/15/2023).

Lee Sangmin, Kim Seongyeop, Kim Hak Gu, and Ro Yong Man (May 2022). "Assessing Individual VR Sickness Through Deep Feature Fusion of VR Video and Physiological Response". In: *IEEE Transactions on Circuits and Systems for Video Technology* 32.5, pp. 2895–2907. (Visited on 07/02/2025).

Lee Yonggun and Alamaniotis Miltiadis (Oct. 2020). "Unsupervised EEG Cybersickness Prediction with Deep Embedded Self Organizing Map". In:

2020 IEEE 20th International Conference on Bioinformatics and Bioengineering (BIBE), pp. 538–542. (Visited on 07/02/2025).

Li Gang, Pohlmann Katharina, McGill Mark, Chen Chao Ping, Brewster Stephen, and Pollick Frank (Mar. 2023a). "Exploring Neural Biomarkers in Young Adults Resistant to VR Motion Sickness: A Pilot Study of EEG". In: *2023 IEEE Conference Virtual Reality and 3D User Interfaces (VR)*. Shanghai, China: IEEE, pp. 328–335. (Visited on 07/02/2025).

Li Gang, Wang Yu–Kai, McGill Mark, Pöhlmann Katharina, Brewster Stephen, and Pollick Frank (Dec. 2023b). "Resting-State EEG in the Vestibular Region Can Predict Motion Sickness Induced by a Motion-Simulated in-Car VR Platform". In: *2023 IEEE Symposium Series on Computational Intelligence (SSCI)*, pp. 47–52. (Visited on 07/02/2025).

Li Xiaolu, Zhu Changrong, Xu Cangsu, Zhu Junjiang, Li Yuntang, and Wu Shanqiang (May 2020). "VR Motion Sickness Recognition by Using EEG Rhythm Energy Ratio Based on Wavelet Packet Transform". In: *Computer Methods and Programs in Biomedicine* 188, p. 105266. (Visited on 03/09/2023).

Li Yan, Liu Aie, and Ding Li (Mar. 2019). "Machine Learning Assessment of Visually Induced Motion Sickness Levels Based on Multiple Biosignals". In: *Biomedical Signal Processing and Control* 49, pp. 202–211. (Visited on 07/02/2025).

Li Zhibin, Zhao Leilei, Chang Jing, Li Wei, Yang Menghui, Li Chong, Wang Rencheng, and Ji Linhong (July 2022). "EEG-based Evaluation of Motion Sickness and Reducing Sensory Conflict in a Simulated Autonomous Driving Environment". In: *2022 44th Annual International Conference of the IEEE Engineering in Medicine & Biology Society (EMBC)*, pp. 4026–4030. (Visited on 07/02/2025).

Liao Chung-Yen, Tai Shao-Kuo, Chen Rung-Ching, and Hendry Hendry (2020). "Using EEG and Deep Learning to Predict Motion Sickness Under Wearing a Virtual Reality Device". In: *IEEE Access* 8, pp. 126784–126796. (Visited on 07/02/2025).

Lim Hyun Kyoon, Ji Kyoungha, Woo Ye Shin, Han Dong-uk, Lee Dong-Hyun, Nam Sun Gu, and Jang Kyoung-Mi (Jan. 2021). "Test-Retest Reliability of the Virtual Reality Sickness Evaluation Using Electroencephalography (EEG)". In: *Neuroscience Letters* 743, p. 135589. (Visited on 04/03/2023).

Lin Chin-Teng, Chuang Shang-Wen, Chen Yu-Chieh, Ko Li-Wei, Liang Sheng-Fu, and Jung Tzyy-Ping (Aug. 2007). "EEG Effects of Motion Sickness

Induced in a Dynamic Virtual Reality Environment". In: *2007 29th Annual International Conference of the IEEE Engineering in Medicine and Biology Society*, pp. 3872–3875. (Visited on 07/02/2025).

Lin Chin-Teng, Tsai Shu-Fang, Lee Hua-Chin, Huang Hui-Lin, Ho Shinn-Ying, and Ko Li-Wei (June 2012). "Motion Sickness Estimation System". In: *The 2012 International Joint Conference on Neural Networks (IJCNN)*. Brisbane, Australia: IEEE, pp. 1–6. (Visited on 07/02/2025).

Liu Mutian, Yang Banghua, Xu Mengdie, Zan Peng, Chen Luting, and Xia Xinxing (Jan. 2024a). "Exploring Quantitative Assessment of Cybersickness in Virtual Reality Using EEG Signals and a CNN-ECA-LSTM Network". In: *Displays* 81, p. 102602. (Visited on 07/02/2025).

Liu Mutian, Yang Banghua, Zan Peng, Chen Luting, Wang Baozeng, and Xia Xinxing (Dec. 2024b). "Exploring the Brain Physiological Activity and Quantified Assessment of VR Cybersickness Using EEG Signals". In: *Displays* 85, p. 102879. (Visited on 07/02/2025).

Liu Ran, Peli Eli, and Hwang Alex D. (Jan. 2017). "Measuring Visually Induced Motion Sickness Using Wearable Devices". In: *Electronic Imaging* 29.14, pp. 218–223. (Visited on 07/02/2025).

Liu Ran, Xu Miao, Zhang Yanzhen, Peli Eli, and Hwang Alex D. (Mar. 2020). "A Pilot Study on EEG-Based Evaluation of Visually Induced Motion Sickness". In: *The Journal of imaging science and technology* 64.2, pp. 20501-1-20501–10. (Visited on 03/09/2023).

Luo Shuhang, Ren Peng, Wu Jiawei, Wu Xiang, and Zhang Xiao (July 2024). "Feature Extraction Method of EEG Based on Wavelet Packet Reconstruction and Deep Learning Model of VR Motion Sickness Feature Classification and Prediction". In: *PLOS ONE* 19.7. Ed. by Mumtaz Wajid, e0305733. (Visited on 07/02/2025).

Luong Tiffany, Martin Nicolas, Raison Anais, Argelaguet Ferran, Diverrez Jean-Marc, and Lécuyer Anatole (Nov. 2020). "Towards Real-Time Recognition of Users' Mental Workload Using Integrated Physiological Sensors Into a VR HMD". In: *ISMAR 2020 - IEEE International Symposium on Mixed and Augmented Reality*. Virtual, Brazil, pp. 1–13. (Visited on 02/21/2024).

Maris Eric and Oostenveld Robert (Aug. 2007). "Nonparametric Statistical Testing of EEG- and MEG-data". In: *Journal of Neuroscience Methods* 164.1, pp. 177–190. (Visited on 03/10/2025).

Mason S.G. and Birch G.E. (Mar. 2003). “A General Framework for Brain-Computer Interface Design”. In: *IEEE Transactions on Neural Systems and Rehabilitation Engineering* 11.1, pp. 70–85. (Visited on 09/25/2025).

Mawalid Moch.Asyroful, Khoirunnisa Alfi Zuhriya, Purnomo Mauridhi Hery, and Wibawa Adhi Dharma (Nov. 2018). “Classification of EEG Signal for Detecting Cybersickness through Time Domain Feature Extraction Using NaÏve Bayes”. In: *2018 International Conference on Computer Engineering, Network and Intelligent Multimedia (CENIM)*, pp. 29–34. (Visited on 07/02/2025).

McAssey Michaela, Brandt Thomas, and Dieterich Marianne (Nov. 2022). “EEG Analysis of the Visual Motion Activated Vection Network in Left- and Right-Handers”. In: *Scientific Reports* 12.1, p. 19566. (Visited on 05/04/2025).

McAssey Michaela, Dowsett James, Kirsch Valerie, Brandt Thomas, and Dieterich Marianne (Dec. 2020). “Different EEG Brain Activity in Right and Left Handers during Visually Induced Self-Motion Perception”. In: *Journal of Neurology* 267.S1, pp. 79–90. (Visited on 05/04/2025).

McCauley Michael and Sharkey Thomas (Jan. 1992). “Cybersickness: Perception of Self-Motion in Virtual Environment.” In: *Presence* 1, pp. 311–318.

Mimnaugh Katherine J., Center Evan G., Suomalainen Markku, Becerra Israel, Lozano Eliezer, Murrieta-Cid Rafael, Ojala Timo, LaValle Steven M., and Federmeier Kara D. (Nov. 2023). “Virtual Reality Sickness Reduces Attention During Immersive Experiences”. In: *IEEE Transactions on Visualization and Computer Graphics* 29.11, pp. 4394–4404. (Visited on 07/02/2025).

Min Byung-Chan, Chung Soon-Cheol, Min Yoon-Ki, and Sakamoto Kazuyoshi (Nov. 2004). “Psychophysiological Evaluation of Simulator Sickness Evoked by a Graphic Simulator”. In: *Applied Ergonomics* 35.6, pp. 549–556. (Visited on 07/02/2025).

Miyazaki Jungo, Yamamoto Hiroki, Ichimura Yoshikatsu, Yamashiro Hiroyuki, Murase Tomokazu, Yamamoto Tetsuya, Umeda Masahiro, and Higuchi Toshihiro (Mar. 2021). “Resting-State Functional Connectivity Predicts Recovery from Visually Induced Motion Sickness”. In: *Experimental Brain Research* 239.3, pp. 903–921. (Visited on 07/02/2025).

Si-Mohammed Hakim (Dec. 2019). “Design and Study of Interactive Systems Based on Brain- Computer Interfaces and Augmented Reality”. PhD thesis. INSA de Rennes. (Visited on 10/24/2022).

Moinnereau Marc-Antoine, Oliveira Alcyr A., and Falk Tiago H. (Oct. 2022). “Instrumenting a Virtual Reality Headset for At-Home Gamer Experience Monitoring and Behavioural Assessment”. In: *Frontiers in Virtual Reality* 3. (Visited on 07/02/2025).

Molefi Emmanuel, McLoughlin Ian, and Palaniappan Ramaswamy (Jan. 2025). “Transcutaneous Auricular Vagus Nerve Stimulation for Visually Induced Motion Sickness: An eLORETA Study”. In: *Brain Topography* 38.1, p. 11. (Visited on 07/02/2025).

Molefi Emmanuel, Palaniappan Ramaswamy, and McLoughlin Ian (July 2022). “Vibro-Motor Reprocessing Therapy towards Managing Motion Sickness Reduction: Evidence from EEG”. In: *Annual International Conference of the IEEE Engineering in Medicine and Biology Society. IEEE Engineering in Medicine and Biology Society. Annual International Conference* 2022, pp. 4781–4784.

Murovec Brandy, Berti Stefan, Yahya Susan, Spaniol Julia, and Keshavarz Behrang (June 2025). “Early Cortical Processing of Coherent vs. Non-Coherent Motion Stimuli in Younger and Older Adults: An Event-Related Potential (ERP) Study Investigating Visually Induced Vection”. In: *Neuropsychologia* 212, p. 109140. (Visited on 05/04/2025).

Nakul Estelle, Bartolomei Fabrice, and Lopez Christophe (Sept. 2021). “Vestibular-Evoked Cerebral Potentials”. In: *Frontiers in Neurology* 12. (Visited on 05/15/2024).

Nam Sungu, Jang Kyoung-Mi, Kwon Moonyoung, Lim Hyun Kyoon, and Jeong Jaeseung (Aug. 2022). “Electroencephalogram Microstates and Functional Connectivity of Cybersickness”. In: *Frontiers in Human Neuroscience* 16, p. 857768. (Visited on 07/02/2025).

Napadow Vitaly, Sheehan James D., Kim Jieun, Lacount Lauren T., Park Kyungmo, Kaptchuk Ted J., Rosen Bruce R., and Kuo Braden (Apr. 2013). “The Brain Circuitry Underlying the Temporal Evolution of Nausea in Humans”. In: *Cerebral Cortex (New York, N.Y.: 1991)* 23.4, pp. 806–813.

Nesbitt Keith, Davis Simon, Blackmore Karen, and Nalivaiko Eugene (July 2017). “Correlating Reaction Time and Nausea Measures with Traditional Measures of Cybersickness”. In: *Displays* 48, pp. 1–8. (Visited on 03/13/2023).

Nolan H., Butler J. S., Whelan R., Foxe J. J., Bülthoff H. H., and Reilly R. B. (May 2012). “Neural Correlates of Oddball Detection in Self-Motion Heading: A High-Density Event-Related Potential Study of Vestibular Integration”. In: *Experimental Brain Research* 219.1, pp. 1–11. (Visited on 06/08/2024).

Nooij Suzanne A. E., Pretto Paolo, Oberfeld Daniel, Hecht Heiko, and Bülthoff Heinrich H. (2017). “Vection Is the Main Contributor to Motion Sickness Induced by Visual Yaw Rotation: Implications for Conflict and Eye Movement Theories”. In: *PloS One* 12.4, e0175305.

Nürnberger Matthias, Klingner Carsten, Witte Otto W., and Brodoehl Stefan (Oct. 2021). “Mismatch of Visual-Vestibular Information in Virtual Reality: Is Motion Sickness Part of the Brains Attempt to Reduce the Prediction Error?” In: *Frontiers in Human Neuroscience* 15, p. 757735. (Visited on 07/02/2025).

Ozkan Alper, Uyan Ufuk, and Celikcan Ufuk (July 2023). “Effects of Speed, Complexity and Stereoscopic VR Cues on Cybersickness Examined via EEG and Self-Reported Measures”. In: *Displays* 78, p. 102415. (Visited on 07/02/2025).

Padmanaban Nitish, Ruban Timon, Sitzmann Vincent, Norcia Anthony M., and Wetzstein Gordon (Apr. 2018). “Towards a Machine-Learning Approach for Sickness Prediction in 360° Stereoscopic Videos”. In: *IEEE Transactions on Visualization and Computer Graphics* 24.4, pp. 1594–1603. (Visited on 09/26/2023).

Page Matthew J, Moher David, Bossuyt Patrick M, Boutron Isabelle, Hoffmann Tammy C, Mulrow Cynthia D, Shamseer Larissa, Tetzlaff Jennifer M, Akl Elie A, Brennan Sue E, Chou Roger, Glanville Julie, Grimshaw Jeremy M, Hróbjartsson Asbjørn, Lalu Manoj M, Li Tianjing, Loder Elizabeth W, Mayo-Wilson Evan, McDonald Steve, McGuinness Luke A, Stewart Lesley A, Thomas James, Tricco Andrea C, Welch Vivian A, Whiting Penny, and McKenzie Joanne E (Mar. 2021). “PRISMA 2020 Explanation and Elaboration: Updated Guidance and Exemplars for Reporting Systematic Reviews”. In: *BMJ*, n160. (Visited on 05/05/2025).

Palmisano Stephen, Allison Robert S., and Kim Juno (2020). “Cybersickness in Head-Mounted Displays Is Caused by Differences in the User’s Virtual and Physical Head Pose”. In: *Frontiers in Virtual Reality* 1. (Visited on 01/30/2023).

Palmisano Stephen, Allison Robert S., Schira Mark M., and Barry Robert J. (2015). “Future Challenges for Vection Research: Definitions, Functional Significance, Measures, and Neural Bases”. In: *Frontiers in Psychology* 6. (Visited on 09/19/2023).

Palmisano Stephen, Apthorp Deborah, Seno Takeharu, and Stapley Paul J. (Apr. 2014). “Spontaneous Postural Sway Predicts the Strength of Smooth Vection”. In: *Experimental Brain Research* 232.4, pp. 1185–1191. (Visited on 09/18/2024).

Palmisano Stephen, Barry Robert J., De Blasio Frances M., and Fogarty Jack S. (2016). “Identifying Objective EEG Based Markers of Linear Vection in Depth”. In: *Frontiers in Psychology* 7, p. 1205.

Pane Evi Septiana, Zuhriya Khoirunnisaa Alfi, Wibawa Adhi Dharma, and Purnomo Mauridhi Hery (Oct. 2018). “Identifying Severity Level of Cybersickness from EEG Signals Using CN2 Rule Induction Algorithm”. In: *2018 International Conference on Intelligent Informatics and Biomedical Sciences (ICIIBMS)*. Vol. 3, pp. 170–176. (Visited on 07/02/2025).

Park Jong-Rack, Lim Dae-Woon, Lee Soo-Yeol, Lee Hang-Woon, Choi Mi-Hyun, and Chung Soo-Cheol (June 2008). “Long-Term Study of Simulator Sickness: Differences in EEG Response Due to Individual Sensitivity”. In: *International Journal of Neuroscience* 118.6, pp. 857–865. (Visited on 07/02/2025).

Pernet Cyril R., Appelhoff Stefan, Gorgolewski Krzysztof J., Flandin Guillaume, Phillips Christophe, Delorme Arnaud, and Oostenveld Robert (June 2019). “EEG-BIDS, an Extension to the Brain Imaging Data Structure for Electroencephalography”. In: *Scientific Data* 6.1, p. 103. (Visited on 09/29/2023).

Pöhlmann Katharina Margareta Theresa, Föcker Julia, Dickinson Patrick, Parke Adrian, and O’Hare Louise (Apr. 2021). “The Effect of Motion Direction and Eccentricity on Vection, VR Sickness and Head Movements in Virtual Reality”. In: *Multisensory Research* 34.6, pp. 623–662. (Visited on 09/19/2023).

— (Jan. 2022). “The Relationship between Vection, Cybersickness and Head Movements Elicited by Illusory Motion in Virtual Reality”. In: *Displays* 71, p. 102111. (Visited on 09/18/2024).

Polich John (Oct. 2007). “Updating P300: An Integrative Theory of P3a and P3b”. In: *Clinical Neurophysiology* 118.10, pp. 2128–2148. (Visited on 02/27/2024).

Prothero Jerrold and Parker Donald (2003). “A Unified Approach to Presence and Motion Sickness”. In: *Virtual and Adaptive Environments: Applications, Implications, and Human Performance Issues*. Mahwah, NJ, US: Lawrence Erlbaum Associates Publishers, pp. 47–66.

Rebenitsch Lisa and Owen Charles (June 2016). “Review on Cybersickness in Applications and Visual Displays”. In: *Virtual Reality* 20.2, pp. 101–125. (Visited on 12/15/2022).

Recenti Marco, Ricciardi Carlo, Aubonnet Romain, Picone Ilaria, Jacob Deborah, Svansson Halldór Á. R., Agnarsdóttir Sólveig, Karlsson Gunnar H., Baeringsdóttir Valdís, Petersen Hannes, and Gargiulo Paolo (Apr. 2021). “Toward Predicting Motion Sickness Using Virtual Reality and a Moving Platform Assessing Brain, Muscles, and Heart Signals”. In: *Frontiers in Bioengineering and Biotechnology* 9. (Visited on 07/02/2025).

Ren Bin and Zhou Qinyu (Apr. 2023). “Assessing Passengers’ Motion Sickness Levels Based on Cerebral Blood Oxygen Signals and Simulation of Actual Ride Sensation”. In: *Diagnostics* 13.8, p. 1403. (Visited on 07/02/2025).

Rietdijk Wim J. R., Franken Ingmar H. A., and Thurik A. Roy (2014). “Internal Consistency of Event-Related Potentials Associated with Cognitive Control: N2/P3 and ERN/Pe”. In: *PloS One* 9.7, e102672.

Rivet Bertrand, Souloumiac Antoine, Attina Virginie, and Gibert Guillaume (Aug. 2009). “xDAWN Algorithm to Enhance Evoked Potentials: Application to Brain-Computer Interface”. In: *IEEE transactions on bio-medical engineering* 56.8, pp. 2035–2043.

Rosanne Olivier, Benesch Danielle, Kratzig Gregory, Paré Simon, Bolt Nicole, and Falk Tiago H. (Jan. 2025). “To Pre-Process or Not to Pre-Process? On the Role of EEG Enhancement for Cybersickness Characterization and the Importance of Amplitude Modulation Features”. In: *Frontiers in Virtual Reality* 6, p. 1468971. (Visited on 07/02/2025).

Roy Raphaëlle N., Bonnet Stéphane, Charbonnier Sylvie, and Campagne Aurélie (July 2013). “Mental Fatigue and Working Memory Load Estimation: Interaction and Implications for EEG-based Passive BCI”. In: *2013 35th Annual International Conference of the IEEE Engineering in Medicine and Biology Society (EMBC)*, pp. 6607–6610. (Visited on 02/21/2024).

Sameri Javad, Coenegracht Hendrick, Van Damme Sam, De Turck Filip, and Torres Vega Maria (Nov. 2024). “Physiology-Driven Cybersickness Detection in Virtual Reality: A Machine Learning and Explainable AI Approach”. In: *Virtual Reality* 28.4, p. 174. (Visited on 07/02/2025).

Schurger Aaron, Marti Sebastien, and Dehaene Stanislas (Oct. 2013). “Reducing Multi-Sensor Data to a Single Time Course That Reveals Experimental Effects”. In: *BMC Neuroscience* 14.1, p. 122. (Visited on 03/05/2025).

Sclocco Roberta, Kim Jieun, Garcia Ronald G., Sheehan James D., Beissner Florian, Bianchi Anna M., Cerutti Sergio, Kuo Braden, Barbieri Riccardo, and Napadow Vitaly (Aug. 2014). “Brain Circuitry Supporting Multi-Organ Autonomic Outflow in Response to Nausea”. In: *Cerebral Cortex*, bhu172. (Visited on 07/02/2025).

Seno Takeharu, Murata Kayoko, Fujii Yoshitaka, Kanaya Hidetoshi, Ogawa Masaki, Tokunaga Kousuke, and Palmisano Stephen (2018). “Vection Is Enhanced by Increased Exposure to Optic Flow”. In: *I-Perception* 9.3, p. 2041669518774069.

Shen Zhenqian, Liu Xingru, Li Wenqiang, Li Xueyan, and Wang Qiang (June 2024). “Classification of Visually Induced Motion Sickness Based on Phase-Locked Value Functional Connectivity Matrix and CNN-LSTM”. In: *Sensors* 24.12, p. 3936. (Visited on 07/02/2025).

Da-Silva P. J. G., Cagy M., and Infantosi A. F. C. (2015). “A New Dynamic Virtual Stimulation Protocol to Evoke M-VEP and Linear Vection during Orthostatic Posture Control”. In: *World Congress on Medical Physics and Biomedical Engineering, June 7-12, 2015, Toronto, Canada*. Springer, Cham, pp. 1220–1223. (Visited on 05/04/2025).

Slater Mel (Jan. 2003). “A Note on Presence Terminology”. In: *Presence Connect* 3.

Stanney Kay M., Kennedy Robert S., and Drexler Julie M. (Oct. 1997). “Cybersickness Is Not Simulator Sickness”. In: *Proceedings of the Human Factors and Ergonomics Society Annual Meeting* 41.2, pp. 1138–1142. (Visited on 03/14/2023).

Steuer Jonathan (Dec. 1992). “Defining Virtual Reality: Dimensions Determining Telepresence”. In: *Journal of Communication* 42.4, pp. 73–93. (Visited on 09/11/2025).

Stróżak Paweł, Francuz Piotr, Augustynowicz Paweł, Ratomska Marta, Fudali-Czyż Agnieszka, and Bałaj Bibianna (Dec. 2016). “ERPs in an Oddball Task under Vection-Inducing Visual Stimulation”. In: *Experimental Brain Research* 234.12, pp. 3473–3482. (Visited on 05/04/2025).

Suwandi Galih Restu Fardian, Khotimah Siti Nurul, Haryanto Freddy, and Suprijadi (Sept. 2024). “Exploring the Impact of Motion Parameter Variations in Virtual Reality Content on Visually Induced Motion Sickness:

An Electroencephalography Signal Analysis Approach". In: *International Journal of Online and Biomedical Engineering (iJOE)* 20.12, pp. 160–176. (Visited on 07/02/2025).

Teixeira Joel, Miellet Sebastien, and Palmisano Stephen (Apr. 2022). "Unexpected Vection Exacerbates Cybersickness During HMD-Based Virtual Reality". In: *Frontiers in Virtual Reality* 3. (Visited on 09/18/2024).

Thilo Kai V., Kleinschmidt Andreas, and Gresty Michael A. (Aug. 2003). "Perception of Self-Motion From Peripheral Optokinetic Stimulation Suppresses Visual Evoked Responses to Central Stimuli". In: *Journal of Neurophysiology* 90.2, pp. 723–730. (Visited on 09/26/2023).

Tian Nana and Boulic Ronan (2024). "Who Says You Are so Sick? An Investigation on Individual Susceptibility to Cybersickness Triggers Using EEG, EGG and ECG". In: *IEEE Transactions on Visualization and Computer Graphics*, pp. 1–11. (Visited on 03/26/2024).

Todd Neil Pm, Govender Sendhil, and Colebatch James G (Nov. 2019). "Modulation of the Human Electro-Cerebellogram (ECeG) during Vestibular and Optokinetic Stimulation". In: *Neuroscience Letters* 712, p. 134497. (Visited on 05/04/2025).

Tokumaru Osamu, Kaida Kenichi, Ashida H, Yoneda I, and Tatsuno J (Apr. 1999). "EEG Topographical Analysis of Spatial Disorientation". In: *Aviation, space, and environmental medicine* 70, pp. 256–63.

Toschi Nicola, Kim Jieun, Sclocco Roberta, Duggento Andrea, Barbieri Riccardo, Kuo Braden, and Napadow Vitaly (Jan. 2017). "Motion Sickness Increases Functional Connectivity between Visual Motion and Nausea-Associated Brain Regions". In: *Autonomic Neuroscience* 202, pp. 108–113. (Visited on 07/02/2025).

Treisman Michel (July 1977). "Motion Sickness: An Evolutionary Hypothesis". In: *Science* 197.4302, pp. 493–495. (Visited on 07/09/2025).

Tu Shen, Cao Xiaojun, Yun Xuyan, Wang Kangcheng, Zhao Guang, and Qiu Jiang (Feb. 2014). "A New Association Evaluation Stage in Cartoon Apprehension: Evidence from an ERP Study". In: *Journal of Behavioral and Brain Science* 4.2, pp. 75–83. (Visited on 09/24/2023).

Uyan Ufuk and Celikcan Ufuk (July 2024). "CDMS: A Real-Time System for EEG-guided Cybersickness Mitigation through Adaptive Adjustment of VR Content Factors". In: *Displays* 83, p. 102704. (Visited on 07/02/2025).

Van der Lee Gael, Cabestaing François, Lécuyer Anatole, Scherer Reinhold, and Si-Mohammed Hakim (2024). "EEG Markers of Acceleration Percep-

tion in Virtual Reality". In: *Proceedings of the 9th Graz Brain-Computer Interface Conference 2024*. Graz, pp. 249–253.

Vidal J. J. (June 1973). "Toward Direct Brain-Computer Communication". In: *Annual Review of Biophysics* 2.Volume 2, 1973, pp. 157–180. (Visited on 09/06/2025).

von Helmholtz Hermann (Dec. 1896). "Handbuch der physiologischen Optik". In: *Monatshefte für Mathematik und Physik* 7.1, A60–A61. (Visited on 07/22/2024).

Wang Regina W.Y., Kuo Hsien-Chu, and Chuang Shang-Wen (Aug. 2017). "Humor Drawings Evoked Temporal and Spectral EEG Processes". In: *Social Cognitive and Affective Neuroscience* 12.8, pp. 1359–1376. (Visited on 09/24/2023).

Weech Séamas, Kenny Sophie, and Barnett-Cowan Michael (2019). "Presence and Cybersickness in Virtual Reality Are Negatively Related: A Review". In: *Frontiers in Psychology* 10. (Visited on 12/15/2022).

Wei Chun-Shu, Chuang Shang-Wen, Wang Wan-Ru, Ko Li-Wei, Jung Tzyy-Ping, and Lin Chin-Teng (May 2011a). "Implementation of a Motion Sickness Evaluation System Based on EEG Spectrum Analysis". In: *2011 IEEE International Symposium of Circuits and Systems (ISCAS)*, pp. 1081–1084. (Visited on 07/02/2025).

Wei Chun-Shu, Ko Li-Wei, Chuang Shang-Wen, Jung Tzyy-Ping, and Lin Chin-Teng (Apr. 2011b). "EEG-based Evaluation System for Motion Sickness Estimation". In: *2011 5th International IEEE/EMBS Conference on Neural Engineering*. Cancun: IEEE, pp. 100–103. (Visited on 07/02/2025).

— (July 2011c). "Genetic Feature Selection in EEG-based Motion Sickness Estimation". In: *The 2011 International Joint Conference on Neural Networks*, pp. 365–369. (Visited on 07/08/2025).

Wei Yue, Okazaki Yuka O., So Richard H.Y., Chu Winnie C.W., and Kitajo Keiichi (Nov. 2019). "Motion Sickness-Susceptible Participants Exposed to Coherent Rotating Dot Patterns Show Excessive N2 Amplitudes and Impaired Theta-Band Phase Synchronization". In: *NeuroImage* 202, p. 116028. (Visited on 05/04/2025).

Wolpaw Jonathan R. and Wolpaw Elizabeth W. (2012). *Brain-Computer Interfaces: Principles and Practice / Edited by Jonathan R. Wolpaw, Elizabeth Winter Wolpaw*. Oxford New York: Oxford University Press.

Woo Ye Shin, Jang Kyoung-Mi, Nam Sun Gu, Kwon Moonyoung, and Lim Hyun Kyoon (Apr. 2023). "Recovery Time from VR Sickness Due to Susceptibility:

Objective and Quantitative Evaluation Using Electroencephalography". In: *Heliyon* 9.4, e14792. (Visited on 07/02/2025).

Wu Jintao, Zhou Qianxiang, Li Jiaxuan, Kong Xiangjie, and Xiao Yi (July 2020). "Inhibition-Related N2 and P3: Indicators of Visually Induced Motion Sickness (VIMS)". In: *International Journal of Industrial Ergonomics* 78, p. 102981. (Visited on 12/13/2023).

Xu Mengdie, Yang Banghua, Liu Mutian, Huang Yiling, Xia Xinxing, and Zhang Jie (Aug. 2023). "SE-CNN Attention Structure for Quantitative EEG-Based Assessment of VR Motion Sickness". In: *Proceedings of the 2023 9th International Conference on Computing and Artificial Intelligence*. ICCAI '23. New York, NY, USA: Association for Computing Machinery, pp. 606–611. (Visited on 07/02/2025).

Xu Wenge, Liang Hai-Ning, Yu Yifan, Monteiro Diego, Hasan Khalad, and Fleming Charles (June 2019). "Assessing the Effects of a Full-Body Motion-Based Exergame in Virtual Reality". In: *Proceedings of the Seventh International Symposium of Chinese CHI*. Xiamen China: ACM, pp. 1–6. (Visited on 07/02/2025).

Yadav Drishti, Yadav Shilpee, and Veer Karan (Dec. 2020). "A Comprehensive Assessment of Brain Computer Interfaces: Recent Trends and Challenges". In: *Journal of Neuroscience Methods* 346, p. 108918. (Visited on 01/04/2023).

Yamamura Hiroo, Baldauf Holger, and Kunze Kai (July 2021). "HemodynamicVR - Adapting the User's Field Of View during Virtual Reality Locomotion Tasks to Reduce Cybersickness Using Wearable Functional Near-Infrared Spectroscopy". In: *Proceedings of the Augmented Humans International Conference 2021*. AHs '21. New York, NY, USA: Association for Computing Machinery, pp. 223–227. (Visited on 07/02/2025).

Yang Alexander Hui Xiang, Kasabov Nikola Kirilov, and Cakmak Yusuf Ozgur (Dec. 2023). "Prediction and Detection of Virtual Reality Induced Cybersickness: A Spiking Neural Network Approach Using Spatiotemporal EEG Brain Data and Heart Rate Variability". In: *Brain Informatics* 10.1, p. 15. (Visited on 07/02/2025).

Yeo Sang Seok, Kwon Jung Won, and Park Seo Yoon (Oct. 2022). "EEG-based Analysis of Various Sensory Stimulation Effects to Reduce Visually Induced Motion Sickness in Virtual Reality". In: *Scientific Reports* 12.1, p. 18043. (Visited on 03/09/2023).

Yeo Sang Seok, Park Seo Yoon, and Yun Seong Ho (Apr. 2024). “Investigating Cortical Activity during Cybersickness by fNIRS”. In: *Scientific Reports* 14.1, p. 8093. (Visited on 07/02/2025).

Yu Yi-Hsin, Lai Pei-Chen, Ko Li-Wei, Chuang Chun-Hsiang, Kuo Bor-Chen, and Lin Chin-Teng (July 2010). “An EEG-based Classification System of Passenger’s Motion Sickness Level by Using Feature Extraction/Selection Technologies”. In: *The 2010 International Joint Conference on Neural Networks (IJCNN)*, pp. 1–6.

Zander Thorsten O. and Kothe Christian (Apr. 2011). “Towards Passive Brain-Computer Interfaces: Applying Brain-Computer Interface Technology to Human-Machine Systems in General”. In: *Journal of Neural Engineering* 8.2, p. 025005.

Zhang Chenyang, Li Shuguang, Li Yaohua, Li Shengbo Eben, and Nie Bingbing (2020). “Analysis of Motion Sickness Associated Brain Activity Using fNIRS: A Driving Simulator Study”. In: *IEEE Access* 8, pp. 207415–207425. (Visited on 07/02/2025).

Zhang Li-Li, Wang Jun-Qin, Qi Rui-Rui, Pan Lei-Lei, Li Min, and Cai Yi-Ling (Jan. 2016). “Motion Sickness: Current Knowledge and Recent Advance”. In: *CNS neuroscience & therapeutics* 22.1, pp. 15–24.

Zhou Lu, Hu Haixu, Qin Bing, Zhu Qiaoqiao, and Qian Zhiyu (Sept. 2023). “Brain Activity Differences between Susceptible and Non-Susceptible Populations under Visually Induced Motion Sickness Based on Sensor-Space and Source-Space Analyses”. In: *Brain Research* 1815, p. 148474. (Visited on 05/04/2025).

Résumé

La Réalité Virtuelle (RV) provoque fréquemment de la cybercinétose (nausées, désorientation, fatigue visuelle), ce qui limite l'utilisation prolongée des casques en formation, santé et divertissement. Cette thèse recherche des neuromarqueurs objectifs, mesurables en temps réel, pour comprendre pourquoi certains utilisateurs tombent malades et permettre à la RV de s'adapter avant l'apparition des symptômes.
En enregistrant l'Électroencéphalographie (EEG) pendant des stimulations de vection en RV, nous identifions deux potentiels évoqués robustes : un potentiel d'accélération (300–700 ms, positivité fronto-centrale) reflétant l'encodage des changements brusques de flux optique, et un potentiel P600 de vection (600 ms, positivité pariétale avec négativité frontale) lié de manière fiable à l'intensité de vection ressentie. La topographie pariéto-frontale de ce P600 et ses corrélations avec la nausée et la désorientation apportent un soutien quantitatif à la théorie du conflit sensoriel de la cybercinétose.
Enfin, nous montrons que le filtrage spatial xDAWN améliore significativement la détection de ces réponses par rapport à des méthodes classiques. Ces résultats ouvrent la voie à des interfaces cerveau-ordinateur (ICO) passives capables de surveiller en continu l'état cérébral et d'adapter automatiquement le contenu RV pour réduire la cybercinétose tout en préservant l'immersion.

Abstract

Head-mounted Virtual Reality (VR) often induces cybersickness (nausea, disorientation, and visual discomfort) that prevents many users from completing longer sessions in training, healthcare, and entertainment. This thesis seeks objective, real-time neural markers that explain why some users become sick and enable VR systems to adapt before symptoms emerge.
By recording electroencephalography (EEG) during visually induced self-motion (vection) in VR, we identify two robust event-related potentials: an acceleration-related component (300–700 ms, fronto-central positivity) that encodes sudden changes in optic flow, and a vection P600 (600 ms, parietal positivity with frontal negativity) that is reliably linked to the strength of perceived vection. The P600's parieto-frontal topography and its correlations with nausea and disorientation scores provide quantitative support for sensory conflict accounts of cybersickness.
Finally, we show that xDAWN spatial filtering enhances the detection of these responses compared to alternative methods. Together, these findings pave the way for passive brain–computer interfaces (BCIs) that continuously monitor brain state and adapt VR content to reduce cybersickness while preserving immersion.